MINERALOGY OF THE TETRAHEDRITE SERIES

A dissertation submitted to

The Graduate School

of the University of Cincinnati

in partial fulfillment of the
requirements for the degree of

DOCTOR OF PHILOSOPHY

1964

by

Harold Bohmer, Jr.

B.A. Amherst College 1958
M.S. University of Cincinnati 1960

UNIVERSITY OF CINCINNATI

MAY 19, 19 64

I hereby recommend that the thesis prepared under my supervision by HAROLD BOHMER, JR.

entitled MINERALOGY OF THE TETRAHEDRITE SERIES

be accepted as fulfilling this part of the requirements for the degree of DOCTOR OF PHILOSOPHY

Approved by:

Frank L. Kourkey

William F. Jones

Form 668—Grad. Sch.—1M—4-61

CONTENTS

	Page
Abstract	1
Introduction	4
Acknowledgments	7
Abbreviations	8
Previous work	8
Chemical analyses and stoichiometry	9
Structure	10
Structural classification	12
Order - disorder	15
Phase relationships	17
X-ray diffraction data	18
Methods and procedures	19
Natural specimens	19
Separatory techniques	19
Polished sections	23
Synthetics	23
GE XRD-5 and diffractometer	25
Nonius-Guinier camera	30
X-ray fluorescence analysis	30
Structure	30
Chemistry	42
Analytical results	42
Atom sizes and radius ratios	43

Page

Element associations and limitations..... 52

Ag..... 53

Zn..... 55

Fe..... 55

Fe + Zn..... 58

Hg..... 58

Limitations in the complete isomorphous series... 58

Streak..... 64

Unit cell dimensions..... 69

Synthetics..... 70

Natural specimens..... 73

Disordered substitutions..... 75

"Extra" reflections belonging to tetrahedrite structure..... 87

Tetrahedrite as a derivative structure..... 89

Differences in chemistry..... 95

Differences in stacking..... 96

Differences in structure..... 97

Conclusions..... 98

Appendix A..... 101

Detailed procedures..... 101

Separatory procedures..... 101

Mineral synthesis procedure..... 103

Appendix B..... 105

Polished section data..... 105

Page

Appendix C..... 121

Data from x-ray diffraction powder patterns..... 121

References..... 167

TABLES

Table 1 Localities of natural specimens..... 20

Table 2 Data from gravimetric and magnetic mineral separations..... 24

Table 3 Data from mineral synthesis..... 26

Table 4 Composition of standards for x-ray fluorescence analysis..... 32

Table 5 Chemical analyses..... 44

Table 6 Minimum percent for Cu and maximum percentages of substituting elements..... 49

Table 7 Radius ratios for constituent elements of the tetrahedrite series..... 51

Table 8 Cell dimensions of natural and synthetic specimens..... 71

Table 9 Nonius-Guinier x-ray data showing "extra" lines..... 90

Table 10 Calculations for "extra" lines on Nonius-Guinier photographs..... 91

FIGURES

Figure 1. Graph of a_o with 2θ for all specimens.... 29

Figure 2. X-ray fluorescence patterns for tetrahedrite and tennantite..... 31

Figure 3. Standard curve for x-ray fluorescence analysis - Cu..... 33

Figure 4. Standard curves for x-ray fluorescence analysis - Fe..... 34

Page

Figure 5. Standard curves for x-ray fluorescence analysis - Zn and Ag..... 35

Figure 6. Standard curves for x-ray fluorescence analysis - As and Sb..... 36

Figure 7. Stacking of the tetrahedrite series..... 38

Figure 8. Tetrahedrite unit cell - forward half (after Pauling and Neuman, 1934..... 41

Figure 9. Limits for Ag in tetrahedrite series (vertical lines outline composition gap). 54

Figure 10. Distribution of Zn in tetrahedrite series (vertical lines outline composition gap). 56

Figure 11. Distribution of Fe in tetrahedrite series (vertical lines outline composition gap). 57

Figure 12. Distribution of Fe + Zn in tetrahedrite series (vertical lines outline composition gap)..... 59

Figure 13. Composition diagram for As-Sb-Bi..... 61

Figure 14. X-ray diffraction powder pattern and polished section of unmixing tetrahedrite -tennantite..... 63

Figure 15. X-ray diffraction powder pattern and polished section of single phase of tetrahedrite-tennantite (containing little silver) in composition gap..... 65

Figure 16. Preliminary diagram of the fields of stability for the tetrahedrite series.... 66

Figure 17. Streaks fields for the tetrahedrite series..... 68

Figure 18. X-ray diffraction powder patterns of members of the tetrahedrite series differing in cell size..... 72

Figure 19. Variation of cell size with Ag and Bi.... 74

Figure 20. Variation of cell size with Ag + Sb..... 76

Page

Figure 21. Variation of cell size in tetrahedrite series..... 77

Figure 22. Unit cell of sphalerite..... 79

Figure 23. Unit cell of chalcopyrite..... 80

Figure 24. X-ray powder diffraction patterns of sphalerite, chalcopyrite, tetrahedrite... 81

Figure 25. Variation of intensity of reflections in tetrahedrite series..... 85

Figure 26. Variation of intensity of (400) and (220) with Sb-As..... 86

Figure 27. Variation of intensity of reflections with Ag..... 88

PLATES
(Photomicrographs)

Plate 1..... 108

Plate 2..... 109

Plate 3..... 110

Plate 4..... 111

Plate 5..... 112

Plate 6..... 113

Plate 7..... 114

Plate 8..... 115

Plate 9..... 116

Plate 10..... 117

Plate 11..... 118

Plate 12..... 119

Plate 13..... 120

ABSTRACT

The tetrahedrite series is both a common group of sulfosalts and an important contributor to ores of copper and silver. The general formula is $X_{12}Y_4S_{13}$, where X is Cu, Fe, Zn, Ag, Pb, Hg, Ni, or Co; and Y is As or Sb with occasionally minor Bi. The occurrence is in low to moderate-temperature hydrothermal veins with other ore minerals of copper, lead, zinc and silver. Microscopic textural relationships of the minerals are difficult to interpret in part because of lack of knowledge of solid phase relationships. This study is based on synthetic specimens and worldwide natural specimens of the tetrahedrite series and correlates data from chemical analyses, x-ray diffraction patterns, and polished sections. The results have implications in geothermometry and the paragenesis of ore minerals. In addition, some limitations in the chemistry of the tetrahedrite series are defined and variation of the unit cell size with chemistry analyzed.

Despite variations in size and valence states of atoms substituting in tetrahedrite-tennantite, complete solid solution between Sb and As has been assumed for all varieties. Chemical analyses of natural specimens show a composition gap, where few analyses fall, between 6 and 11 atomic percent As. X-ray powder diffraction data suggest that this gap marks an unmixing field for varieties having greater than 2.5 atomic percent Ag. The critical

temperature for unmixing might be useful as a geological thermometer.

Limitations in the quantities of various substituting elements have not previously been determined. Suggested upper limits for Fe, Zn and Ag have been determined for the series, and the solid solution field for As-Sb-Bi outlined. The sum Fe + Zn approaches a constant value in the tennantite field, suggesting the formula $Cu_{10}(Fe,Zn)_2(As,Sb)_4S_{13}$. A brown streak is related quantitatively to the Zn content and in a permissive way to the As content.

Knowledge of the range in unit cell size and the effects of chemistry on cell size has been quite limited. A complete range of dimensions from 10.20 (10.18) Å to 10.55 Å exists. The variation of cell size with chemistry has been approached quantitatively for the tetrahedrite series.

Most workers have stressed the similarity of the tetrahedrite structure to the sphalerite type, and classified it as a derivative of the basic sphalerite structure. However, data from synthetic and natural specimens seem to rule out an order-disorder relationship for all the metals within a stable sulfur network in the tetrahedrite structure. The explanation is to be found in important differences from sphalerite in chemistry, stacking and structure. In view of these findings, the

tetrahedrite series could not exsolve in quantity from a common high-temperature phase with sphalerite and chalcopyrite.

Two "extra" reflections belonging to the tetrahedrite structure appear in long-exposure Nonius-Guinier powder camera photographs. These are anomalous reflections for the published structure and may be due to slight ordering of metal atoms not previously indicated.

INTRODUCTION

The tetrahedrite series is a group of sulfosalts classified under the Type Formula A_3BX_3 (Palache and others, 1944, p. 348). The general composition is $X_{12}Y_4S_{13}$, where X is predominantly Cu with lesser amounts of Fe, Zn, Ag, Pb, Hg, Ni or Co. A complete isomorphous series exists between Y = Sb and Y = As with the dividing line between tetrahedrite and tennantite placed by definition at Sb:As = 1:1. In addition, Y = Bi is found to a minor extent in some members of the series.

The name tetrahedrite is derived from the usual tetrahedral habit of the crystals, and tennantite from the English chemist Smithson Tennant. Fahlerz (German, gray ore) is an obsolete term (Commission on New Minerals and Mineral Names, 1960, 1962, p. 224). A number of compositional names have been coined for members of the series. The most noteworthy are freibergite for silver-bearing tetrahedrite (Freiberg, Germany); schwatzite for mercury-bearing tetrahedrite (Schwatz, Tirol); rionite for bismuth-bearing tennantite; and binnite for crystals of tennantite with dominant form $\{100\}$ (Binnental, Switzerland).

Members of the tetrahedrite series are among the most common sulfosalts and are important ore minerals of copper and silver. Typically the occurrence is in low to moderate-temperature hydrothermal veins with other ore minerals of

copper, lead, zinc and silver. Commonly associated minerals are chalcopyrite, pyrite, galena, sphalerite, bornite, argentite, bournonite, and the gangue minerals quartz, calcite, siderite, and barite.

The assignment of a paragenetic sequence of deposition for minerals in hydrothermal ore deposits depends on the interpretation of the textural relationships of the minerals in polished sections. The correct interpretation of these textural relationships must be founded in part on a knowledge of solid phase relationships for individual minerals. At present, textures resulting from exsolution, replacement or simultaneous crystallization may often be confused with one another because of lack of knowledge of these phase relations.

This paper presents results of a study of the chemical composition, structural variations and textural relationships in polished section of a variety of minerals of the tetrahedrite series representing world-wide occurrences. Previous work has been confined primarily to determination of the general stoichiometric formula through chemical analysis and to determination and refinement of the structure from single specimens. Correlation of data from x-ray diffraction, chemical analysis and polished sections provides information about the tetrahedrite series which applies to geologic thermometry and to the interpretation of the paragenesis of ore minerals.

A complete isomorphous series between As and Sb members has been tacitly assumed to exist for all compositions of the tetrahedrite series, though limiting values for various substituting elements have not previously been well-defined. Considerable size disparity among substituting elements suggested that complete isomorphism ought not to exist for all compositions. Chemical analyses as well as x-ray and polished section data suggest an unmixing field for certain composition in the tetrahedrite series. The critical temperature for this unmixing phenomenon might be useful as a geologic thermometer.

The dimensions of the unit cell (a_o) in minerals of the tetrahedrite series vary considerably. The values have been reported to range from 10.19 Å in tennantite to 10.33 Å in tetrahedrite, with 10.40 Å for silver-rich tetrahedrite from Freiberg. Data presented in this paper record a continuum of values from 10.20 to 10.55 for the cell edges of minerals of the tetrahedrite series. Further the variation of cell edges with some of the substituting elements has been assessed in a quantitative manner. This information may be used to determine, in a general way, the composition of a member of the tetrahedrite series from its cell dimensions.

Many workers have stressed the structural similarity between tetrahedrite and sphalerite. Tetrahedrite (like chalcopyrite) may be considered a derivative of the basic sphalerite-type structure. At sufficiently high temperature,

chalcopyrite has been found to disorder in such a manner that the sphalerite-type unit cell is produced. Similarly the complex, defect-derivative tetrahedrite might be expected to have such a high-temperature disordered phase. Such a relationship, or lack of it, would be important to geologic thermometry as well as to the interpretation of the paragenesis of the commonly associated ore minerals sphalerite, chalcopyrite and tetrahedrite-tennantite. X-ray analysis of natural and synthetic members of the tetrahedrite series has suggested that no quenchable high-temperature disordered phase exists. The explanation lies in the chemistry and atom coordinations in the tetrahedrite series, which result in some basic differences in stacking and structure from the sphalerite type. It is considered inappropriate to conceive of the structural differences in tetrahedrite as defects in a derivative of the sphalerite-type structure.

Aknowledgements

I wish to thank Dr. Frank L. Koucky for his help during the research and for criticism of the paper. Most natural specimens were generously provided by the U. S. National Museum and by the Chicago Museum of Natural History. The major part of the work was done with the support of NSF Fellowships during 1961-62, 1962-63.

Abbreviations

The following standard mineral abbreviations used throughout this paper are taken from Chace (1956):

tetrahedrite	td
tennantite	tn
chalcopyrite	ccp
sphalerite	sp
pyrite	py
galena	gn
argentite	arg
bornite	bn
chalcocite	cc
malachite	mc
chrysocolla	chrys
quartz	qtz
calcite	calc
siderite	sid
barite	ba
bournonite	bo
hematite	hem

PREVIOUS WORK

Previous work on the tetrahedrite series has been limited primarily to determination of the stoichiometric formula from chemical analyses; descriptive mineralogy; and to determination and refinement of the structure from single specimens. With the notable exception of Wuensch's (1963) confirmation and refinement of the structure, few studies have been made since the publication of Vol. I of the seventh edition of Dana's System of Mineralogy (Palache and others, 1944). In this volume the data are summarized on which present knowledge of the tetrahedrite series is based.

The general formula $X_{12}Y_4S_{13}$ is known, but limits of substitution for various elements have not previously been proposed. Complete solid solution has been assumed to exist between Sb and As, and no limitation on the introduction of Bi into this series has been advanced. Until Wuensch's (1963) work the structure was based on the Pauling and Neuman (1934) determination, which was made from a limited number of reflections. X-ray data for the tetrahedrite series is sketchy, consisting of a few incomplete diffraction patterns. As a result, neither the range in cell dimensions nor the effects of individual elements on cell size have been known. X-ray diffraction patterns of natural materials have not been investigated for the effects of possible ordered substitution of elements. Although tetrahedrite-tennantite is classified as a defect-derivative of sphalerite, no search has been made for a possible order-disorder relationship with the sphalerite-type structure.

Chemical Analyses and Stoichiometry

Many of the analyses of the tetrahedrite series were made prior to 1900, and a number of different formulas were proposed. Prior and Spencer (1899) proposed the formula $Cu_6Sb_2S_6$ and Wherry and Foshag (1921) $Cu_{10}(Zn,Fe,Cu)_2Sb_4S_{13}$. Winchell (1926) collected 33 analyses of the tetrahedrite

series considered best up to that time and recalculated them to atomic percentage composition. These analyses were judged to fit either the Wherry and Foshag or the Prior and Spencer formula. Winchell concluded tentatively that divalent Zn and Fe and Cu are not always present in the structure in standard amount, as indicated by the Wherry and Foshag formula, but that divalent Zn and Fe substitute for Cu with concurrent addition of S to maintain charge balance, as advocated by Prior and Spencer. Machatschki's (1928) structure determination resulted in the type formula R_3RS_3. In fifteen analyses of tetrahedrite minerals, Pauling and Neuman (1934) noted a consistent excess of sulfur over the formula used by Machatschki. They adopted the ideal formula $(Cu_{10}Zn_2)Sb_4S_{13}$ for the tetrahedrite group.

Structure

Machatschki (1928) made the first determination of the structure of tetrahedrite (fahlerz) from a specimen from Colquechaca, Bolivia. He concluded that the mineral crystallized in space group T_d^3 and worked out the general nature of the structure. Essentially, Machatschki's unit cell was similar to the one shown in Figure 8 without the S-II atoms. Machatschki noted that, except for one atom missing in each octant, the tetrahedrite unit cell was

similar to a stack of eight cells of zincblende (sphalerite). By comparing lattice constants with partial analyses of some 21 specimens, Machatschki judged that Ag substituting in a "customary" Cu-Sb tetrahedrite ($a_o = 10.32$) raised the cell dimensions to 10.40, and As lowered them to 10.19.

Pauling and Neuman (1934) determined the structure of binnite, a variety of tennantite from Binnenthal, Wallis, Switzerland, which resulted in a refinement of the structure proposed by Machatschki. Using data from oscillation and Laue photographs, he calculated cell dimensions 10.19 ± 0.020 KX units and chose space group T_d^3. The consistent excess of sulfur noted by Pauling and Neuman resulted in the placing of 6-coordinated S-II atoms in the structure.

Wuensch (1963) confirmed and refined the crystal structure of tetrahedrite proposed by Pauling and Neuman. Nearly pure $Cu_{12}Sb_4S_{13}$ was used from Horhausen, Westerwald, Germany. One-hundred and thirty-six reflections, with only two undetectable, were obtained using an equi-inclination diffractometer with proportional point counter. The observed intensities, reduced to a set of structure factors, compared closely with the set of calculated structure factors. Wuensch obtained improved values for the atomic coordinates, interatomic distances and bond angles.

Structural Classification

The structural classification of sulfides into which the tetrahedrite structure fits has evolved with the determination of numerous structures and with the development of order-disorder theory. Strock (1935) outlined a classification of crystal structures with defect lattices. The "structure theory" permitted only those structures composed of two or more interpenetrating lattices, each consisting of only one type atom with no empty points. Strock proposed the term "defect structures" to include those structures which do not fulfill the structure theory. The departures of defect structures from the theory are characterized by:

1. equivalent points not completely filled.
2. equivalent points occupied by different sorts of atoms.
3. a combination of 1 and 2.

Strock pointed out that structures having large atom stable frameworks (oxides, Si-O complexes, sulfides, tellurides, selenides, halogens) permit defects ranging from a perfectly ordered and filled lattice of small interstitial cations to completely random distribution of cations in the lattice. Defect lattices show all transitions from ideal solids to a dispersed state in which the lattice of one atom type is completely destroyed.

Berry (1943) pointed out that the sulpho-salts include

a wide variety of crystal structures. In attempting to find a more modern structural basis on which to classify them, instead of the traditional chemical grouping, he suggested that the only common denominator might be certain frequently occurring cell dimensions. Thus the numbers 4, 6, 8, 11, 15, and 19 Å were found to occur frequently in the sulpho-salts (Berry, 1943, p. 23). However, groupings according to these dimensions have no particular structural significance as do the classifications according to packing geometry proposed by Hiller (1953) and Ross (1957).

Hiller (1953) outlined a crystal-chemical classification of the sulfide, telluride and selenide minerals. He pointed out that the classification AB to AB_2 and so forth reflects nothing of the crystal-structure and bonding of the atoms. He asserted that a crystal-chemical classification can be constructed from either one of two points of view:

1. a classification on the basis of the chemical bonding of the lattice-forming atoms.
2. a classification based on the static geometry with coordination numbers and polyhedron arrangement.

Hiller indicated that these two points of view would often show parallels and are not necessarily contradictory. However, witness the structural similarity but bonding differences in NaCl and PbS. In essence, Hiller's

classification was based first on the kind of sulfur lattice and subdivided on the basis of coordination of metal atoms in the sulfur lattice.

Ross (1957) summarized the data basic to a structural classification of the sulfide minerals. Such a classification is based on similarities of packing geometry and of component metals in chemical bonding. The classification is divided into two groups on the basis of cubic or hexagonal closest packing of the sulfur atoms. Under these headings are grouped "type structures" based on differences in coordination of metal atoms in the sulfur lattice. "Simple" structures contain one component metal. "Complex derivative" structures are derived by ordering two or more metals in sites occupied by one metal in the simple structure. "Defect" structures deviate from the ideal composition because of an excess or deficiency of metal or sulfur. "Layered" and "chain" structures are grouped as separate types.

Tetrahedrite-tennantite is classified as a complex defect derivative structure of the basic sphalerite type-structure. Both have cubic closest-packed sulfur atoms. Further, both structures have all tetrahedral voids filled by metal atoms. The geometrical differences in the tetrahedrite structure derive from ordered positions of more than one metal and from "defects" in the packing

of sulfurs, such as the large holes caused by missing sulfurs.

Order-Disorder

Buerger (1949) discussed thermodynamic considerations basic to the order-disorder concept and outlined the kinds of disorder in crystals of non-metals. Of the four recognized kinds (interchange disorder, interstitial disorder, orientation disorder and distortional disorder), interchange disorder and interstitial disorder are important in sulfides. Disorder is a kind of disarray of atoms produced by temperature energy. As an illustration of interchange disorder, consider a crystal of three components ABC. There are two possible arrangements of atoms. (1) The atoms may be in classical order. (2) Some A atoms may be interchanged with B atoms. If the first arrangement has minimal internal or bond energy, the second arrangement has higher energy which can be supplied by heat. Except at absolute zero, some A is always interchanging with B. With increasing T, the amount of interchange of A and B increases until A and B are randomly oriented on positions ideally occupied by A or B. The crystal is then completely disordered with respect to A and B.

Buerger discussed in a general manner some crys-

tallographic implications of the order-disorder relationship. Complete disorder with respect to atoms A and B produces a hybridized atom, with resultant higher symmetry operations for the crystal. Thus, the sequence A B A B A B with disordering and resultant hybridization of A and B becomes H H H H H H with period one-half t. Diagrammatically, the following conditions may be expected in crystals with order-disorder possibilities:

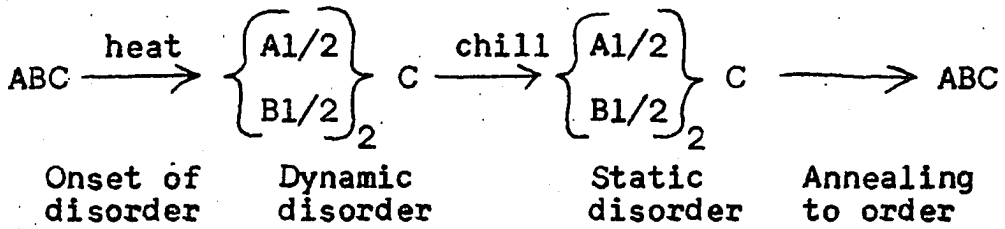

Frueh (1950)asserted that sulfides are good choices for continuation of work by metallurgists and physicists on disorder in intermetallic compounds. Sulfides have a sub-metallic character, contain atoms of similar size and properties and commonly show evidence of exsolution textures, indicating diffusion in the solid state.

Frueh (1958) discussed the application of the disorder relationship in sulfides to geologic thermometry. Polymorphic transitions have long been used as temperature indicators, but less attention has been given to high-low inversions in ore minerals. X-ray crystallographic criteria may be applied to answer the questions:

1. Which crystalline modification is now present?
2. Did this form or another crystallize originally?
3. If it is not the original and there are more than two modifications, which did form first?

Reordered forms may be characterized by indistinct morphology or polycrystalline aggregates. X-ray crystallographic effects in pictures of single crystals may be (1) diffuseness of returned reflections due to small size of domains, (2) appearance of additional reflections due to more than one crystallographic orientation for ordered domains, (3) angular differences in crystallographic axes due to non-parallel alignment of domains because axes of ordered forms are not perfect multiples of axes of disordered forms.

Phase Relationships

Gaudin and Dicke (1939) synthesized many sulfides and sulfosalts including tetrahedrite-tennantite and studied the phase relationships under the microscope. In the Cu-Sb-S system, six phases were synthesized: covellite, chalcocite, chalcostibite, tetrahedrite, famatinite and stibnite. Though an excess of sulfur over the "ideal" formula A_3BS_3 occurs in tetrahedrite, the structure shows sulfur missing from the cubic closest-packed arrangement, suggesting tetrahedrite is a sulfur-deficient compound. The experimental results of Gaudin and Dicke suggest that the production of tetrahedrite is inhibited by excess

sulfur and favored by sufficient or deficient sulfur. The following sequences were obtained:

1. With excess S and increasing Cu:
   stibnite ⟶ famatinite ⟶ chalcocite
2. With sufficient S and increasing Cu:
   stibnite ⟶ chalcostibite ⟶ tetrahedrite ⟶ chalcocite
3. With decrease in S due to reaction with Fe of bomb:
   famatinite ⟶ tetrahedrite
4. With very deficient S:
   metal as exsolution blebs from tetrahedrite and other minerals.

In the Cu-As-S system, four phases were synthesized: realgar, orpiment, enargite, and tennantite. Relationships were rather similar to the Cu-Sb-S system. The following sequences were obtained:

1. With excess S and increasing Cu:
   enargite ⟶ chalcocite
2. With deficient S and increasing Cu:
   tennantite ⟶ chalcocite

X-ray Diffraction Data

Little x-ray diffraction data has been published for the tetrahedrite series. Waldo (1935) and Harcourt (1942) published incomplete powder patterns for three specimens. Berry and Thompson (1962) reported observed intensities and d-spacings for powder patterns of two tetrahedrites and one tennantite. Wuensch (written communication, 1963) supplied indices for all his observed reflections as well

as the set of observed and calculated structure factors.

METHODS AND PROCEDURES

Natural Specimens

Seventy-five specimens of natural material were procured for investigation. Many of these proved to be misidentified specimens, most commonly confused with bournonite or chalcocite. Ores of massive sulfides as well as mineral specimens of euhedral crystals are included in the samples. Of the total, 40 are foreign and 14 U.S. occurrences, with localities in 14 countries and seven states represented. (table 1). The majority of specimens were obtained from the U.S. National Museum; the Chicago Museum of Natural History; and the University of Cincinnati. Additional specimens were collected from mines and private individuals.

Separatory Techniques. It was desirable to effect a clean separation of tetrahedrite-tennantite from some specimens in order to obtain reliable chemical and x-ray data. Commonly, the "contaminating" minerals were chalcopyrite, pyrite, bornite, sphalerite, and galena, as well as the gangue minerals quartz, calcite, siderite, barite and occasional hematite and malachite. Specimens were crushed, sized, and separated by means of Clerici solution and the Frantz Isodynamic Separator. Rosenblum

TABLE 1

LOCALITIES OF NATURAL SPECIMENS

Spec. #	Name	X	C	P[E]	Locality	Obtained
					Foreign	
46455	td	X	C		Tadergount, Constantine, Algeria	U.S. Nat. Museum
M11654	td	X	C	P	Pulganbar, New South Wales, Australia	Chicago Museum
103164	td	X	C	P	Pulacaya Mine, Huanchaca, Bolivia	U.S. Nat. Museum
66819	td	X	C		Huanchaca, Bolivia	U.S. Nat. Museum
C4995	td	X	C		Animas Mine, Chocaya, Bolivia	U.S. Nat. Museum
R1110	tn	X	C	P	Sherbrooke Co., Canada	U.S. Nat. Museum
96332	td	X	C	P	O'Brien Mine, Cobalt, Ontario, Canada	U.S. Nat. Museum
Wedge 1	td	X	C		Bathurst Dist., New Brunswick, Canada	R.A. Jones
Wedge 2	td			P	Bathurst Dist., New Brunswick, Canada	R.A. Jones
R1089	tn	X	C		Braden Copper Mines, Chile	U.S. Nat. Museum
C819	tn	X	C		Rancagua, Chile	U.S. Nat. Museum
6997				P	Elgin, Chile	U.S. Nat. Museum
115110	td	X	C		Rudnany, near Spisska, Nova Ves, E. Slovakia, Czechoslovakia	U.S. Nat. Museum
M609	tn	X	C	P	Zips, Czechoslovakia	Chicago Museum
103658	td	X	C		Cornwall, England	U.S. Nat. Museum
M354	td	X	C		Cornwall, England	Chicago Museum
C5262	td	X	C	P	Georg Mine, Wilbroth, Horhausen, Westerwald, Germany	U.S. Nat. Museum
104553	td	X	C		Clausthal, Harz, Germany.	U.S. Nat. Museum
M631				P	Dillenburg, Nassau, Germany	Chicago Museum
M728				P	Kapnik, Hungary	Chicago Museum
D148 A877	td	X	C		Kapnik, Hungary	U. of Cincinnati
D148 A1772	td	X	C		Kapnik, Hungary	U. of Cincinnati

TABLE 1 (continued)

Spec. #	Name	X	C	P	Locality	Obtained
61823	tn	X	C	P	Ikuno, Japan	U.S. Nat. Museum
61901				P	Migusawa (Ugo), Japan	U.S. Nat. Museum
103201	tn	X	C		Zenigame-Zawa Mine, Hokkaido, Japan	U.S. Nat. Museum
90864				P	Tsubaki, Akita-Ken, Japan	U.S. Nat. Museum
64941				P	Lolita Mine, Arispe, Sonora, Mexico	U.S. Nat. Museum
90942				P	Sultepec, Mexico	U.S. Nat. Museum
R11609		X			Bonanza Mine, Concepcion del Oro, Saltio, Mexico	U.S. Nat. Museum
92347	td	X	C		Urique, Chihuahua, Mexico	U.S. Nat. Museum
64981		X		P	Cueva Santa Mine, Attar Dist., Sonora, Mexico	U.S. Nat. Museum
M18004				P	Mina Bonanza, Concepcion del Oro, Zecatecas, Mexico	Chicago Museum
108759	tn	X	C	P	Carlos Francisco, 1200 level, Casapalca, Peru	U.S. Nat. Museum
90875	td	X	C		Peru	U.S. Nat. Museum
98503	td	X	C		El Rayo Mine, Casapalca, Peru	U.S. Nat. Museum
90776	tn	X	C	P	Alpamina Mine, Ymbi, Peru	U.S. Nat. Museum
No # B	td	X	C	P	Huachocolpa, Peru	U.S. Nat. Museum
R1096	tn	X	C	P	Yanli, Peru	U.S. Nat. Museum
D148 A315	td	X	C		Tasmania	U. of Cincinnati
M14982	td	X	C		Gornig, Vasuf, Bosnia, Yugoslavia	Chicago Museum
					U. S.	
51746				P	Hightower Mine, Cleburne Co., Alabama	U.S. Nat. Museum
91562				P	Copper Mt., Prince of Wales Island, Alaska	U.S. Nat. Museum

TABLE 1 (continued)

Spec. #	Name	X	C	P	Locality	Obtained
14252	tn	X	C	P	Arizona	U.S. Nat. Museum
115256	td	X	C	P	Cole Mine, Bisbee, Arizona	U.S. Nat. Museum
74553	td	X	C	P	Royal Tiger Mine, Silverton, Colorado	U.S. Nat. Museum
86172				P	Della S. Mine, Aspen, Colorado	U.S. Nat. Museum
19174		X		P	Moose Mine, Park Co., Colorado	U.S. Nat. Museum
39411				P	Moose Mine, Park Co., Colorado	U.S. Nat. Museum
M14761	tn	X	C	P	Yankee Girl Mine, Ouray Co., Colorado	Chicago Museum
Sunshine 3	td	X	C	P	Sunshine Mine, Kellogg, Idaho	Sunshine Mine
18267	td	X	C		Newburyport, Massachusetts	U.S. Nat. Museum
88118	td	X	C		Daly Judge Mine, Park City, Utah	U.S. Nat. Museum
Bingham	tn	X	C		Bingham, Utah	U. of Cincinnati
MB380	tn	X	C		Ophir, Utah	Chicago Museum

■ X x-rayed
C chemically analyzed
P polished section

(1958) gathered and tabulated data on the magnetic susceptibilities of about 50 minerals. These data were useful as a basis from which to work to find settings on the Frantz Separator which allowed for separation of a clean fraction of tetrahedrite-tennantite. By this method, contaminant was generally less than one percent (table 2). Even specimens of massive, fine-grained sulfides were separable. Only microscopic mineral intergrowths (such as tetrahedrite and bornite) proved inseparable by this method.

Polished Sections. About 45 polished sections were made from suitable material. Many of the specimens proved difficult to polish because of crustification textures, friability and differences in mineral hardnesses. Mountings were made in lucite thermo-plastic by means of the Buehler Press. Grinding and polishing was done according to standard procedures on the Sampson-Patmore Polisher (Sampson, 1949, 1956). Good quality reflective surfaces without relief were achieved. Photomicrographs of the polished sections were taken using the Zeiss Attachment Camera for Photomicrographs mounted on a Baush and Lomb reflecting microscope. The photos were taken with 35 mm Panatomic X film and printed on F5 paper.

Synthetics.

Nine varieties of synthesized tetrahedrite-tennantite

TABLE 2

DATA FROM GRAVIMETRIC AND MAGNETIC MINERAL SEPARATIONS

Spec. #	Discarded Fraction Clerici Sol'n	Discarded Fraction Magnetic Separator	Recovered Fraction
92347			td, (trace qtz)
66819			td, (about 1% qtz and sp, trace gn)
91755			td, (conchoidal grains, granular mass
Sunshine 3	qtz, calc, td	py (euhedral), td	td
Bingham	sp, tn, qtz, py	py, sp, tn, gn, qtz	tn, (trace sp)
C819	tn, qtz, ccp	ccp, tn, qtz	tn, (about 1/2% ccp)
88118	td, sp, qtz	gn, td, qtz, sp, py	td
C4995	qtz, td	td, qtz, py	td
46455	calc, td, qtz	td, qtz, calc	td (total contam. less than 1%)
M14982	qtz, td, sp	trace qtz	td
R1096	sp, tn		tn
64981	qtz, tn	gn, tn	tn
No # B	qtz, td, ccp	gn, td	td
Wedge 1		td, ccp, qtz	td (attached ccp less than 1%)
6997	qtz, bn		td and bn intergrowth
90864	qtz, py-td		td and py mixture

contain various amounts of Cu, Fe, Zn, Ag, Sb, and As. These were prepared from stoichiometric amounts of reagent grade CuS, reduced iron powder, ZnS, sulfur, antimony powder, powdered arsenic, and silver, weighed to 0.0001 g. on a chain or Sartorius balance. These dry chemicals were compressed into pellets under 50,000 psi and sealed in evacuated Vycor silica glass tubing. The specimens were synthesized just below 600° C. over a 16-24 hour interval and quenched in cold water immediately upon removal from the furnace. X-ray diffraction patterns verified formation of the single mineral phase. The results are tabulated in Table 3.

GE XRD-5 and Diffractometer.

All specimens were x-rayed by the powder method to identify phases and obtain structural data. Samples were taken from among the mineral separates or hand-picked from specimens and investigated under the binocular microscope for purity. Despite precautions, some x-ray diffraction powder patterns showed contamination by other minerals. Samples were scanned with Ni-filtered Cu radiation ($K\alpha = 1.54050$ Å) at 16 ma and 40 kv. Recordings were made through 15° to 65° 2θ angles at 2°/minute.

Peak positions were recorded as accurately as

TABLE 3

DATA FROM MINERAL SYNTHESIS

Spec. #	Composition	Temp. °C	Results
S1-1	$Cu_{11.8}Fe_{0.3}Sb_4S_{13}$	500 - 650	Solid at 500, melted at 650. Porous with crystal-coated vugs. Trace of red (S?) coating on tube.
S1-2	"	540 - 552	Pellet solid with tiny crystals on surface.
S1-3	"	584 - 600	Solid at 600, melted at 618.
S2	$Cu_9Fe_3Sb_4S_{13}$	560 - 614	Pellets solid with fine-grained crystalline surface.
S3-1	$Cu_{10}Fe_2As_4S_{13}$	560 - 614	Pellets solid. Slight yellow and red tube residue possibly orpiment and realgar.
S3-2	"	674 - 684	Pellet solid. (Cooled slowly).
S4	$Cu_{10}Zn_2Sb_4S_{13}$	560 - 614	Pellets partially fused together. Pitted surface.
S5-1	$Cu_{11}Zn_1As_4S_{13}$	560 - 614	Pellet deformed. Slight yellow and red tube residue may be orpiment and realgar.
S5-2	"	642 --654 674 - 684	Pellet solid. Pellet partially melted. (Cooled slowly).
S6	$Cu_9Ag_3Sb_2S_{13}$	580 - 590 635 max.	Pellets fused and deformed into one thick pellet. Very slight S film in tube.

TABLE 3 (continued)

Spec. #	Composition	Temp. °C	Results
S7	$Cu_8Ag_1Fe_3Sb_1As_3S_{13}$	580 - 590 635 max.	Pellets solid and undeformed.
S8	$Cu_6Ag_2Fe_4Sb_3As_1S_{13}$		Pellets fused, bulged and porous.
S9	$Cu_8Fe_1Zn_3Sb_4S_{13}$		Pellets solid. (Anomalous - probably organized after temperature lowered from 635.

■ Specimens in furnace 16-24 hours; T controlled to ± 10°C.

possible to the second place (°2θ) and the observed intensity recorded. Peak intensities were computed as peak height times peak width at one-half the height. The most intense peak (I_1) was picked as unity ($I_1 = 100$) and other peaks logged as I/I_1. From the reflection angles (°2θ) the d-spacings (interplanar spacings) in angstrom units were computed according to Bragg's Law:

$$(1) \qquad n\lambda = 2d\sin\theta$$

The (440) and (622) reflections are sharp, intense peaks lying in a reliable region for the goniometer at 50° to 60° 2θ, respectively. These two peaks were slow-scanned at 0.2°/minute to obtain an accurate value for the unit cell edge (a_o) according to the relationship:

$$(2) \qquad d = \frac{a_o}{\sqrt{h^2+k^2+l^2}}$$

For the isometric system, a body-centered cell such as in tetrahedrite has allowed Bragg reflections following the relationship:

$$(3) \qquad h^2+k^2+l^2 = \text{all even numbers}$$

The fit of each reflection with this scheme was checked by using d (computed in equation 1) and a good estimate of a_o in equation 2. An a_o for each relection was computed according to equation 2. These were graphed versus 2θ (fig. 1) and compared with a_o from the slow-scanned peaks to arrive at an a_o reliable generally to

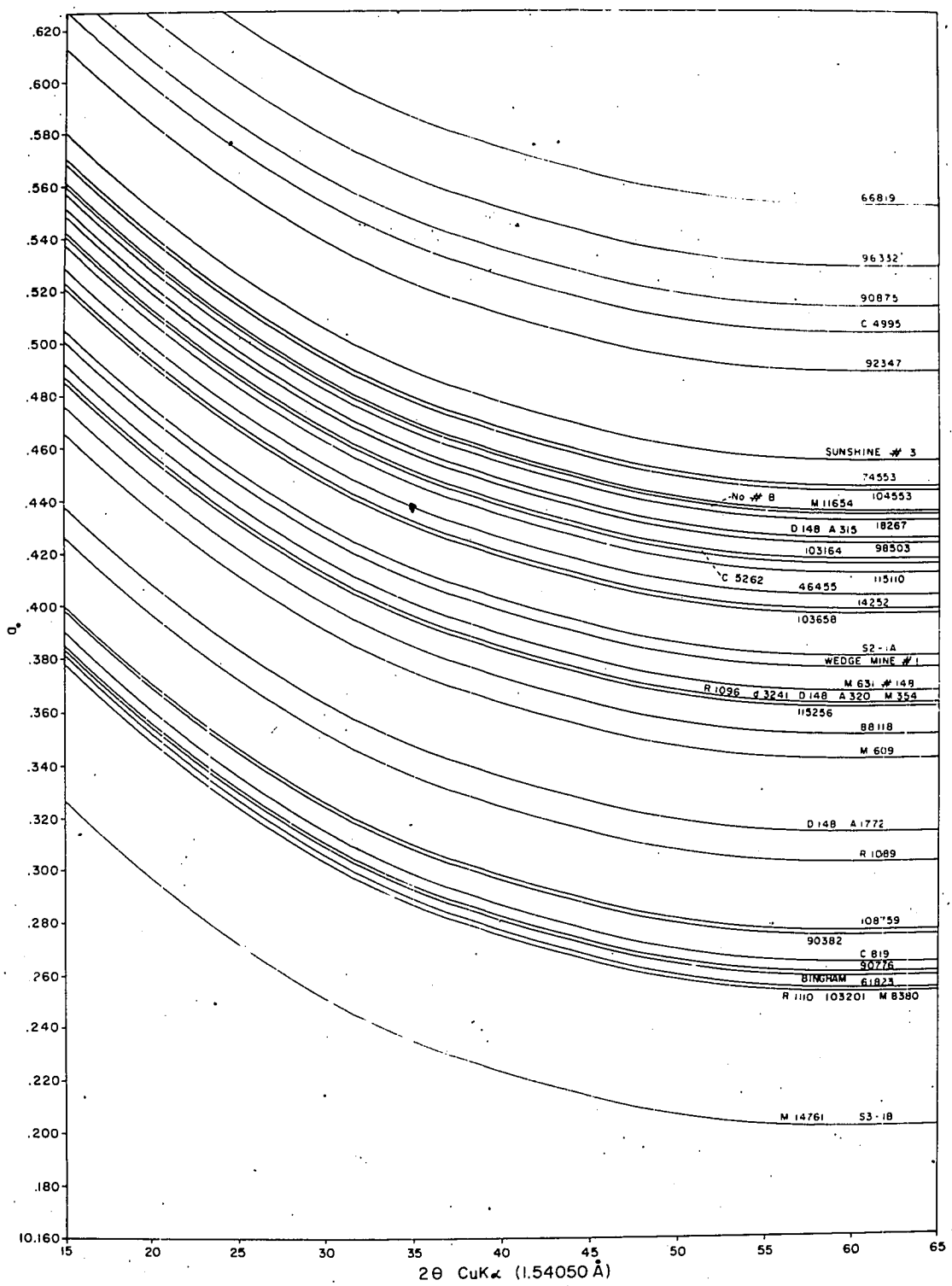

Figure 1. Graph of a_o with 2θ for all specimens.

$\pm$ 0.005 Å. Values for all specimens calculated by means of the IBM 1620 Data Processing System appear in Appendix C.

Nonius-Guinier Camera

Film strips were taken of several powder samples by means of the Nonius-Guinier camera. The camera was mounted on a Picker x-ray unit with Co tube run at about 15 ma, 40 kv. Exposures were about 15 hours. Very weak reflections not detectable by the diffractometer were recorded on the film strips.

X-ray Fluorescence Analysis.

Specimens were analyzed by the x-ray fluorescence method with LiF analyzing crystal and Cr tube run at 30 ma and 40 kv (fig. 2). The nine synthetic specimens were used as standards (table 4). Standard curves were drawn for each element on the basis of peak intensity versus atomic percent for all usable peaks (fig. 3, 4, 5, 6). The elements Bi, Hg and Pb were treated on a semi-quantitative basis.

STRUCTURE

Machatschki (1928) made the first determination of the structure of tetrahedrite (fahlerz) from a specimen

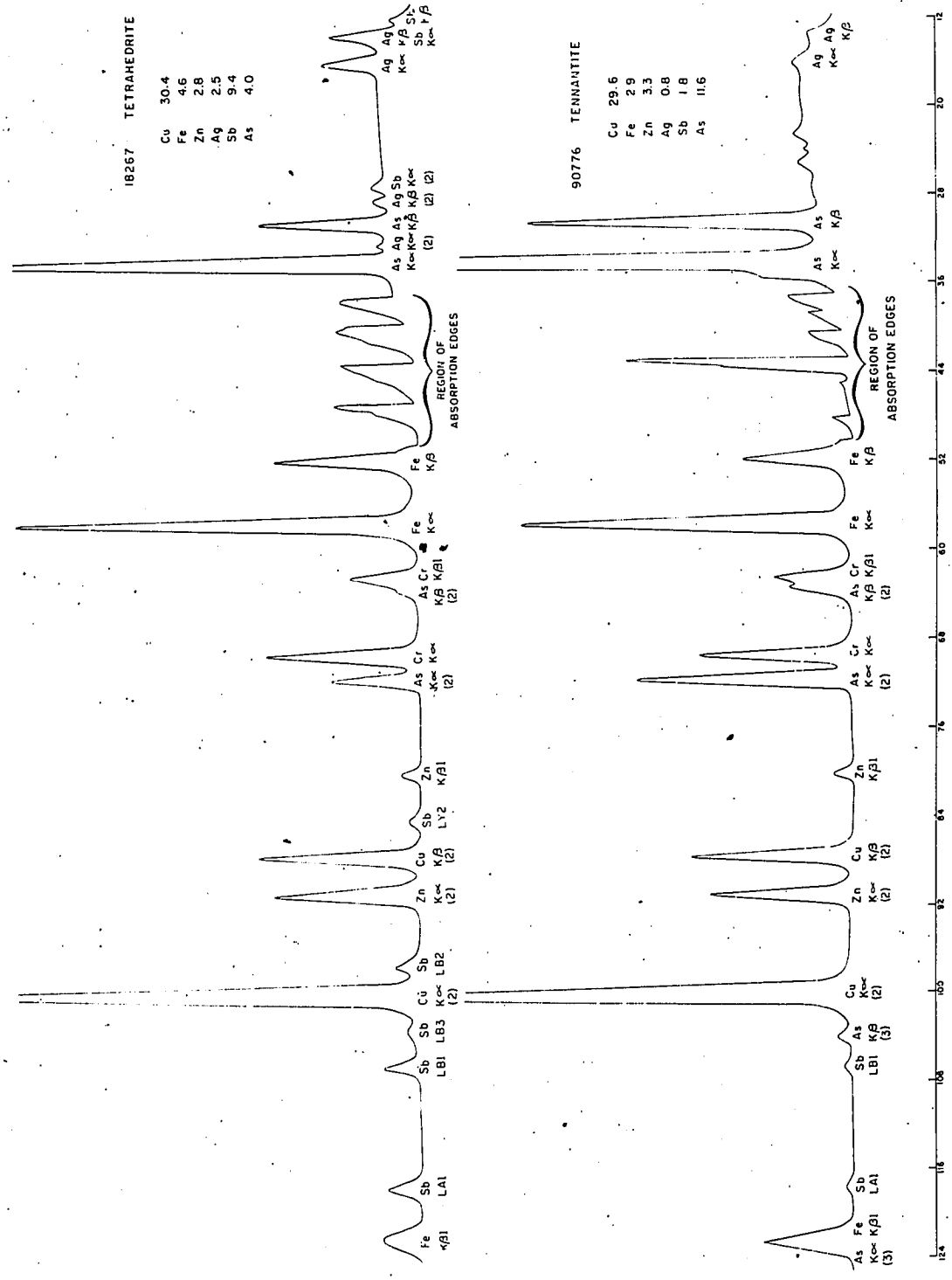

Figure 2. X-ray fluorescence patterns for tetrahedrite and tennantite.

TABLE 4

COMPOSITION OF STANDARDS FOR X-RAY FLUORESCENCE ANALYSIS

	S1-1		S2-1		S3-1		S4-1		S5-1	
	at. %	wt. %	at. %	wt. %	at. %	wt. %	at. %	wt. %	at. %	wt. %
Cu	40.5	44.8	31.0	34.7	34.4	43.4	34.4	38.0	37.9	47.1
Fe	0.8	0.8	10.3	10.1	6.8	7.6	.....	.....	.....	.....
Zn	....	.....	.....	.....	.....	.....	..6.8	7.8	3.4	4.4
Ag	....	.....	.....	.....	.....	.....	.....	.....	.....	.....
Sb	13.7	29.2	13.7	29.6	.....	.....	13.7	29.1	.....	.....
As	....	.....	.....	.....	13.7	20.4	.....	.....	13.7	20.2
S	44.8	25.0	44.8	25.3	44.8	28.4	44.8	24.9	44.8	28.1
Total	99.8	99.8	99.8	99.7	99.7	99.8	99.7	99.8	99.8	99.8

	S6		S7		S8		S9	
	at. %	wt. %	at. %	wt. %	at. %	wt. %	at. %	wt. %
Cu	31.0	33.5	27.5	32.8	20.6	22.7	27.5	30.5
Fe	.....	.....	10.3	10.8	13.7	13.3	3.4	3.3
Zn	.....	.....	.....	.....	.....	.....	10.3	11.7
Ag	10.3	18.9	3.4	6.9	6.8	12.8	.....	.....
Sb	6.8	14.2	3.4	7.8	10.3	21.7	13.7	29.2
As	6.8	8.7	10.3	14.5	3.4	4.4	.....	.....
S	44.8	24.4	44.8	26.9	44.8	24.8	44.8	25.0
Total	99.7	99.7	99.7	99.7	99.6	99.7	99.7	99.7

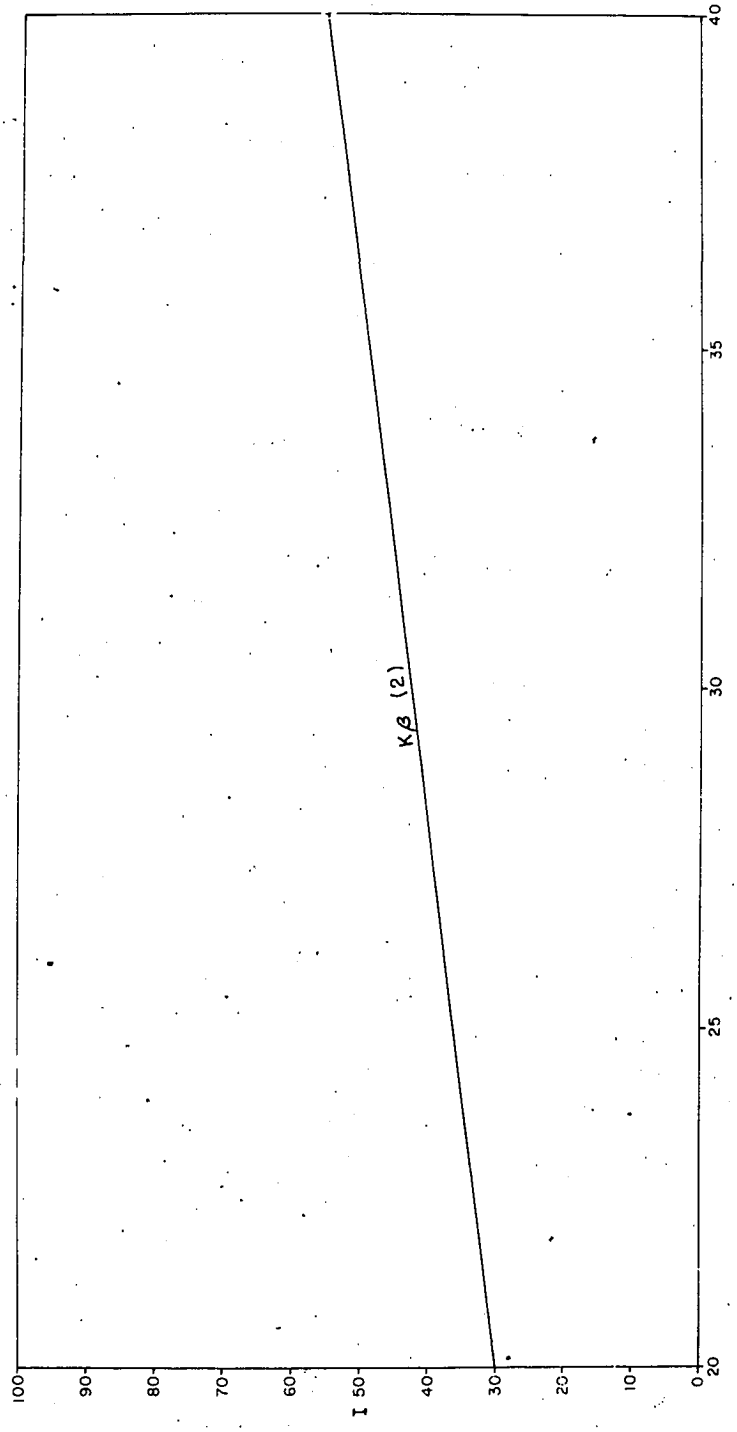

Figure 3. Standard curve for x-ray fluorescence analysis - Cu.

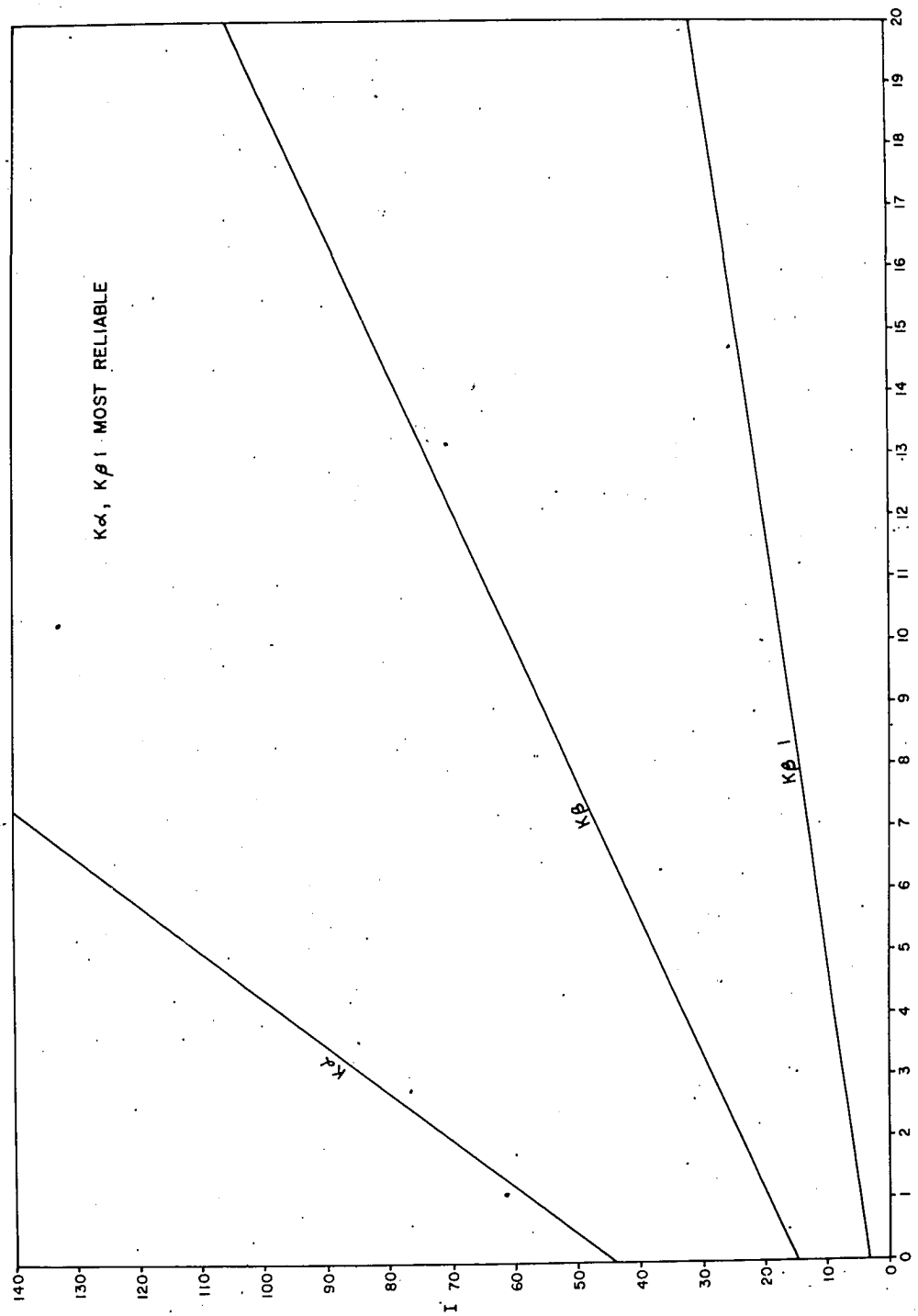

Figure 4. Standard curves for x-ray fluorescence analysis - Fe.

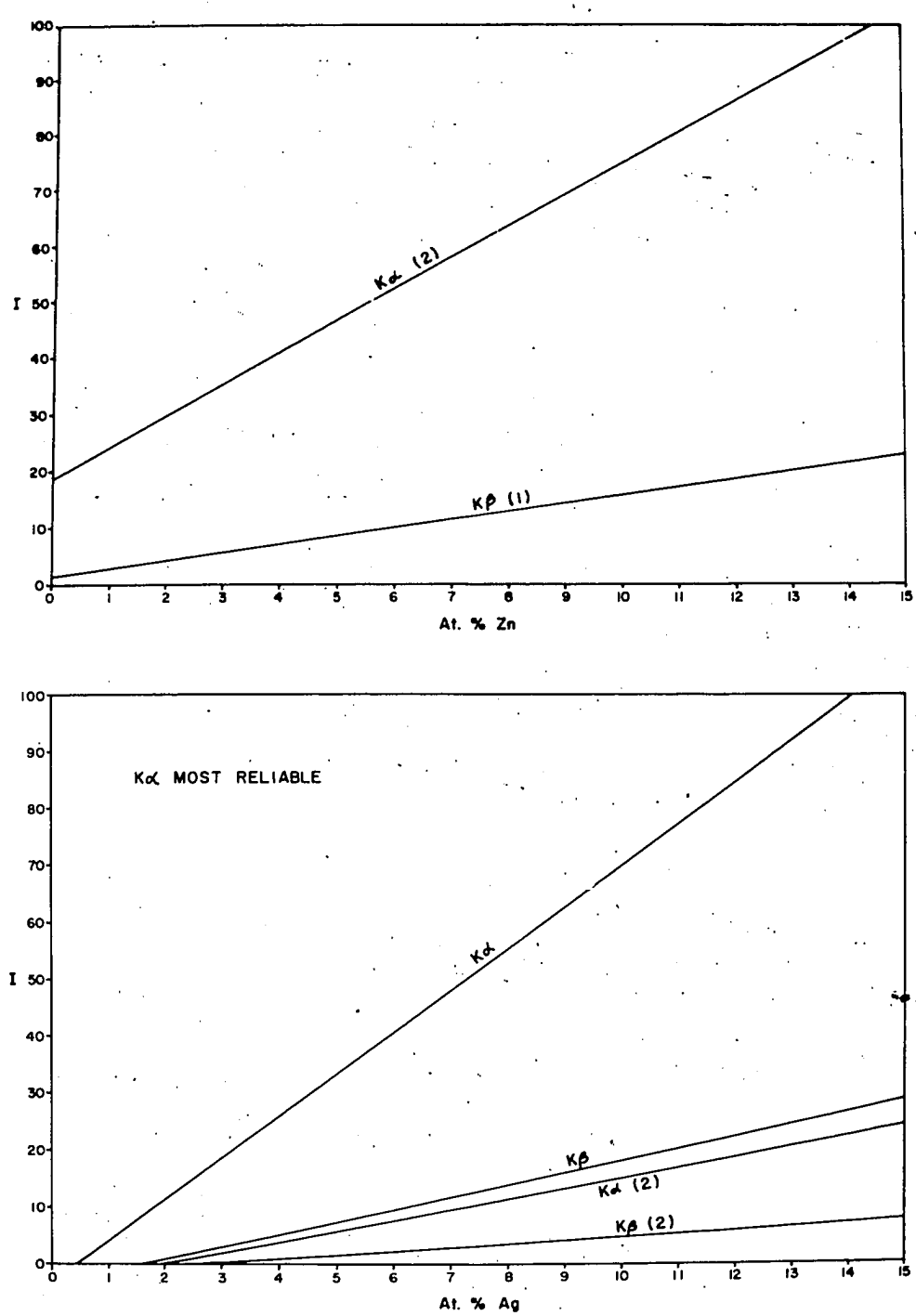

Figure 5. Standard curves for x-ray fluorescence analysis - Zn and Ag.

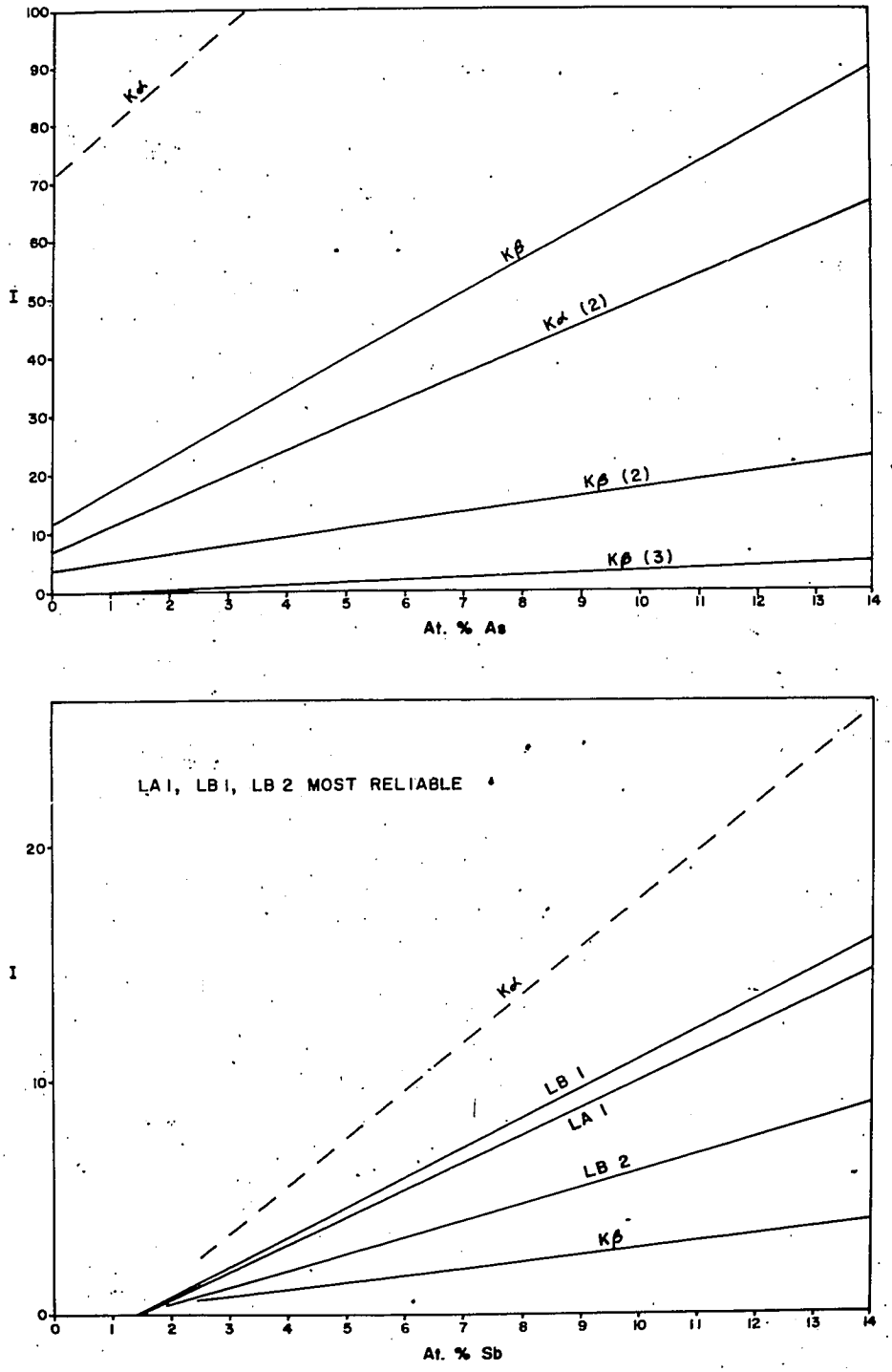

Figure 6. Standard curves for x-ray fluorescence analysis - As and Sb.

from Colquechaca, Bolivia. The structure was modified by Pauling and Neuman (1934) from a crystal of binnite from Binnenthal, Wallis, Switzerland. Wuensch (1963), using nearly pure $Cu_{12}Sb_4S_{13}$ from Horhausen, Westerwald, Germany, confirmed and refined the structure proposed by Pauling and Neuman.

The tetrahedrite series is composed of sulfur and metal atoms in closest packing, forming a lattice of large sulfur atoms and a superlattice of small metal atoms. Essentially, the sulfur lattice is composed of hexagonally closest-packed layers of sulfur atoms stacked in the cubic closest-packed manner (ABC, ABC). The metal atoms occupy all the tetrahedral interstitial sites between sulfur atoms to form the metal superlattice (fig. 7).

The general formula for the tetrahedrite series is $X_{12}Y_4S_{13}$, where X is always predominantly Cu, with lesser amounts of Fe, Zn, Ag, Pb, Hg, Ni and Co. In the Y position, Sb or As always predominate, but some Bi is present in some instances. The atoms Sb, As and Bi are ordered in tetrahedral sites as shown in Figure 7. In the structure, each Y atom forms an apex of a large tetrahedral hole two sulfur layers deep, brought about by four missing sulfur atoms. In each such hole, translated one-half layer distance out of position, a sulfur

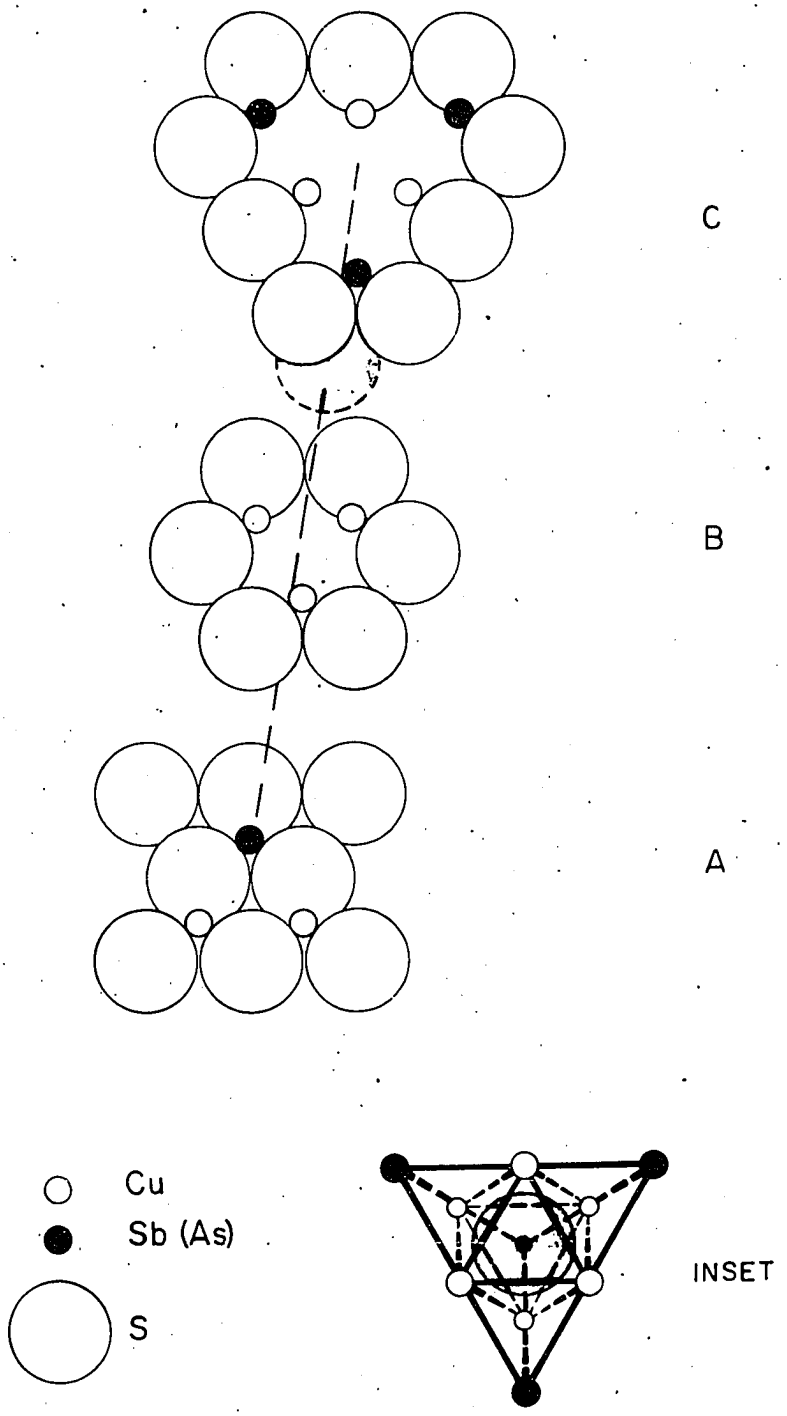

Figure 7. Stacking of the tetrahedrite series.

atom coordinates with six X atoms in their normal positions. The six apices of the resultant octahedron coincide with the midpoints of the edges of the large tetrahedral hole (fig. 7, inset). Thus each hole has only three missing sulfur atoms.

The unit cell is body-centered with symmetry $I\bar{4}3m$ (fig. 8). The following values for the atomic coordinates were obtained by Wuensch (1963):

Sb	in	8c	xxx, etc.	$x = 0.2682 \pm 0.0002$
Cu-I	in	12d	½¼0, etc.	
Cu-II	in	12e	x00, etc.	$x = 0.212(7) \pm 0.0008$
S-I	in	24g	xxz, etc.	$x = 0.115(3) \pm 0.0007$ $z = 0.360(3) \pm 0.0009$
S-II	in	2a	000	

The contents of this large cell are $2(Cu_{12}Sb_4S_{13})$ or 58 atoms. For the pure As-end member (tennantite) containing only the elements Cu, As and S, the cell includes 26 S atoms - 24 S-I and 2 S-II; 24 Cu atoms - 12 Cu-I and 12 Cu-II; and 8 As atoms. Each S-I atom is surrounded by four metal atoms (2 Cu-I, 1 Cu-II, 1 As), forming a tetrahedron, and each S-II atom is surrounded by 6 Cu-II, forming an octahedron. Each tetrahedron is linked to other tetrahedra and to the apex of an octahedron. Each apex of an octahedron is linked to two tetrahedra. The resulting polyhedra structure is an oversimplification, since the picture is complicated by

the three-fold coordination of As and Cu-II with sulfur atoms. The coordinations of all atoms in the structure are:

S-II	with respect to	Cu-II	6
S-I	with respect to	Cu-II	1
S-I	with respect to	Cu-I	2
S-I	with respect to	As	1
Cu-II	with respect to	S-II	1
Cu-II	with respect to	S-I	2
Cu-I	with respect to	S-I	4
As	with respect to	S-I	3

Wuensch (1963) found the following interatomic distances and bond angles:

> Cu-I to S-I 2.343 Å with bond angle 110° 47'. This is close to a regular tetrahedron.
>
> Cu-II to S-I 2.292 Å and to S-II 2.210 Å. This triangular planar group of four atoms lies in the (110) symmetry planes of the cell.
>
> S-I to Sb 2.436 Å with bond angle S-I to Sb to S-I 95° 18'. This is a trigonal pyramid with Sb at the apex.

An octahedron is at the center of the cubic cell and a 1/8 octahedron at each of the eight corners, giving the cell two octahedra (fig. 8). The cell also contains 24 tetrahedra, 12 of them bonded to the apices of the central octahedron. The (111) plane of the cell is the direction of stacking of the hexagonally closest-packed sulfur layers. The center of the cell can be considered a large tetrahedrally-shaped hole caused by four sulfur atoms missing from the stacking arrangement. At the center of this space (center of the unit cell) is one S

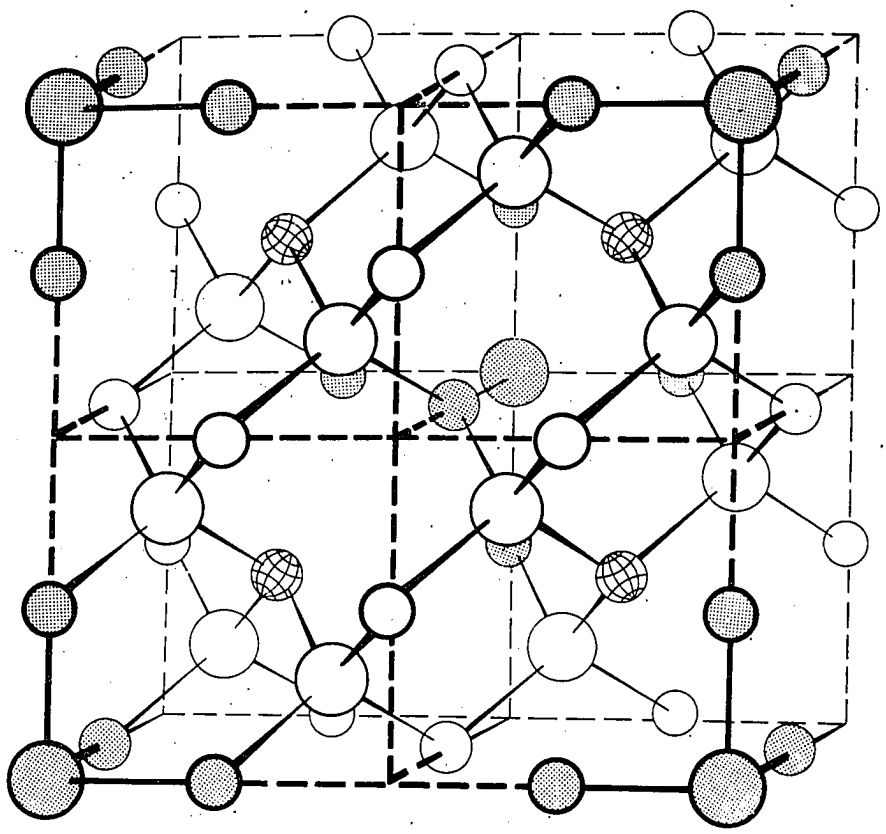

TETRAHEDRITE SERIES

Cu I

Cu II

Sb (As)

S I

S II

$(Cu, Fe, Zn, Ag)_{12} (Sb, As)_4 S_{13}$

$I\bar{4}3m$

$a_0 = 10.18 - 10.55$ Å

Figure 8. Tetrahedrite unit cell - foward half (after Pauling and Neuman, 1934).

atom. Each case of a S atom missing from the normal packing is associated with the bonding of an As to only three S atoms instead of four, as in the case of S-I. Thus four As atoms are arranged about each tetrahedral hole. Since the cell has eight S atoms missing from the normal packing with only two centered S atoms replacing them, space amounts to six missing S atoms.

CHEMISTRY

The many elements substituting in the tetrahedrite series show considerable differences in size and possible valence states. The implications of these differences in terms of limits of substitution of various atoms; associations of atoms of similar size; and the effect of certain substitutions on the tetrahedrite-tennantite isomorphous series have not previously been investigated. Chemical data presented here define limits of most substituting elements, show a segregation of large atoms into varieties in the tetrahedrite series, reveal compositional limitations in the isomorphous series and suggest limits of solid solution between As-Sb and Bi.

Analytical Results.

Thirty-eight specimens of the tetrahedrite series were analyzed by the x-ray fluorescence method ——

quantitatively for Cu, Fe, Zn, Ag, Sb and As; and semi-quantitatively for Bi, Pb and Hg. The results in atomic percents and weight percents and the calculated formulas are tabulated in Table 5. Of the total, 29 analyses are good formula fits and thus quantitatively reliable; 11 analyses are semi-quantitative. Twenty-two of the specimens are tetrahedrites; 13 are tennantites; six are bismuthian varieties.

Table 6 gives the minimum percent for Cu and the maximum percentages for other elements in the specimens analyzed in comparison with the figures in Dana's System of Mineralogy (Palache and others, p. 376). Generally the maximum percentages reported in this paper are lower and expected to be more accurate, since obviously contaminated analyses are omitted. Percentages especially for Pb and possibly Hg may still be high. In view of the antiquity of the analyses and in view of the ensuing discussion in this paper on element associations and limitations in the tetrahedrite series, the high values for Bi and Ag reported in tennantites in Dana are regarded as errors. Further, analyses reporting Ni and Co are old and rare and ought to be considered suspect unless confirmed.

Atom Sizes and Radius Ratios

Little previous work has been done to assess

TABLE 5

CHEMICAL ANALYSES

Tetrahedrites:

	(1) 104553		(2) 103164		(3) Sunshine 3		(4) 90875		(5) 74553	
	at. %	wt. %	at. %	wt. %	at. %	wt. %	at. %	wt. %	at. %	wt. %
Cu	30.4	35.5	28.9	35.9	32.0	36.3	26.5	29.7	33.5	36.7
Fe	4.0	4.2	2.9	3.0	5.2	5.1	2.7	2.7	trace	trace
Zn	3.3	4.1	2.5	3.0	1.7	2.0	3.4	3.9	7.9	8.9
Ag	2.5	4.7	1.7	3.6	3.4	6.6	7.0	13.1	1.7	3.2
As	trace	trace	1.2	1.5	1.3	1.8	2.0	2.7	1.8	2.2
Sb	11.2	24.7	10.5	24.6	10.4	22.4	10.5	22.2	9.5	20.3
Bi	.....	.....	.....	.....	.....	.....	.....	.....	.....	.....
Hg	.....	.....	.....	.....	.....	.....	trace	trace	.....	.....
Pb	.....	.....	.....	.....	.....	.....	.....	.....	1	4
Total[a]	51.4		47.7		54.0		52.1		55.4	
Contam.	.....	.....	.....	.....	.....	.....	sp	sp	sp	sp

	(6) D148 A877		(7) 92347		(8) 66819		(9) 18267		(10) 98503	
	at. %	wt. %	at. %	wt. %	at. %	wt. %	at. %	wt. %	at. %	wt. %
Cu	33.5	35.3	28.8	33.4	25.7	26.2	30.4	35.0	35.1	38.0
Fe	trace	trace	1.2	1.0	1.1	0.9	4.6	4.5	trace	trace
Zn	6.0	6.3	4.6	5.3	4.4	4.6	2.8	3.2	6.0	6.5
Ag	1.1	1.8	5.7	11.4	8.9	15.4	2.5	4.7	2.9	5.0
As	3.4	4.3	2.0	2.8	1.8	2.0	4.0	5.6	5.3	6.5
Sb	10.4	20.9	8.9	19.8	8.3	16.1	9.4	20.6	9.4	19.2
Bi	.....	.....	.....	.....	.....	.....	.....	.....	.....	.....
Hg	.....	.....	.....	.....	.....	.....	.....	.....	.....	.....
Pb	2	7	.....	.....	4	12	.....	.....	.....	.....
Total	54.4		51.2		54.2		53.7		58.7	
Contam.	.....	.....	.....	.....	sp?	sp?	.....	.....	.....	.....

TABLE 5 (continued)

	(11) No # B		(12) M14982		(13) 88118		(14) 103658		Tennantites: (15) 14252	
	at. %	wt. %	at. %	wt. %	at. %	wt. %	at. %	wt. %	at. %	wt. %
Cu	31.1	34.8	34.3	36.9	32.7	38.2	27.4	27.0	27.4	28.3
Fe	3.1	3.0	2.6	2.6	trace	trace	0.5	0.3	trace	trace
Zn	5.2	5.9	.....	.....	5.6	6.6	3.1	3.1	4.2	4.4
Ag	3.0	5.9	.....	.....	1.0	2.0	2.1	3.4	2.6	4.8
As	5.0	6.8	5.0	7.0	5.9	8.0	5.0	6.0	6.8	8.4
Sb	8.2	17.8	8.2	17.1	8.3	18.5	7.8	15.0	5.8	11.6
Bi	.....	.....	.....	.....	.....	.....	.....	.....	.....	.....
Hg	.....	.....	3.5	11.7	.....	.....	.....	.....	.....	.....
Pb	.....	.....	.....	.....	.....	.....	7.0	22.3	6.0	18.7
Total	55.6		53.6		53.5		52.9		52.8	
Contam.	.....	.....	.....	.....	.....	.....	gn	gn	.....	.....

	(16) R1096		(17) R1089		(18) 108759		(19) 90776		(20) C819	
	at. %	wt. %	at. %	wt. %	at. %	wt. %	at. %	wt. %	at. %	wt. %
Cu	28.0	32.4	30.3	37.0	34.7	40.5	29.6	38.7	34.4	40.2
Fe	8.3	8.4	8.8	9.6	trace	trace	2.9	3.1	1.7	1.7
Zn	5.7	6.9	0.7	0.8	5.6	6.6	3.3	4.6	3.6	4.1
Ag	0.8	1.3	.....	.....	.....	.....	0.8	1.5	0.9	2.0
As	9.1	12.2	11.8	27.5	12.6	17.6	11.6	18.0	13.6	18.4
Sb	5.6	12.2	3.5	8.0	3.8	8.5	1.8	4.3	3.0	6.9
Bi	.....	.....	.....	.....	.....	.....	.....	.....	.....	.....
Hg	.....	.....	.....	.....	.....	.....	.....	.....	.....	.....
Pb	.....	.....	.....	.....	.....	.....	.....	.....	.....	.....
Total	57.5		55.1		56.7		50.0		57.2	
Contam.	py,sp		py,ccp		qtz		ccp		.....	.....

TABLE 5 (continued)

	(21) M8380		(22) 103201		(23) R1110		(24) M14761		(25) Bingham	
	at. %	wt. %	at. %	wt. %	at. %	wt. %	at. %	wt. %	at. %	wt. %
Cu	25.7	35.0	32.7	41.7	23.3	29.7	35.2	40.4	32.8	41.1
Fe	12.5	14.7	trace	trace	10.7	11.9	2.1	2.0	1.1	1.1
Zn	0.2	0.4	5.9	7.6	2.1	2.6	2.9	3.2	5.2	6.6
Ag	.....	.....	.....	.....	.....	.....	2.2	4.0	0.9	2.2
As	11.1	17.6	13.3	20.2	11.5	17.0	12.0	16.3	13.7	20.4
Sb	.....	.....	.....	.....	.....	.....	.....	.....	trace	trace
Bi	.....	.....	.....	.....	.....	.....	.....	.....	.....	.....
Hg	.....	.....	.....	.....	.....	.....	.....	.....	.....	.....
Pb	0.5	1.5	0.5	1.5	2.5	9.9	2.0	7.7	.....	.....
Total	50.0		52.4		50.1		56.4		53.7	
Contam.	py,ccp, qtz		.....	.....	py		gn,bn(?)		sp(?)	

Bi Varieties:

	(26) Wedge 1		(27) 115110		(28) 46455		(29) C4995		Semi-quantitative: (30) M609
	at. %	wt. %	at. %	wt. %	at. %	wt. %	at. %	wt. %	at. % wt. %
Cu	35.2	39.8	30.4	33.5	37.5	40.7	29.6	29.8	25.7
Fe	3.3	3.4	7.3	7.0	3.7	3.6	4.8	4.2	4.0
Zn	3.4	4.0	trace	trace	trace	trace	trace	trace	trace
Ag	.....	.....	.....	.....	.....	.....	6.5	11.2	.....
As	3.6	4.6	4.5	5.8	9.8	20.0	0.3	0.4	5
Sb	8.7	18.6	8.3	17.5	2.0	2.6	8.7	16.6	7
Bi	1.0	3.8	1.0	3.7	1.3	4.9	4.5	14.8	2
Hg	.....	.....	2.0	7.2	1.0	3.5	.....	.....	1
Pb	.....	.....	.....	.....	.....	.....	.....	.....	.....
Total	55.2		53.5		55.3		54.4		45
Contam.	.....	.....	.....	.....			.....	.....	.....

TABLE 5 (continued)

	(31) 96332	(32) 115256	(33) M11654	(34) M354	(35) 61823
	at. %	at. %	at. %	at. %	at. %
Cu	13	30	11	27	30
Fe	3	2	19	3	6
Zn	trace	1	trace	3	trace
Ag	14	1	.....	1	.....
As	trace	3	1	4	13
Sb	8	10	5	6	1
Bi	6	.....	.....	.....	.....
Hg	.....	.....	1	.....	.....
Pb	.....	.....	.....	2	.....
Total	44	47	37	46	50
Contam.	.....	.....	py(high)	gn	qtz

	(36) D148 A315	(37) D148A1772	(38) C5262
	at. %	at. %	at. %
Cu	20	25	29
Fe	8	trace	3
Zn	trace	3	3
Ag	2	.....	trace
As	trace	3	trace
Sb	7	9	11
Bi	.....	.....	.....
Hg	.....	.....	.....
Pb	7	.....	.....
Total	37	40	46
Contam.	py(slight)	.....	.....

■ Total based on total atomic percent of X + Y = 55.1 in $X_{12}Y_4S_{13}$

TABLE 5 (continued)

Calculated formulas (S_{13} assumed) for analyses (1) - (29):

(1) $Cu_{8.8}Fe_{1.2}Zn_{1.0}Ag_{0.7}Sb_{3.2}$

(2) $Cu_{8.4}Fe_{0.8}Zn_{0.7}Ag_{0.5}Sb_{3.0}As_{0.3}$

(3) $Cu_{9.3}Fe_{1.5}Zn_{0.5}Ag_{1.0}Sb_{3.0}As_{0.4}$

(4) $Cu_{7.7}Fe_{0.8}Zn_{1.0}Ag_{2.0}Sb_{3.0}As_{0.6}$

(5) $Cu_{9.7}Zn_{2.3}Ag_{0.5}Pb_{0.3}Sb_{2.8}As_{0.5}$

(6) $Cu_{9.7}Zn_{1.7}Ag_{0.3}Pb_{0.6}Sb_{3.0}As_{1.0}$

(7) $Cu_{8.4}Fe_{0.3}Zn_{1.3}Ag_{1.7}Sb_{2.6}As_{0.6}$

(8) $Cu_{7.5}Fe_{0.3}Zn_{1.3}Ag_{2.6}Pb_{1.0}Sb_{2.4}As_{0.5}$

(9) $Cu_{8.8}Fe_{1.3}Zn_{0.8}Ag_{0.7}Sb_{2.7}As_{1.2}$

(10) $Cu_{10.2}Zn_{1.7}Ag_{0.8}Sb_{2.7}As_{1.5}$

(11) $Cu_{9.0}Fe_{0.9}Zn_{1.5}Ag_{0.9}Sb_{2.4}As_{1.5}$

(12) $Cu_{9.9}Fe_{0.8}Hg_{1.0}Sb_{2.4}As_{1.6}$

(13) $Cu_{9.5}Zn_{1.6}Ag_{0.3}Sb_{2.4}As_{1.7}$

(14) $Cu_{7.9}Fe_{0.1}Zn_{0.9}Ag_{0.6}Pb_{2.0}Sb_{2.3}As_{1.5}$

(15) $Cu_{7.9}Zn_{1.2}Ag_{0.8}Pb_{1.6}Sb_{1.7}As_{2.0}$

(16) $Cu_{8.1}Fe_{2.4}Zn_{1.7}Ag_{0.2}Sb_{1.6}As_{2.6}$

(17) $Cu_{8.8}Fe_{2.6}Zn_{0.2}Sb_{1.0}As_{3.4}$

(18) $Cu_{10.0}Zn_{1.6}Sb_{1.1}As_{3.7}$

(19) $Cu_{8.6}Fe_{0.8}Zn_{1.0}Ag_{0.2}Sb_{0.5}As_{3.4}$

(20) $Cu_{10.0}Fe_{0.5}Zn_{1.0}Ag_{0.3}Sb_{0.9}As_{3.9}$

(21) $Cu_{7.5}Fe_{3.6}Zn_{0.1}Pb_{0.1}As_{3.2}$

(22) $Cu_{9.5}Zn_{1.7}Pb_{0.1}As_{3.9}$

(23) $Cu_{6.8}Fe_{3.1}Zn_{0.6}Pb_{0.7}As_{3.3}$

(24) $Cu_{10.2}Fe_{0.6}Zn_{0.8}Ag_{0.6}Pb_{0.6}As_{3.5}$

(25) $Cu_{9.5}Fe_{0.3}Zn_{1.5}Ag_{0.3}As_{4.0}$

(26) $Cu_{10.2}Fe_{1.0}Zn_{1.0}Sb_{2.5}As_{1.0}Bi_{0.3}$

(27) $Cu_{8.8}Fe_{2.1}Hg_{0.6}Sb_{2.4}As_{1.3}Bi_{0.3}$

(28) $Cu_{10.9}Fe_{1.1}Hg_{0.3}Sb_{2.8}As_{0.6}Bi_{0.4}$

(29) $Cu_{8.6}Fe_{1.4}Ag_{1.9}Sb_{2.5}As_{0.1}Bi_{1.3}$

TABLE 6

MINIMUM PERCENT FOR Cu AND
MAXIMUM PERCENTAGES OF SUBSTITUTING ELEMENTS ■

	TETRAHEDRITE				TENNANTITE			
	This Paper			Dana	This Paper			Dana
	Spec. #	at. %	wt. %	wt. %	Spec. #	at. %	wt. %	wt. %
Cu	66819	25.7	26.2		R1110	23.3	29.7	
Fe	115110	7.3	7.0	13	61823	6	--	11
Zn	98503	6.0	6.5	8	103201	5.9	7.6	9
Ag	96332	14?	--					
	66819	8.9	15.4	18	14252	2.5	4.8	14
Hg	M14982	3.5?	11.7?	17	--	none	none	--
Pb	66819	4?	12?	16?	14252	6?	18?	4?
Bi	96332	6	--	4	46455	1.3	4.9	13
Ni	--	none	none	4	--	none	none	--
Co	--	none	none	4	--	none	none	1

■ Analyses this paper obviously biased by contamination omitted.

quantitatively what limitations might apply to substitution of constituent elements for one another in the tetrahedrite series. From radius ratio considerations, only certain of the elements are "allowed" in tetrahedral voids in a cubic closest-packed arrangement of sulfur atoms.

If simplified, the tetrahedrite structure consists of sulfur and metal atoms tetrahedrally coordinated with each other. From geometrical considerations, the radius ratio limits for the 4:4 coordinations are 0.225 - 0.414 (Hurlbut, 1959, p. 196). This means that tetrahedral coordination has maximum stability when the cation/anion ratio lies within this range. If the ratio is larger, we approach the lower limiting value of octahedral coordination; if smaller, we approach the upper limiting value of triangular coordination.

The assignment of specific radii to atoms is difficult, since many variables are involved. The size of an atom is affected by its coordination number as well as the electrostatic forces between atoms (Azaroff, 1960, p. 80). Atomic radii of various elements have been determined from strongly ionic, covalent or metallic substances. The sub-metallic character of the tetrahedrite series means that it has bonding of more than one type, in common with other sulfides. Bonding has both a covalent and ionic

character and thus is partly metallic. In view of the complex coordination and valence picture in the tetrahedrite series, the radii in Table 7 (Pauling, 1948, p. 346, Azaroff, 1960, p. 438) are crude approximations meant to afford a qualitative look at the consequences of large size discrepancies between atoms.

TABLE 7

RADIUS RATIOS FOR CONSTITUENT ELEMENTS OF THE TETRAHEDRITE SERIES

■ r/S^{-2} within range 0.225 - 0.414

element	valence	radius	radius ratio
As	+5	0.46	0.250
As	+3	0.58	0.315
Sb	+5	0.62	0.336
Fe	+3	0.64	0.347
Cu	+2	0.72	0.391
Fe	+2	0.74	0.402
Bi	+5	0.74	0.402
Zn	+2	0.74	0.402
Sb	+3	0.76	0.413

■ r/S^{-2} exceeds 0.414

element	valence	radius	radius ratio
Pb	+4	0.84	0.456
Ag	+2	0.89	0.483
Cu	+1	0.96	0.521
Bi	+3	0.96	0.521
Hg	+2	1.10	0.597
Pb	+2	1.20	0.652
Ag	+1	1.26	0.684

■ S^{-2} taken as 1.84

These data show several illuminating groupings. Divalent Cu, Fe and Zn are closely similar in size,

differing in radius by only three percent, and ought to substitute easily for one another. Trivalent As and Sb, which apparently randomize in ordered positions in the tetrahedrite structure, differ greatly in size by 25 percent, with Sb at about the upper limit for tetrahedral coordination. The association of larger atoms with tetrahedrite, rather than tennantite, may be anticipated. Although Pb is a ubiquitous element as shown by the frequent association of galena with the tetrahedrite series, it is a fairly infrequent substituting atom. Analyses in Table 5 show only seven specimens with Pb which is not explained by contamination, and only four of these have Pb greater than one atomic percent. Contrastingly, Ag was present in 25 of the specimens in amounts up to 8.9 and possibly 14 atomic percent. The element Pb may either be too large or have too high a valency to be an important constituent. Silver may then be divalent rather than the large monovalent atom. These radius ratio considerations anticipate the segregation of large atoms in the tetrahedrite series as well as the possibility of limited solid solution between tetrahedrite and tennantite.

Element Associations and Limitations

Chemical analyses disclose probable near upper limits in the tetrahedrite series for the important substituting

elements Ag, Fe and Zn. In addition, a tendency for a fixed content of Fe plus Zn, at least in the tennantite field, is strongly suggested. High amounts of the larger elements Ag, Bi and Hg associate preferentially with Sb in the tetrahedrite field.

A gap in the As-Sb solid solution series is indicated by analyses of natural specimens in this study, and supported by the best analyses from the literature. The gap coincides with a low-temperature unmixing field for members rich in Ag. This relationship is also supported by x-ray diffraction data and by relationships in polished sections. In addition, solid solution between As and Bi is apparently quite restricted, but more extensive between Sb and Bi.

Ag. Figure 9 illustrates the distribution of Ag in the tetrahedrite series. Tennantites are restricted to about 2.5 atomic percent Ag (14252). Above this value, specimens are tetrahedrites with eight or more atomic percent Sb. Of the 25 Ag-bearing specimens analyzed, 19 are tetrahedrites and only 6 tennantites. Of a total of 21 tetrahedrites analyzed, only 2 contain no Ag. In Ag-bearing tetrahedrites, Ag averages 3.8 atomic percent; in Ag-bearing tennantites, Ag averages only 1.3 atomic percent. In summation, Ag is associated with tetrahedrites in quantity and frequency of occurrence.

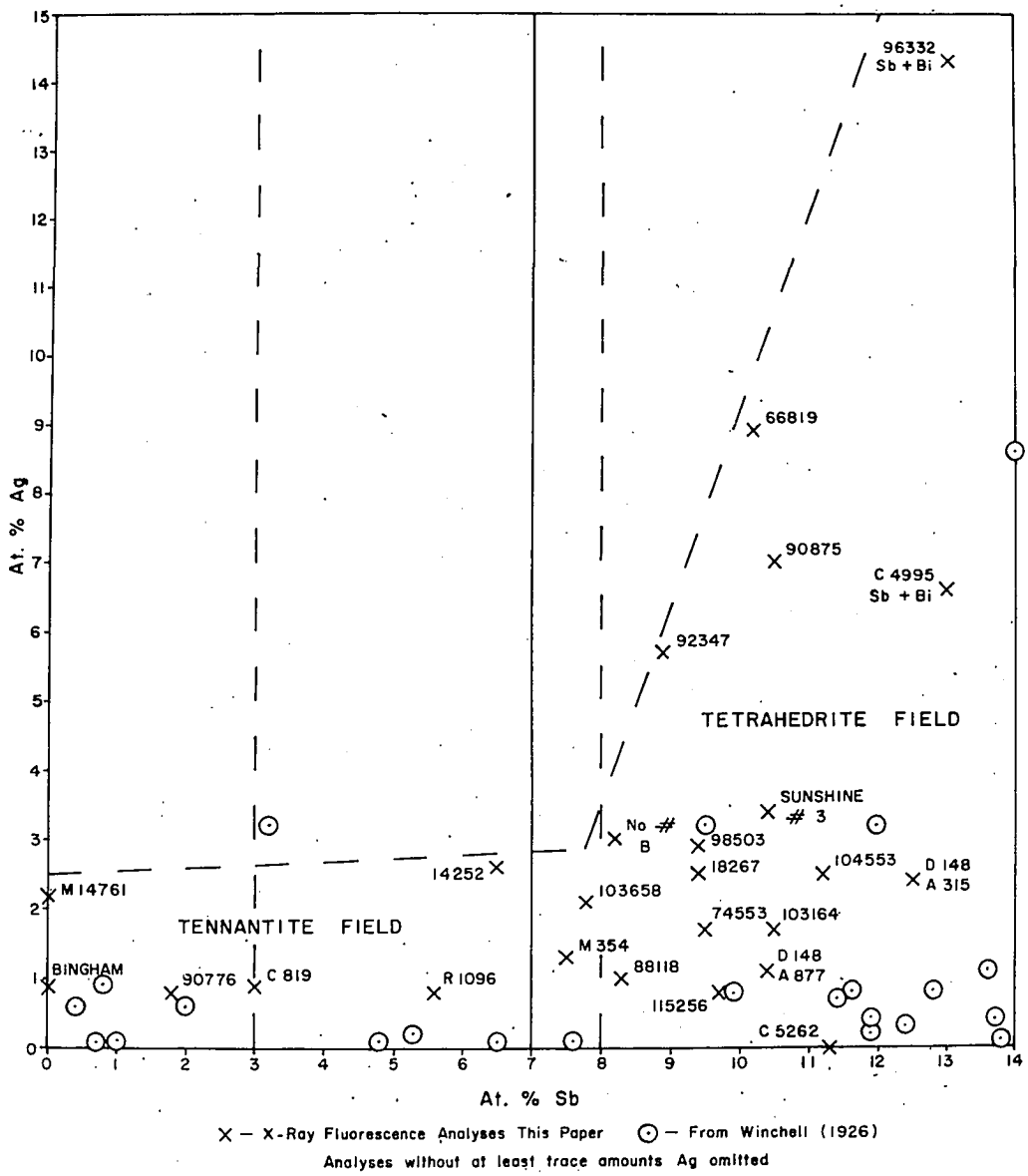

Figure 9. Limits for Ag in tetrahedrite series (vertical lines outline composition gap).

With increasing Sb in the tetrahedrite field, Ag rises from an upper limit of about 3 atomic percent to 9 (66819) and possibly to 14 (96332) atomic percent.

Zn. Figure 10 illustrates the random distribution of Zn in the tetrahedrite series. Zinc shows no propensity to associate with either As or Sb-rich phases of the series. The range is from no Zn to a pronounced upper limit at 6.5 atomic percent. Of 38 specimens analyzed, 37 contained at least trace amounts of Zn.

Fe. Figure 11 illustrates the distribution of Fe in the tetrahedrite series. The distribution is random, ranging from no Fe, but with more vague limits in the tetrahedrite and tennantite fields than in the case of Zn. All specimens analyzed contained at least trace amounts of Fe. Very high analyses above the dashed line show contamination by Fe-bearing minerals in x-ray diffraction patterns. Polished sections of M11654, R1110, M609 and R1096 have been investigated (Appendix B). Textural relations of the first three give evidence that tetrahedrite or tennantite is a later phase than the contaminant. In M11654, tetrahedrite fills interstices and apparently replaces pyrite in an intergrowth of quartz and euhedral pyrite. In M609, tennantite bears apparent replacement relationships to chalcopyrite and subhedral pyrite. In R1110,

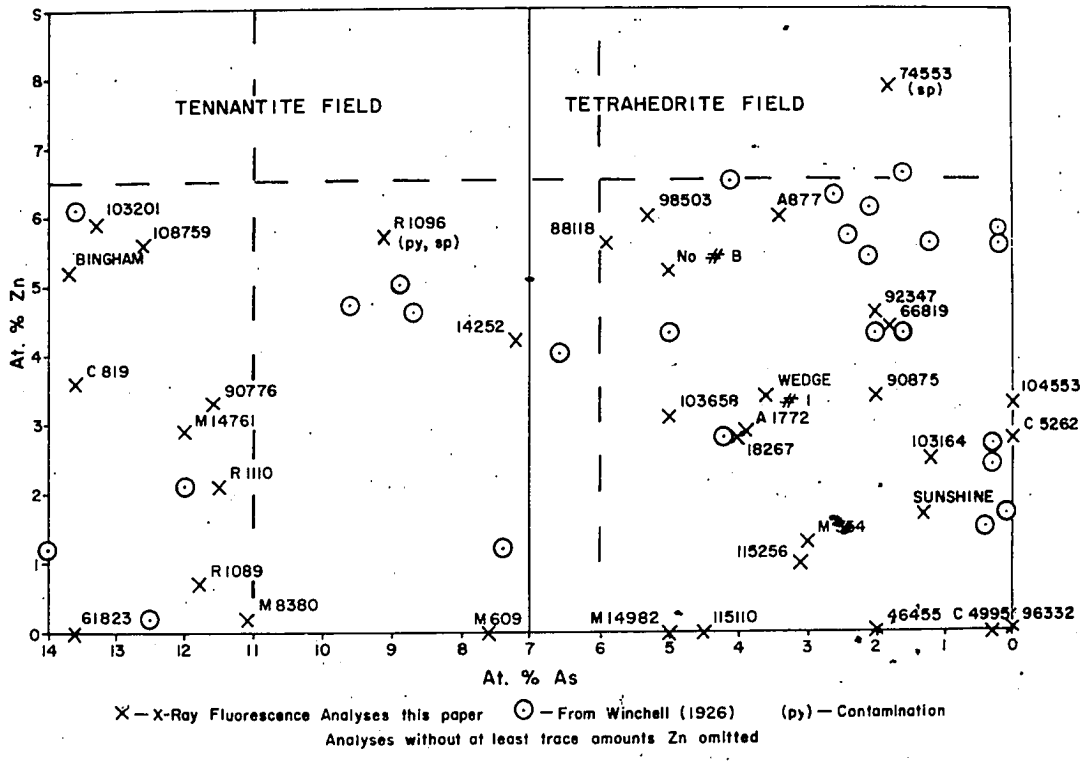

Figure 10. Distribution of Zn in tetrahedrite series (vertical lines outline composition gap).

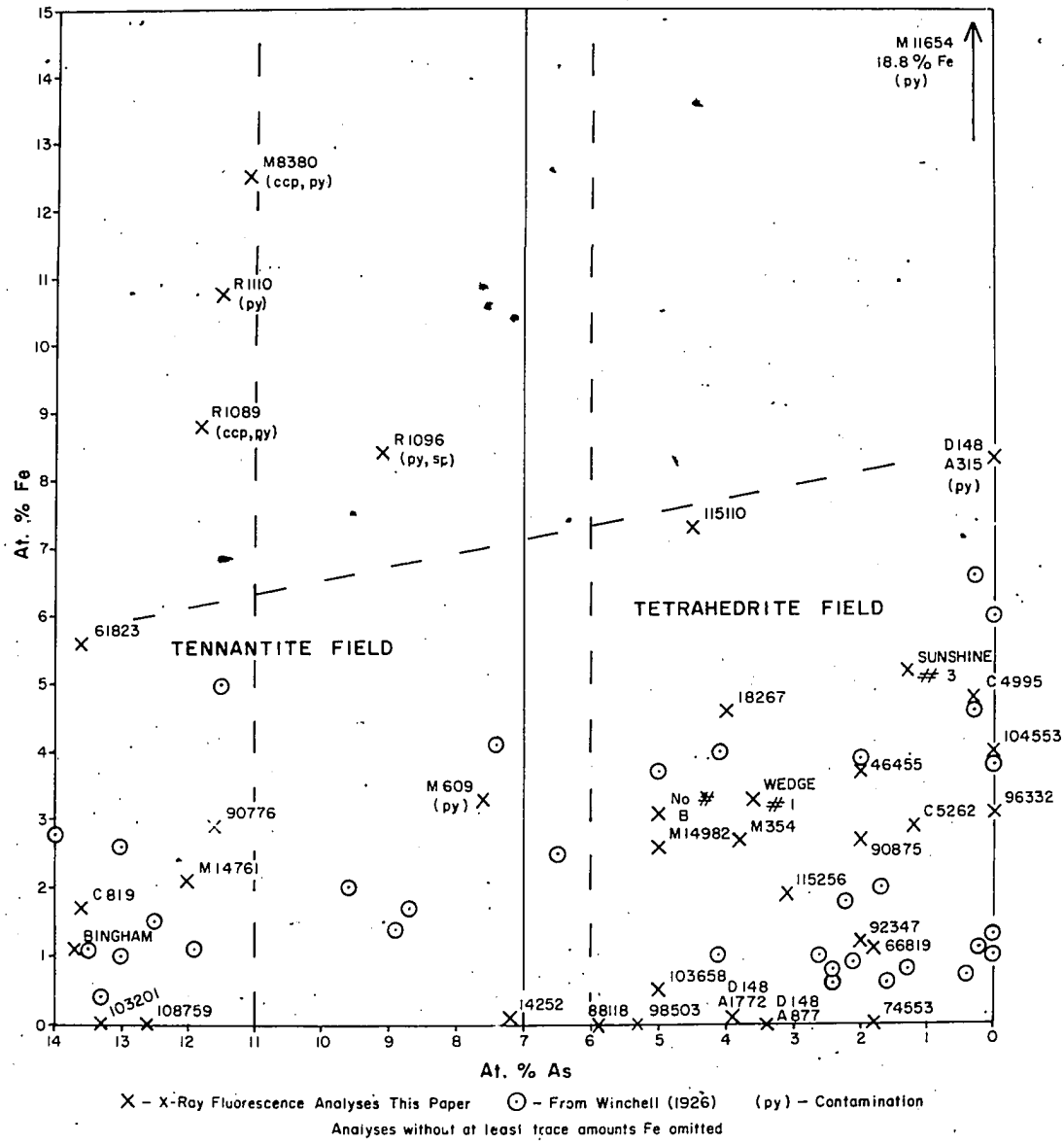

Figure 11. Distribution of Fe in tetrahedrite series (vertical lines outline composition gap).

tennantite fills interstices of a field of pyrite crystals. The texture of R1096 is more difficult to interpret and may represent essentially isochronous phases of tennantite and pyrite. A tennantite front appears to advance into sphalerite, with pyrite blebs distributed along the contact and numerous blebs in tennantite near the contact. In this case, pyrite may have exsolved from tennantite.

Fe + Zn. Figure 12 illustrates the distribution of Fe + Zn in the tetrahedrite series. All samples analyzed contain either Fe or Zn. The sum does not fall below 2.5, except for analyses from Winchell (1926). Neglecting the Winchell analyses and contaminated specimens, the sum ranges from 2.5 to about 8 in the tetrahedrite field and from about 5 to 6.5 in the tennantite field. This distribution suggests that the sum Fe + Zn tends to have a fixed value, at least in tennantite. The formula may be $Cu_{10}(Fe, Zn)_2(As, Sb)_4S_{13}$.

Hg. All specimens containing the rare, large element Hg are tetrahedrites or bismuthian tetrahedrites.

Limitations in the Complete Isomorphous Series

Analyses in this paper and from Winchell (1926) indicate a composition gap in the As-Sb solid solution series. This is revealed in the above graphs and in the

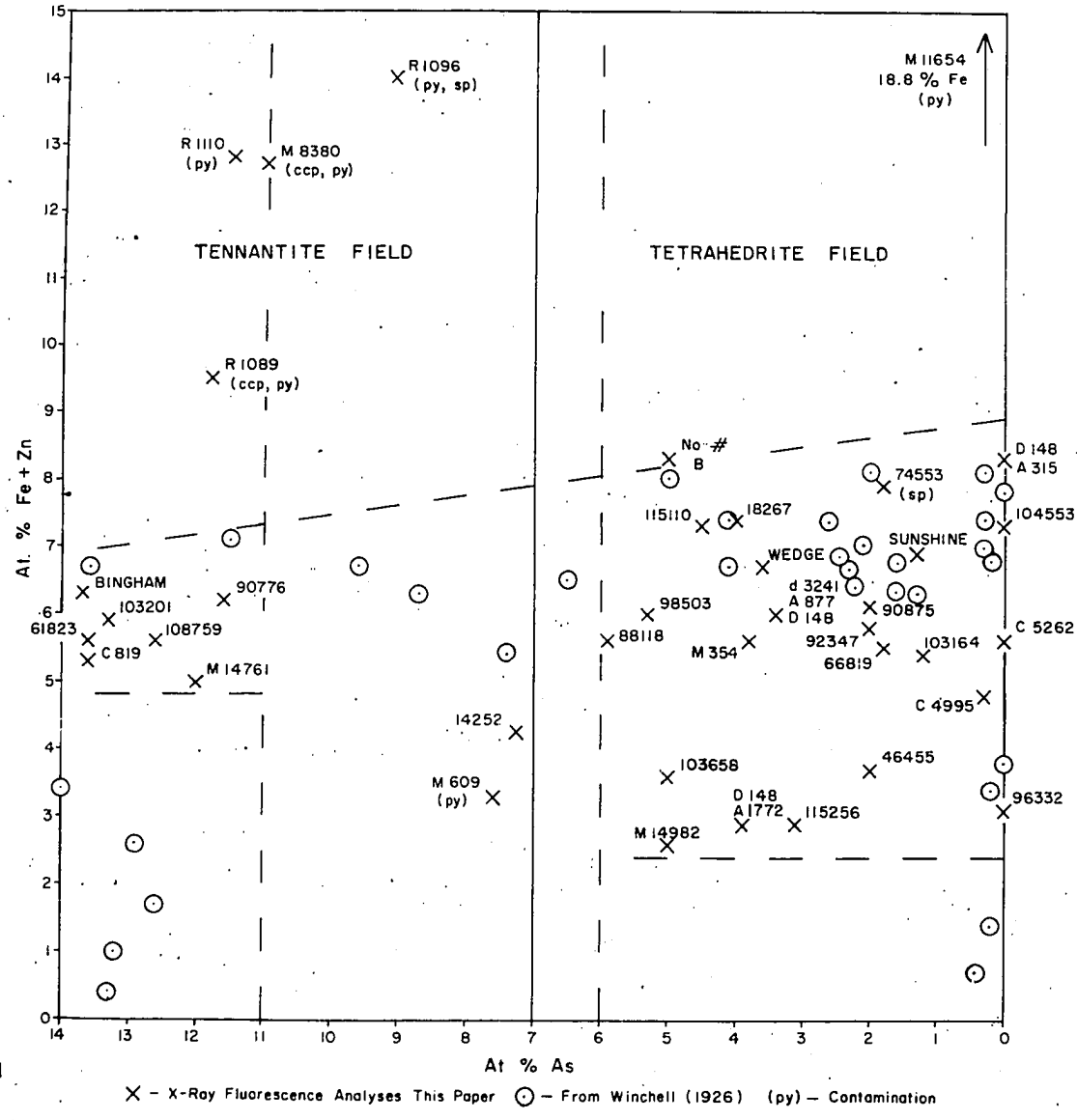

Figure 12. Distribution of Fe + Zn in tetrahedrite series (vertical lines outline composition gap).

As-Sb-Bi composition diagram (fig. 13) as a region between 6 and 11 atomic percent As in which few analyses fall. Thus the gap lies predominantly in the tennantite field with analyses of the tetrahedrite series clustering in the regions 11 to 14 atomic percent As and 8 to 14 atomic percent Sb. Further, Figure 13 indicates extreme restriction of As-Bi solid solution, which is limited to less than one atomic percent Bi even in an intermediate As-Sb member. Solid solution between Sb and Bi is much more extensive, reaching four to six atomic percent Bi in antimonian members of the series.

The composition gap between As and Sb is transgressed by several analyses. Discounting contamination, these analyses are all low in percentages of the large atoms Ag, Hg and Bi. Despite the size disparity between As and Sb, both fall within the radius ratio limits for tetrahedral coordination. The differences between them are accentuated by the incorporation of considerable quantities of Ag (also Hg and Bi) in tetrahedrites and the exclusion of these quantities in tennantites. The data suggest that complete solid solution exists between As and Sb only for members with insignificant Bi and Hg and with Ag not greater than 2.5 atomic percent (fig. 9).

X-ray and polished section investigations suggest that the composition gap may mark a low-temperature un-

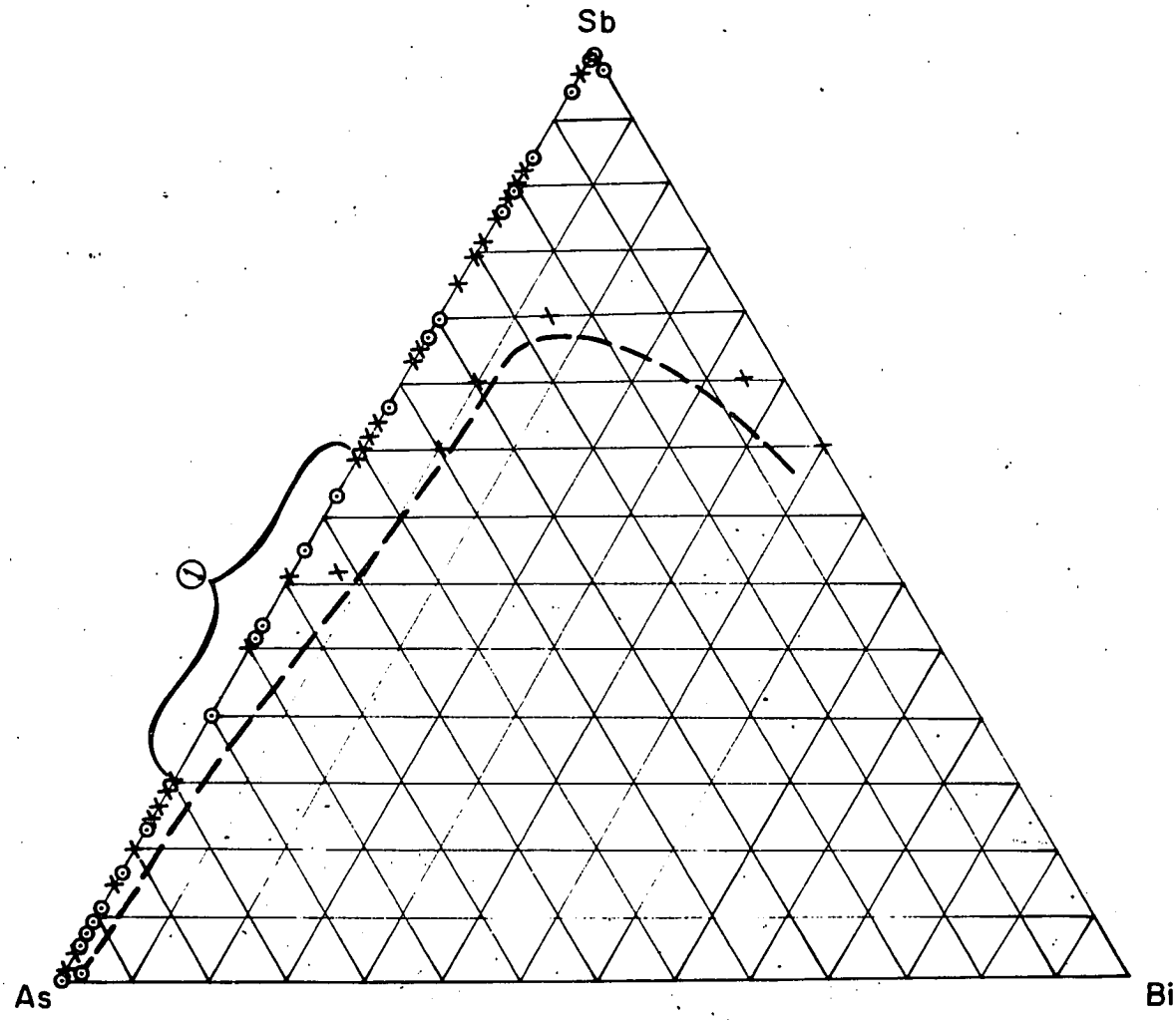

X - X-RAY FLUORESCENCE ANALYSES THIS PAPER

⊙ - FROM WINCHELL (1926)

① - REGION OF IMMISCIBILITY FOR Ag > 2.5 At.%

Figure 13. Composition diagram for As-Sb-Bi.

mixing field for members having Ag in excess of 2.5 atomic percent. A semi-quantitative wet chemical analysis of specimen 64981 indicates that it is intermediate in As and Sb content and contains Ag in excess of 2.5 atomic percent. The x-ray diffraction powder pattern of this specimen (fig. 14) shows double peaks for all substantial reflections except those in the front region, where resolution is not likely. This indicates the occurrence in the same specimen of two species of the tetrahedrite series. The slightly different peak positions reflect different size unit cells which are a function of the different chemistry of the two species. Since two phases are not detected in the photomicrograph of this specimen, the mixture is probably sub-microscopic. These features are interpreted as an unmixing of this material in the solid state. Cell dimensions computed for the (440); (510, 431); and (400) reflections give the following values:

	(440)	$a_o = 10.42(3)$ Å $a_o = 10.37(5)$
(510)	(431)	$a_o = 10.43(0)$ $a_o = 10.30(2)$
	(400)	$a_o = 10.45(2)$ $a_o = 10.30(6)$

According to results presented in the ensuing section on cell size variation, the larger cell size is consistent with Ag-bearing tetrahedrite and the smaller with

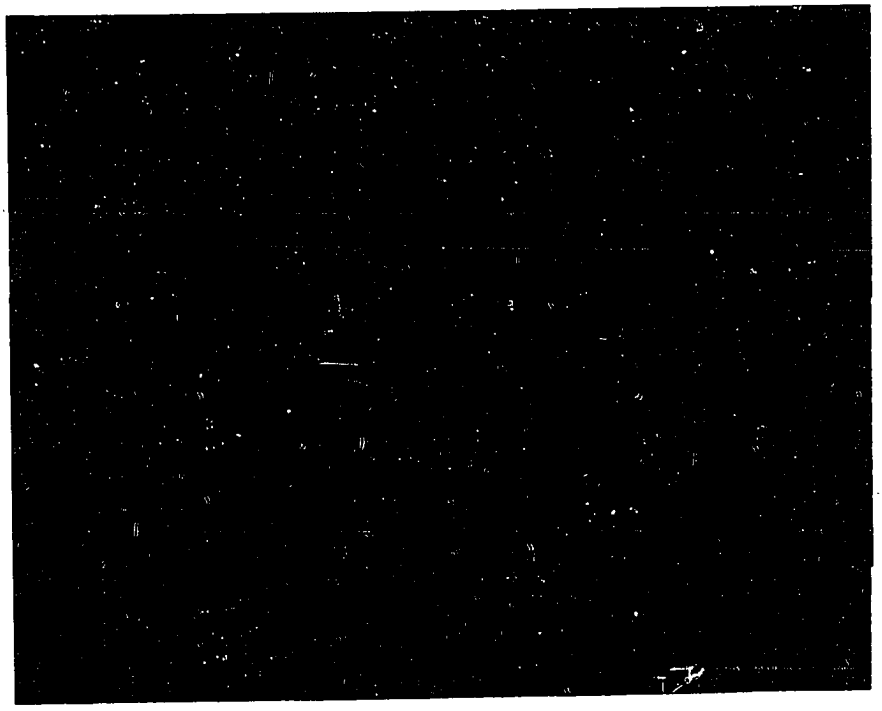

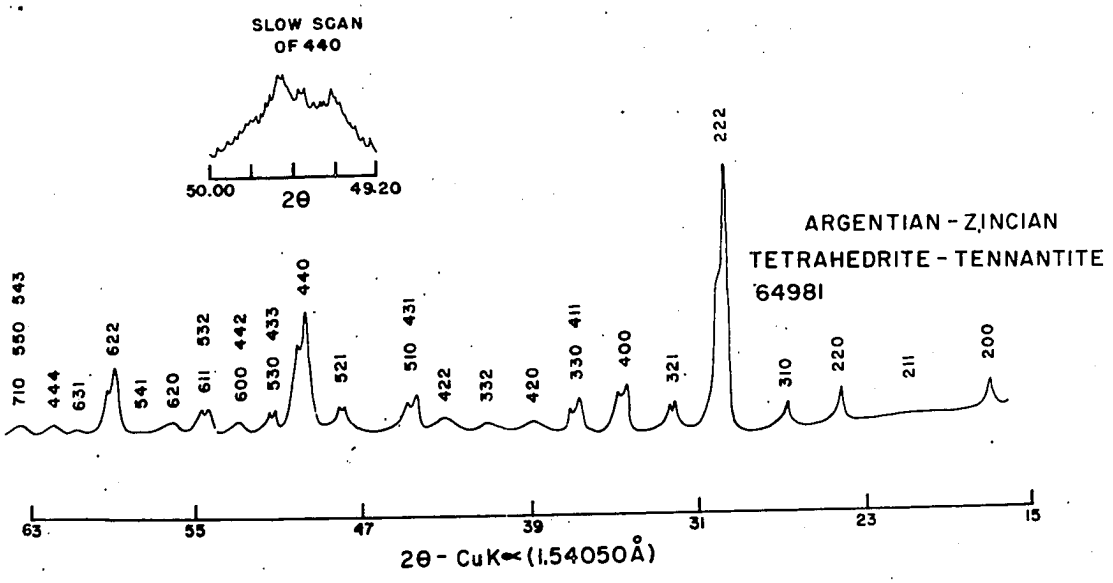

Figure 14. X-ray diffraction powder pattern and polished section of unmixing tetrahedrite-tennantite.

tennantite. The complexity revealed by the slow-scanned (440) reflection probably indicates this material has domains of differing cell sizes due to differing chemistry.

Figure 15 shows relationships for specimen R1096, which also occurs in the composition gap but has less than one atomic percent Ag. The x-ray diffraction pattern shows sharp, single peaks characteristic of a single phase.

Figure 16 is a preliminary diagram of the fields of stability for the tetrahedrite series based on chemical and x-ray diffraction data from natural specimens. The melting temperatures were obtained from experimental results on synthetic members of the series. The miscibility gap may be transgressed by two situations:

1. Small atom (i.e. Fe, Zn) varieties in the tetrahedrite series.
2. Unstable large atom (Ag) varieties which crystallized at high temperature, where complete miscibility in the series is indicated.

Streak

In the tetrahedrite series, streak ranges from black to light brown. The various streak colors were determined by inspection of very finely powdered amounts dried on glass slides. The color is a function of the

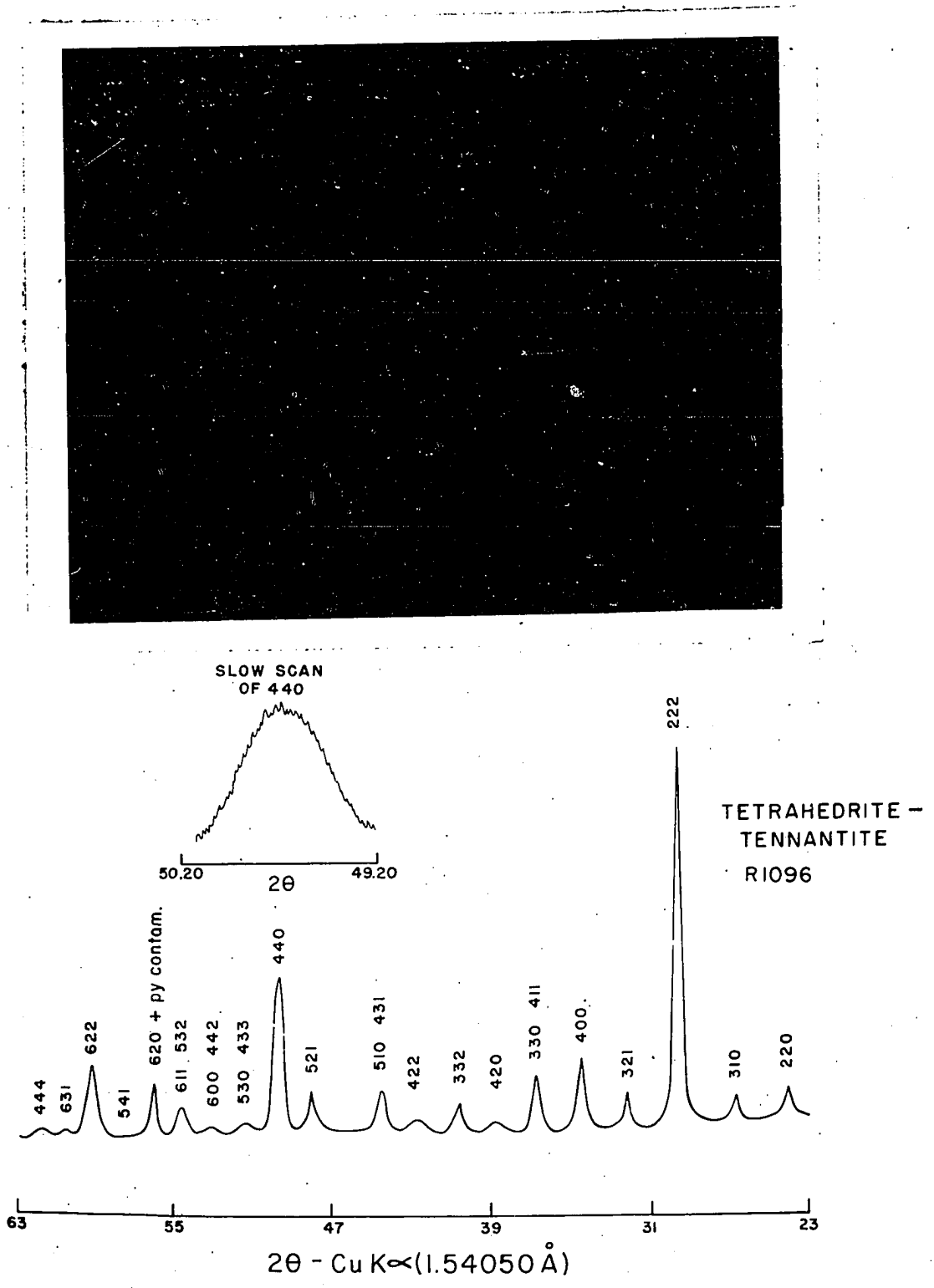

Figure 15. X-ray diffraction powder pattern and polished section of single phase of tetrahedrite-tennantite (containing little silver) in composition gap.

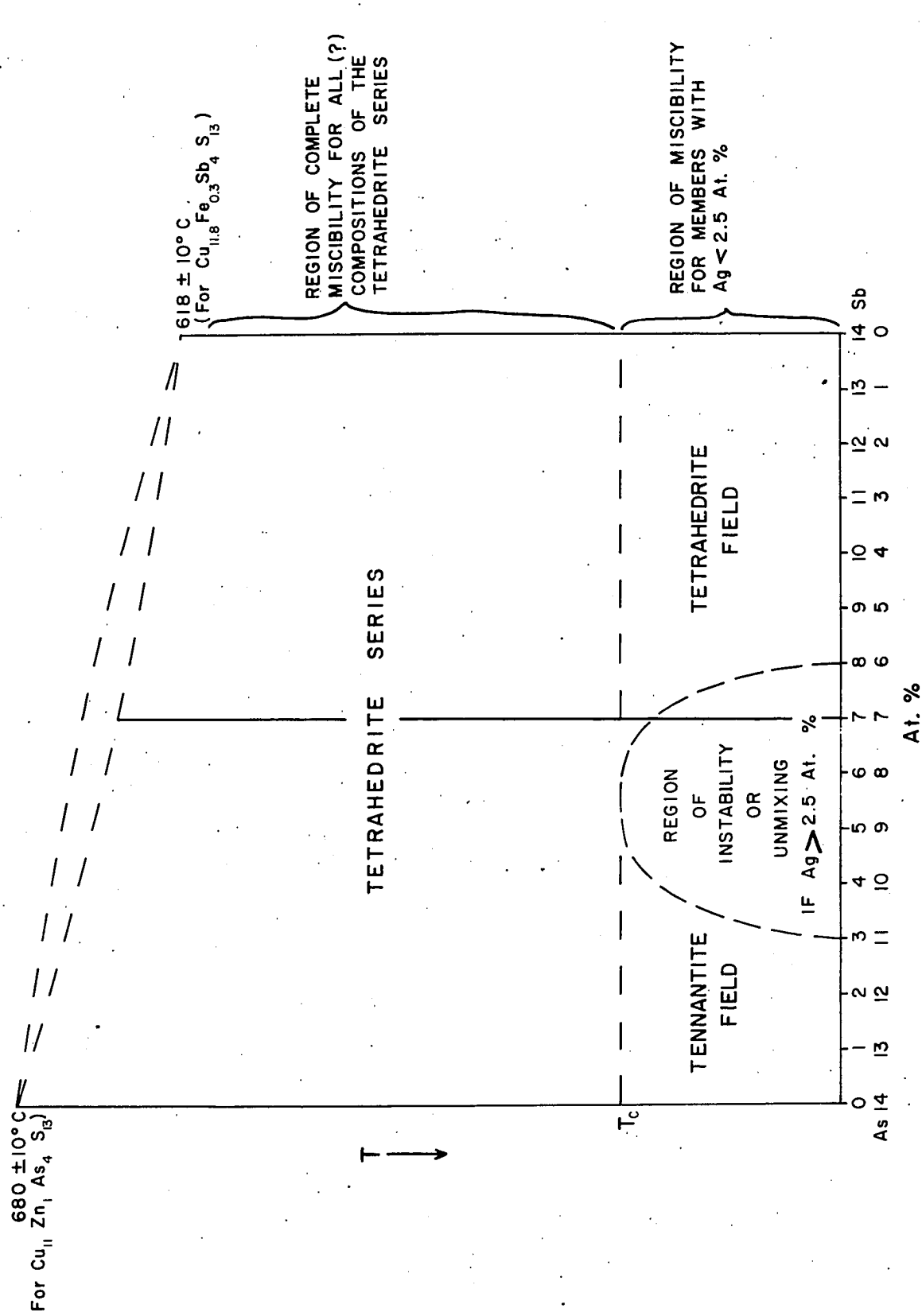

Figure 16. Preliminary diagram of the fields of stability for the tetrahedrite series.

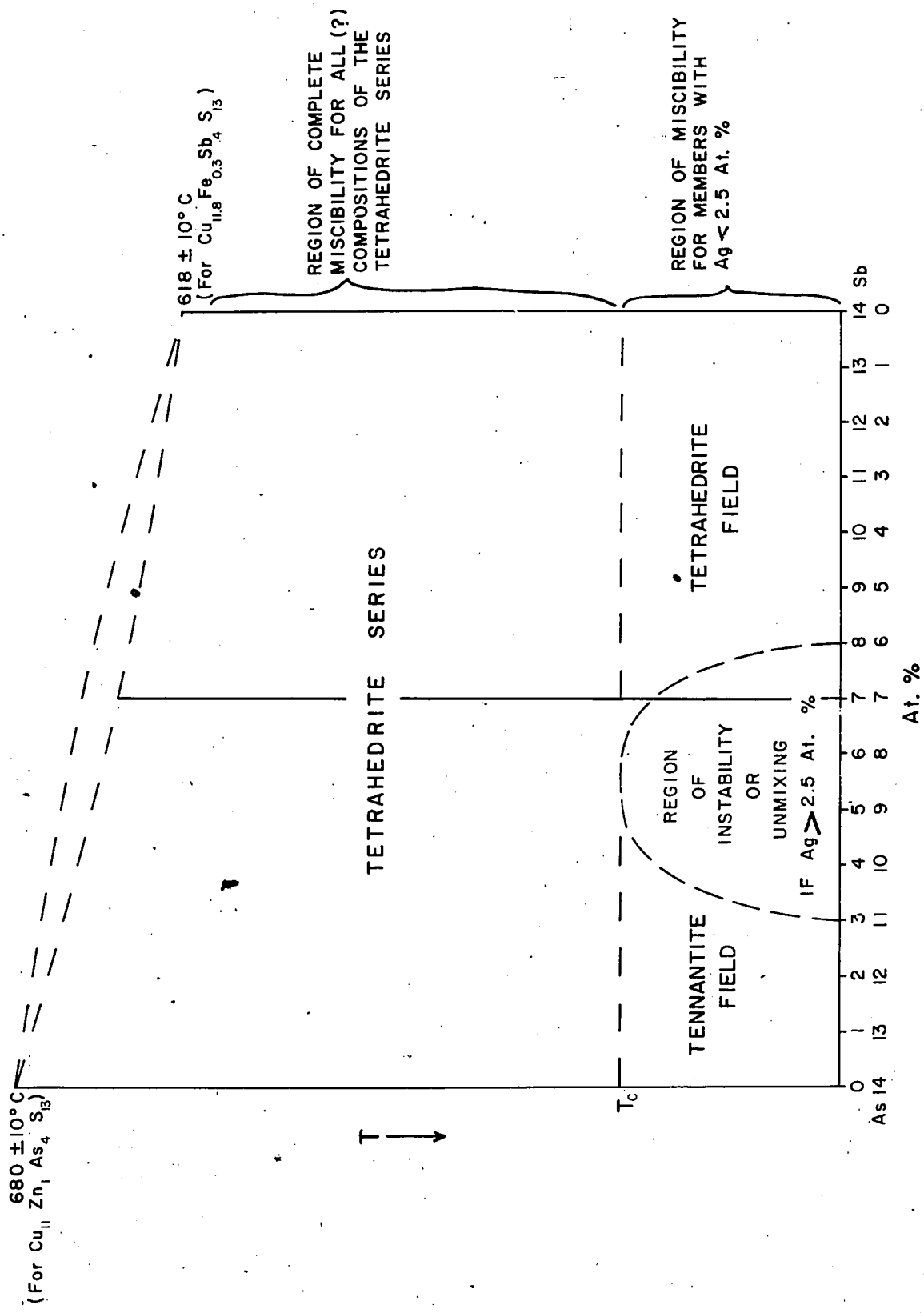

Figure 16. Preliminary diagram of the fields of stability for the tetrahedrite series.

quantities of the common elements Fe, Zn, Sb and As. The trend to a light brown streak is related to the amount of Zn and in a permissive way to the amount of As. That is, a tennantite with a given amount of Zn will show a more brownish streak than a tetrahedrite with the same amount. Both Zn and As occur in sulfide minerals which have non-metallic or sub-metallic streaks. Examples are:

Sphalerite	ZnS	Streak colorless
Orpiment	As_2S_3	Streak yellow
Realgar	AsS	Streak red

On the other hand, sulfide minerals of Fe and Sb have a black metallic streak:

Pyrite	FeS_2	Streak black
Stibnite	Sb_2S_3	Streak black

Black streak is related to metallic and colored streak to a more non-metallic character.

Figure 17 illustrates the dependence of brown streak color in the tetrahedrite series on the quantity of Zn. Since Sb and As are interdependent, the plot is made atomic percent Fe plus Sb versus atomic percent Zn for the analyzed samples. In this manner streak fields are delineated from black to light brown. From these data can be drawn the conclusion that if the streak is black, Zn must be less than 3 atomic percent. If the streak is light brown, Zn must be greater than a minimum of 4 atomic percent.

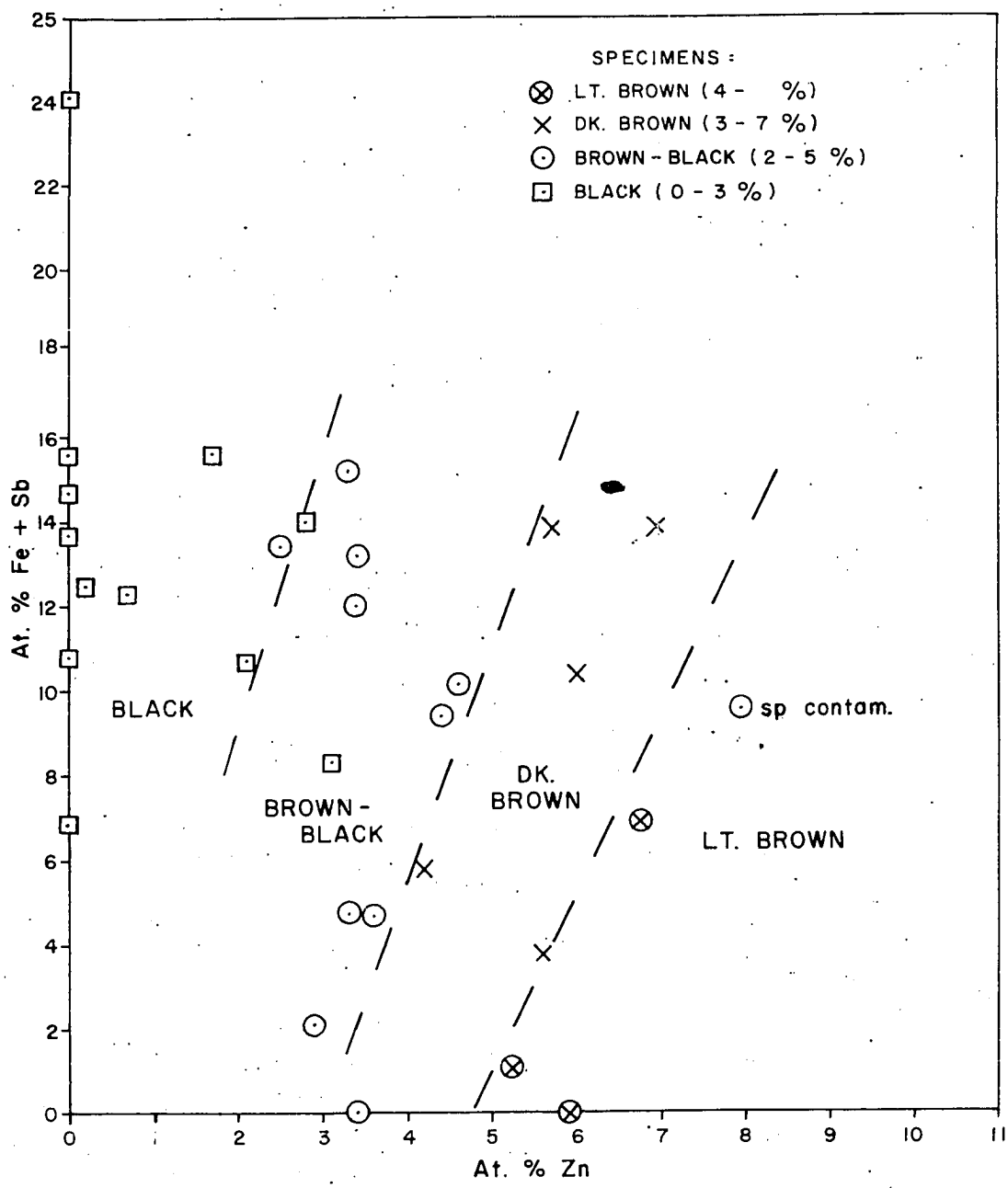

Figure 17. Streak fields for the tetrahedrite series.

UNIT CELL DIMENSIONS

Machatschki (1928) indicated that the cell dimensions of the tetrahedrite series were lowered by As and raised by both Sb and As. Since that time no further attempt has been made to assess quantitatively what effects the substituting atoms have on the cell sizes in the tetrahedrite series.

A number of studies have been made of the effect of atom substitutions on cell dimensions for some chemically simpler compounds. For example, Skinner (1961) and Skinner and Bethke (1961) demonstrated that the unit cell edges in natural and synthetic sphalerites and in synthetic wurtzites are linear functions of composition in mol percent. In these studies, only the effect of substitution of Fe or Mn separately for Zn needed to be considered.

In contrast, the tetrahedrite series has chemically complex species in natural specimens, with many different atoms interacting on the size of the unit cell. From a complete spectrum of cell sizes, the variation due to several of the constituent atoms has been assessed in a generally quantitative way. These results may be useful for a rough approximation of the chemistry of members of the series when the unit cell size is known.

In the 38 natural specimens investigated by the powder

method, cell dimensions were computed ranging continuously from 10.201 to 10.552 ±.005 Å. The most common values fall in the region 10.25 to 10.45 Å. Table 8 lists the cell sizes determined for tetrahedrites, tennantites and synthetic specimens. The lowest value (10.201 Å) is from a pure tennantite (M14761). This is undoubtedly an Fe and Zn-bearing variety with the reported Ag (table 5) due to contaminant. The synthetic S5 ($Cu_{11}Zn_1As_4S_{13}$) has a very small cell (10.188 Å). This figure is close to the low figure for nearly pure tennantite given in Dana's System of Mineralogy (Palache and others, 1944, p. 374) and represents the lowest limit for cell dimensions of natural material. The range to 10.55 is considerably higher than the 10.40 for Ag-rich tetrahedrite reported by Machatschki (1928).

Since large atoms tend to associate with Sb in the tetrahedrite field, only a narrow region of overlap in cell dimensions occurs between tetrahedrites and tennantites. The latter range from 10.20 to 10.39 Å (14252) in Ag-rich varieties; the former range from 10.31 (D148, A1772) to 10.55 Å. In Figure 18 is shown the magnitude of variation of 2θ in x-ray powder diffraction patterns of specimens differing greatly in cell size.

Synthetics. From synthetic material, insufficient data have been procured to demonstrate quantitatively

TABLE 8

CELL DIMENSIONS OF NATURAL AND SYNTHETIC SPECIMENS *

Tetrahedrites:

Spec. #	a_o (Å)
66819	10.552
96332	10.531
90875	10.512
C4995	10.502
92347	10.487
Sunshine 3	10.453
74553	10.444
104553	10.443
M11654	10.435
No # B	10.433
18267	10.431
D148 A315	10.424
98503	10.423
103164	10.416
C5262	10.414
115110	10.411
46455	10.403
103658	10.392
Wedge 1	10.377
M631 #148	10.368
M354	10.363
115256	10.361
88118	10.350
D148 A1772	10.315 ?

Tennantites:

Spec. #	a_o (Å)
14252	10.398
M609	10.340
R1089	10.301
108759	10.274
90382	10.274
C819	10.264
90776	10.260
Bingham	10.255
61823	10.255
R1110	10.254
103201	10.252
M8380	10.252
M14761	10.201 ?

Synthetics:

Spec. #	a_o (Å)
S1-1	10.308
S2-1	10.380
S3-1	10.200
S4-1	10.365
S5-1	10.188

* Determinations to $\pm$ .005 Å

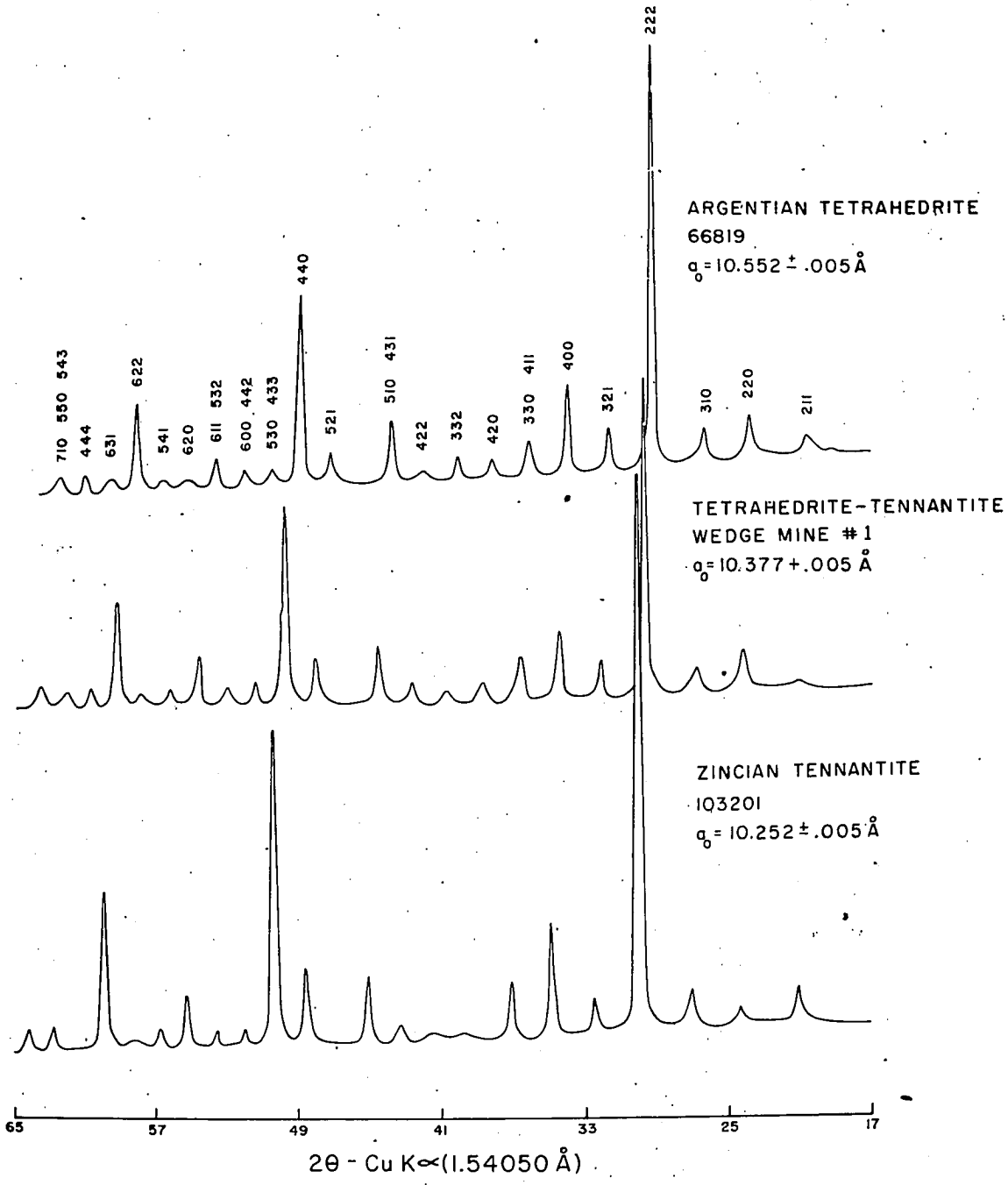

Figure 18. X-ray diffraction powder patterns of members of the tetrahedrite series differing in cell size.

the effect of each atom on the cell size of the tetrahedrite series. This can be done by plotting data from a sufficient number of pure materials. However, except for a few major generalities which are readily attainable, these data could be applied only in a qualitative manner to natural materials which are chemically complex. Nevertheless, some useful generalities can be obtained from the synthetic specimens.

1. The effect of all substituting atoms is to raise the cell dimensions from a lowest case of something less than 10.18 Å (perhaps about 10.16) for ideally pure tennantite $Cu_{12}As_4S_{13}$.
2. Complete substitution of Sb for As causes a_o to expand from 10.18 to about 10.30 Å.
3. Substitution of Fe up to 10.3 atomic percent into ideally pure tetrahedrite $Cu_{12}Sb_4S_{13}$ causes a_o to rise from 10.30 to 10.38 Å.
4. Substitution of Zn has nearly the same effect as Fe on cell dimensions but causes a slightly greater rise.
5. Larger atoms cause a greater rate of change of cell dimensions with composition.

Natural Specimens. Graphs of the variation of a_o with Ag and with Bi (fig. 19) emphasize the association of large atoms which mutually affect cell dimensions in the tetrahedrite series. In tennantites, which have little Ag, the effect of Sb on a_o is most obvious. Specimens poor in Ag below the trend are tennantites. The element Bi is associated with large amounts of Sb, Ag and Hg. Therefore, bismuthian tetrahedrites have

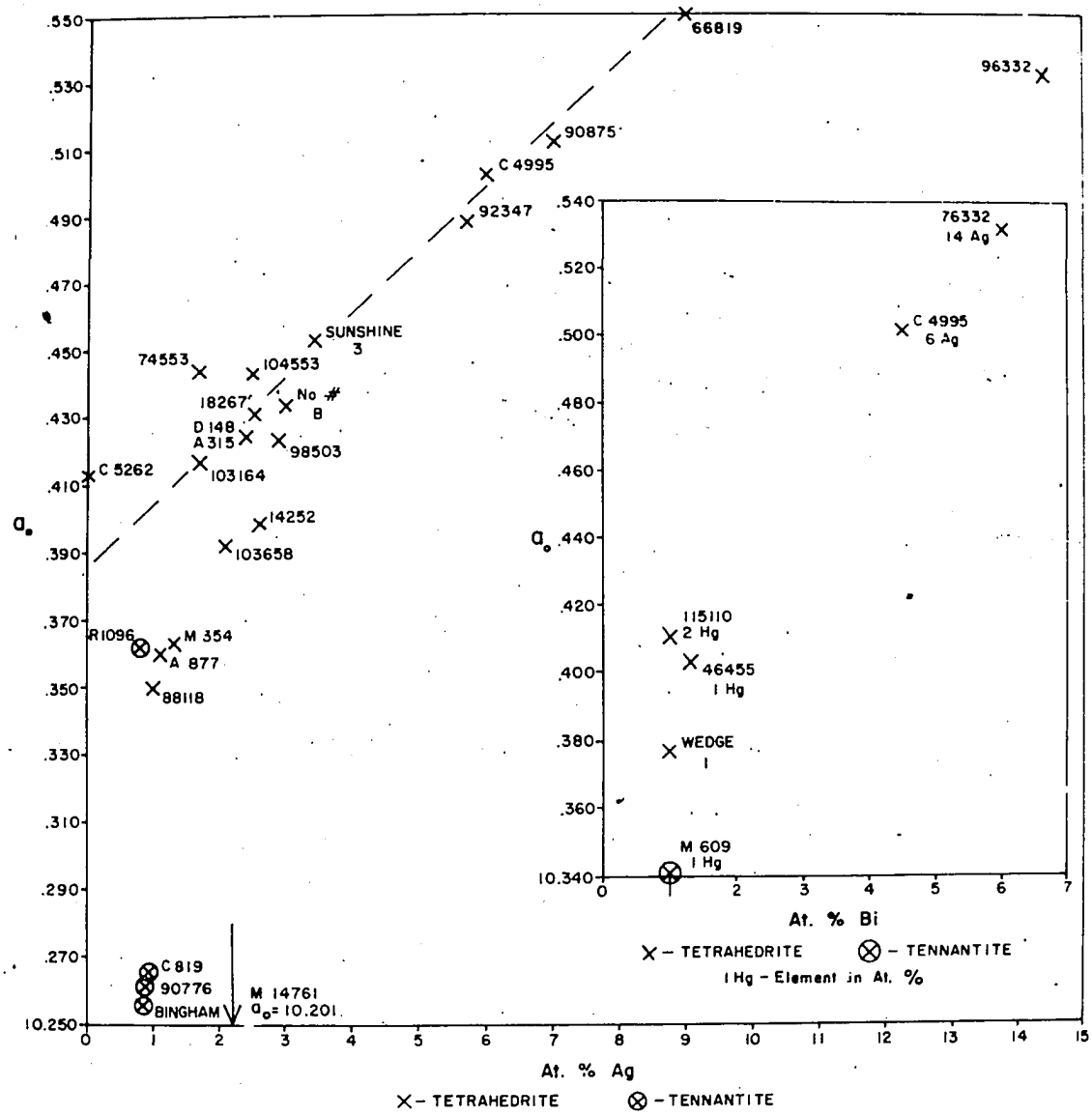

Figure 19. Variation of cell size with Ag and Bi.

big cells ranging from 10.38 at least to 10.53 Å. Since Ag is a fairly common substitute associated with Sb, the plot of a_o versus Ag + Sb approximates a straight-line trend (fig. 20).

The variation of cell size throughout the tetrahedrite series is illustrated in Figure 21. Most of the important relationships of cell size to chemistry can be deduced from this diagram. Tennantites, which have little Ag and rather constant sums of Fe + Zn, tend to cluster in a region 10.25 to 10.28 Å. Varieties poor in Fe + Zn are rare, and consequently members of the tetrahedrite series with a_o less than 10.25 Å are seldom found. Differences in cell dimensions between tennantites and tetrahedrites are rendered more pronounced by the sparsity of specimens in the composition gap. The family of curves represents the rise in a_o with Sb for various Ag contents. The diagram may be used in conjunction with the chemical data for the tetrahedrite series to approximate the chemistry of members when the cell size is known.

DISORDERED SUBSTITUTIONS

The tetrahedrite structure accommodates a variety of substituting atoms --- Fe, Zn, Ag, Hg, Pb, and Bi. X-ray diffraction results indicate that these atoms are

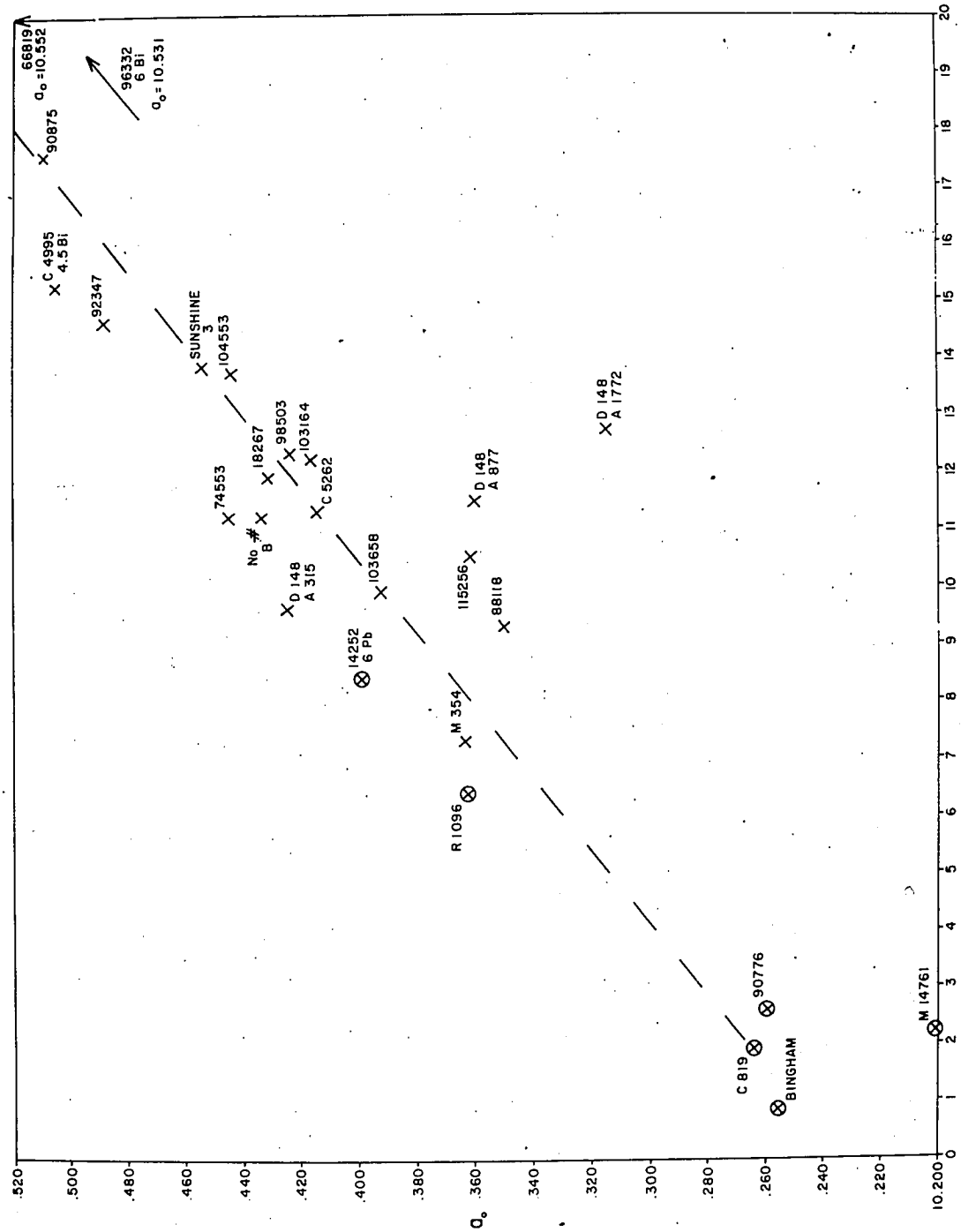

Figure 20. Variation of cell size with Ag + Sb.

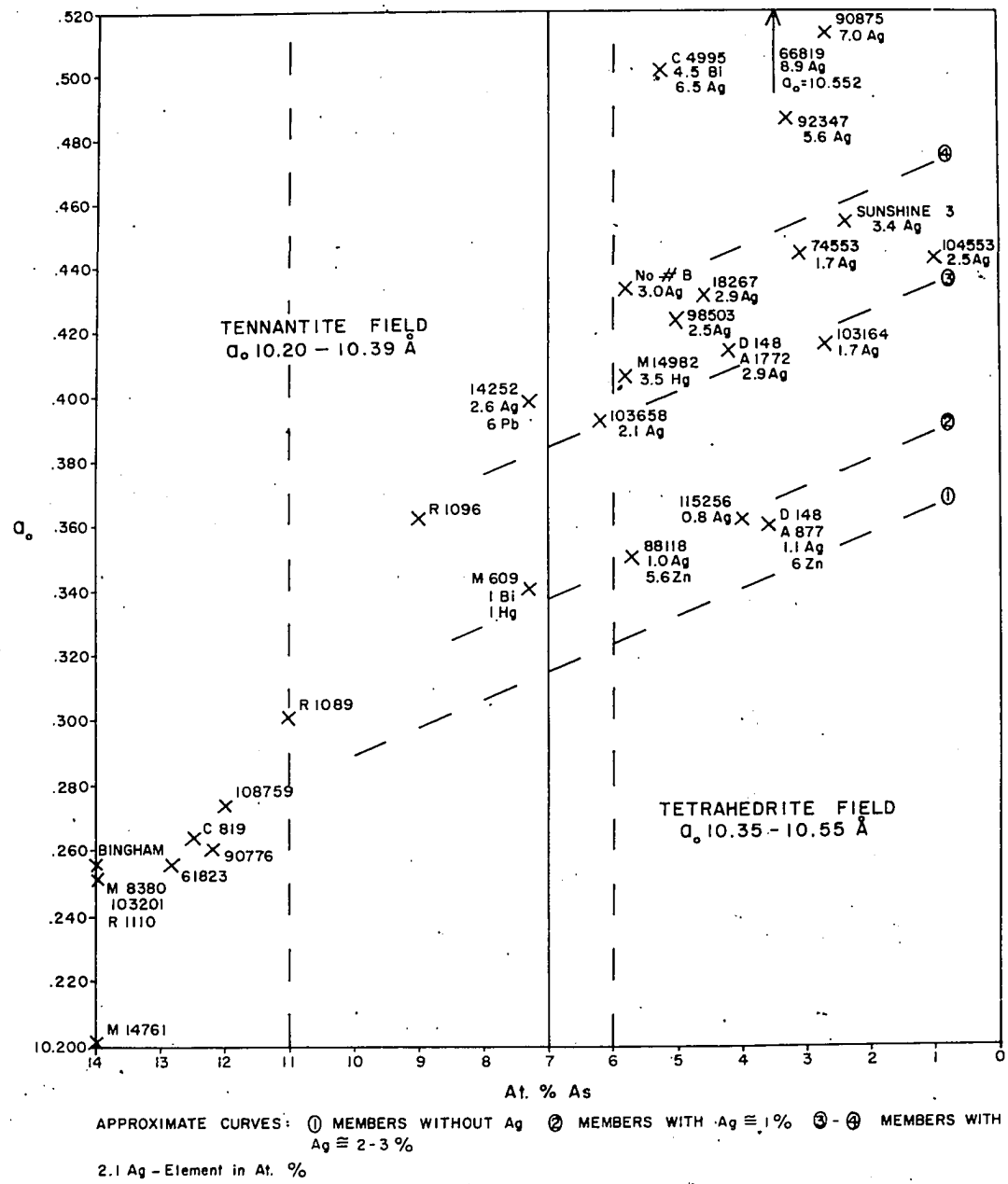

Figure 21. Variation of cell size in tetrahedrite series.

disordered or randomly distributed in metal sites rather than ordered in a regular lattice array in the structure.

Atoms which substitute for others in a structure may be randomized or orderly distributed in equivalent sites. If ordered, the substituting atoms comprise a new set of equivalent points. As a consequence, the substitutions cause changes in the symmetry of the structure. The structures of sphalerite and chalcopyrite may be used as an example. Sphalerite is composed of cubic closest-packed sulfur atoms with all interstitial tetrahedral sites occupied by zinc atoms. The resulting unit cell (fig. 22) is a face-centered cubic structure. Chalcopyrite has the same basic packing of sulfur atoms with all tetrahedral sites occupied by metal atoms. However, the zinc atoms are replaced by regularly alternating atoms of copper and iron. In effect, this is similar to an orderly replacement of one metal atom by another. The chalcopyrite unit cell (fig. 23) has a new tetragonal body-centered symmetry imposed by the ordered arrangement of metals in a superlattice.

Such differences in symmetry are detected in x-ray diffraction powder patterns by the appearance of new lines or reflections. In Figure 24, the three most intense lines in sphalerite, chalcopyrite and tetrahedrite are

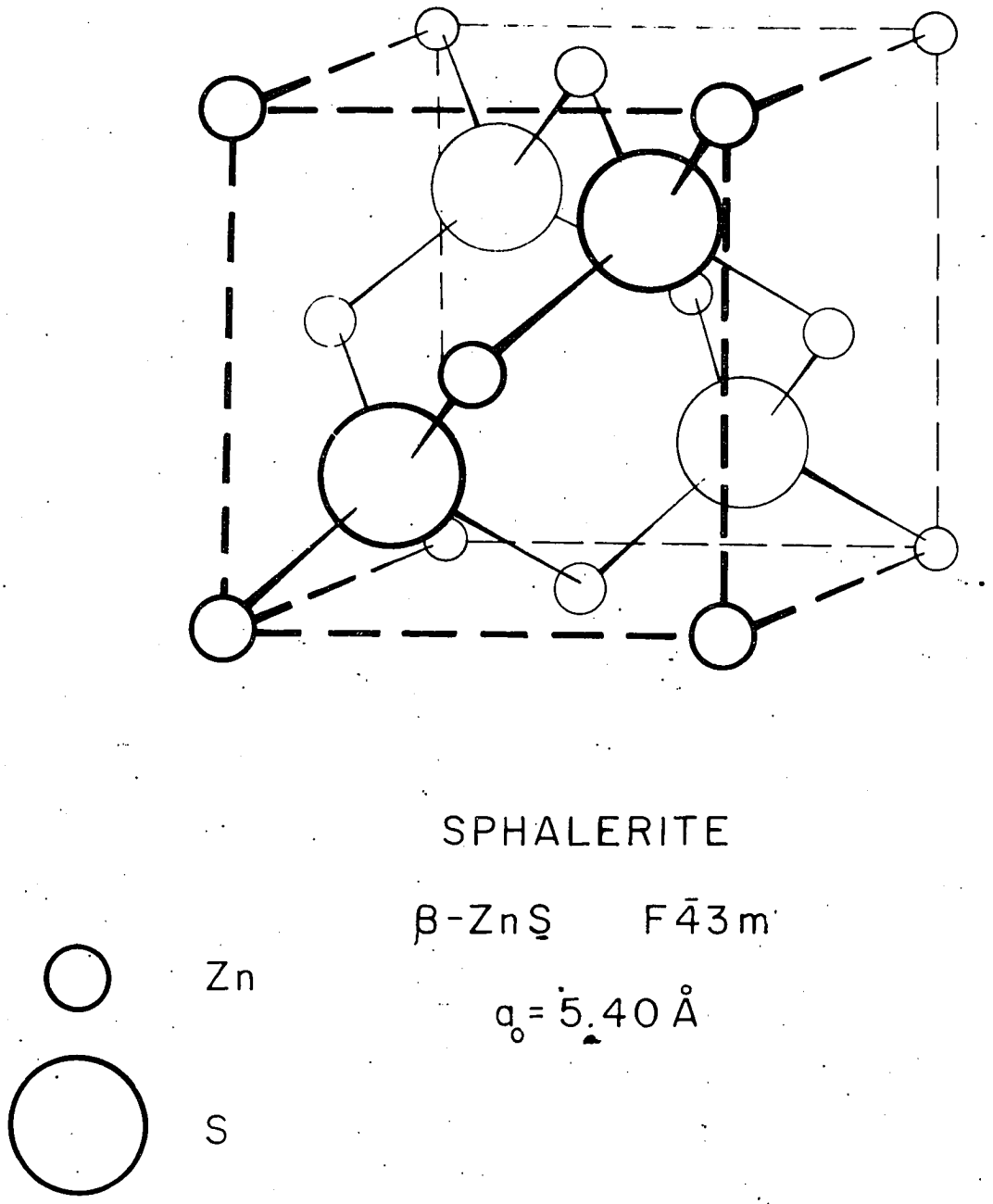

Figure 22. Unit cell of sphalerite.

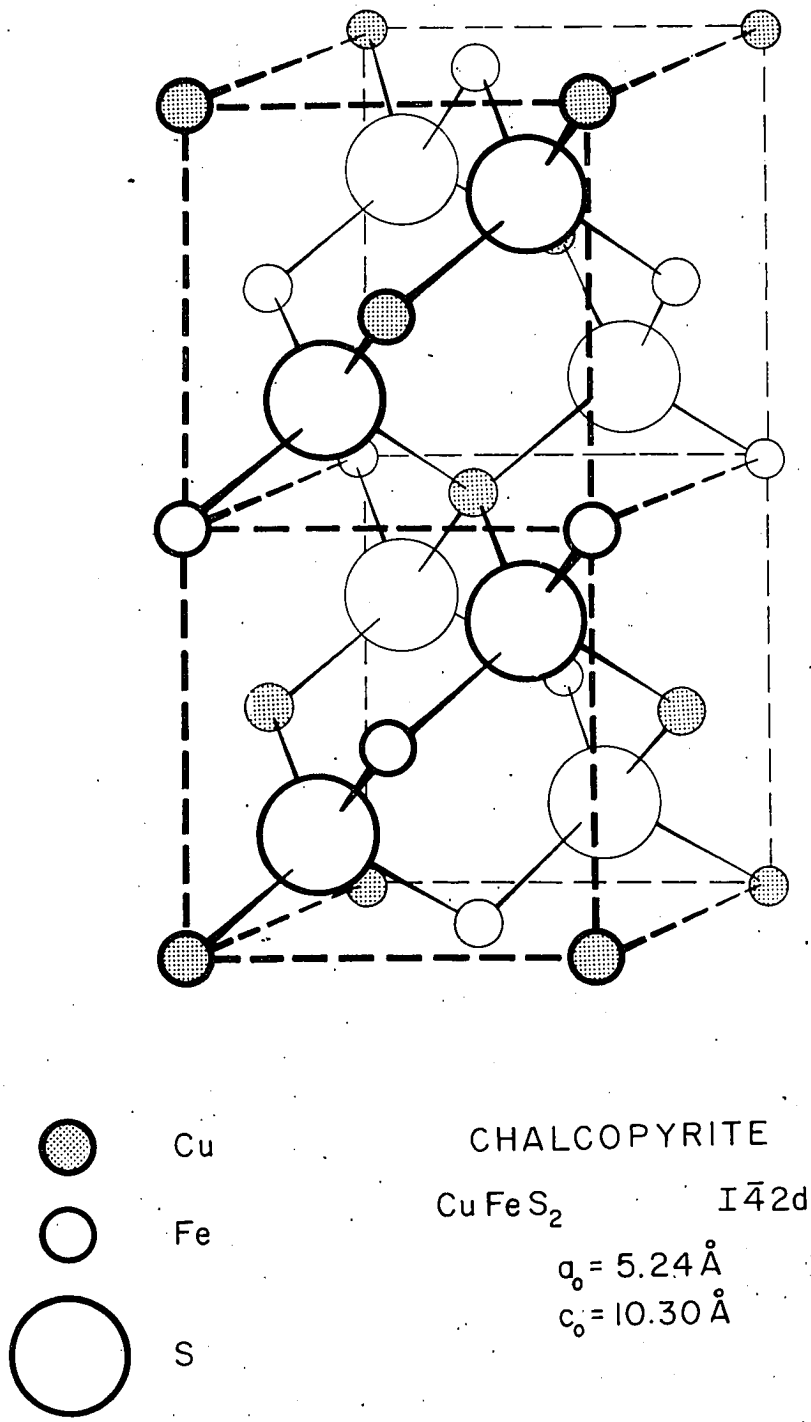

Figure 23. Unit cell of chalcopyrite.

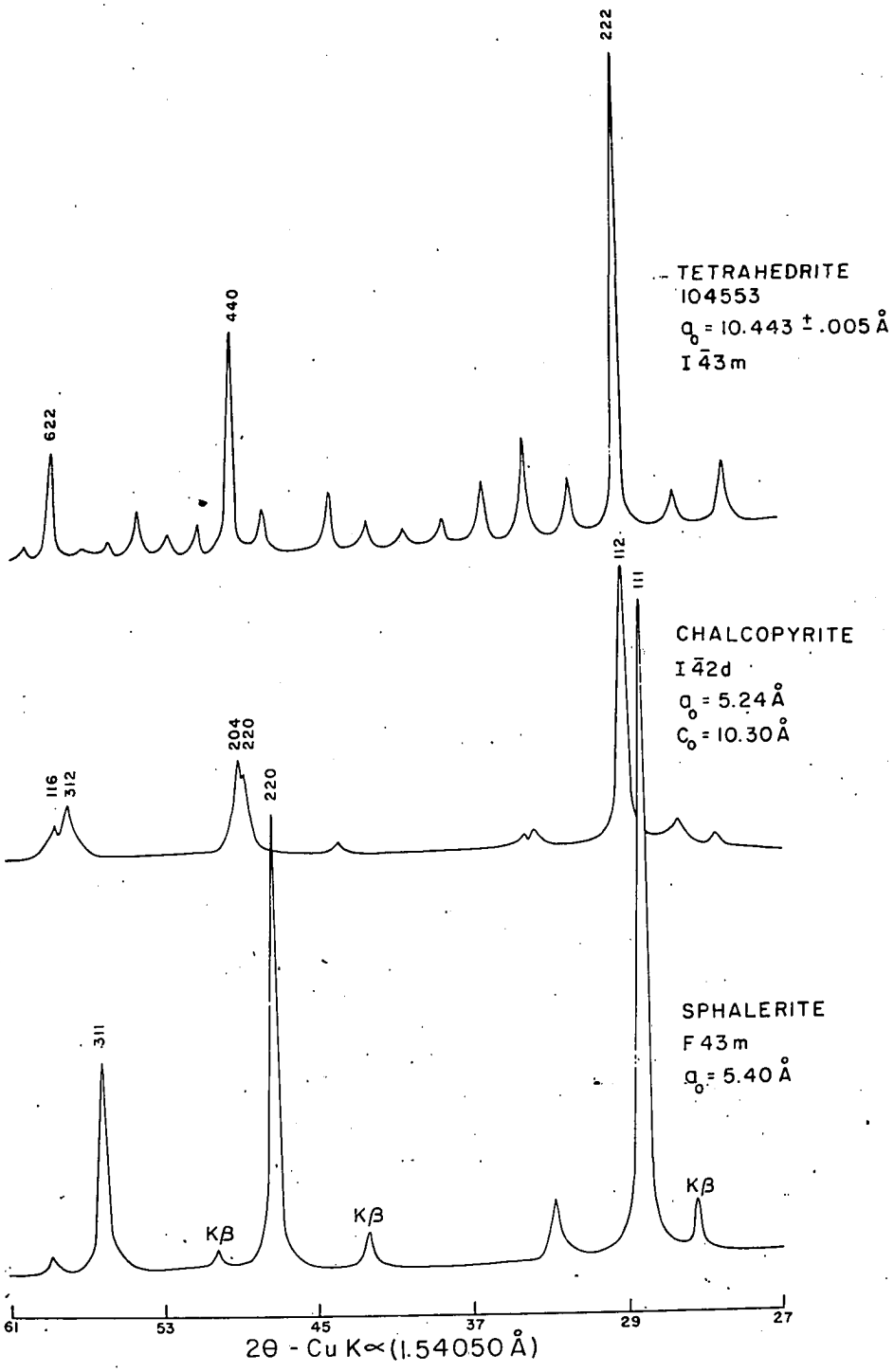

Figure 24. X-ray powder diffraction patterns of sphalerite, chalcopyrite, tetrahedrite.

caused by the cubic closest-packing of sulfur atoms in all three minerals. Theyrrepresent reflections from planes containing sulfur atoms, and are sometimes referred to as "main lines" for these minerals. Discounting K_B reflections, the sphalerite pattern is quite simple, whereas the chalcopyrite pattern shows added reflections caused by the ordered positions of two sets of metal atoms instead of one. These reflections are sometimes referred to as "superstructure reflections". Tetrahedrite, with several sets of ordered metal atoms (Cu-I, Cu-II, As) has many superstructure reflections.

In contrast to ordered substitutions of atoms, substitutions in a disordered manner produce no change in the symmetry of the structure. Instead, the intensity of reflections from planes of atoms affected by the substitution will fluctuate.

The dependence (in part) of the intensity of reflections on type of atom is indicated by the following relationship:

$$I \propto m \cdot p \cdot L \cdot |F|^2$$

where m = the multiplicity of reflection (i.e. number of times this same symmetry direction is repeated for x-ray diffraction powder pattern data).

L = the Lorentz factor.

P = the polarization factor.

F = the atomic structure factor (this factor is dependent on the type of atoms and their positions in a structure.

The way in which F is dependent on the type of atoms and their positioning is shown by the relationship:

$$F = \sum f e^{2\pi i (hx + ky + lz)}$$
$$= \sum f (\vec{A} + \vec{B})$$

where f = the atomic scattering factor for particular atoms.

A and B can be obtained from International Tables for X-ray Crystallography.

X-ray powder diffraction data (Appendix C) for all natural and synthetic specimens of the tetrahedrite series show reflections accounted for by the body-centered cubic structure where allowed reflections are given by the relationship:

$$h^2 + k^2 + l^2 = \text{all even numbers}$$

In the tetrahedrite structure there are possibilities for disordered substitution of metal atoms in several sets of equivalent points. Consider again the tetrahedrite structure (fig. 8). The Cu-I, Cu-II and Sb-As positions are ordered, and any of the substituting metals may selectively disorder in any one of the three sets of equivalent points without changing the structure.

The unique set of points for As and Sb has been

established by the determination of the structure of the tetrahedrite series. These can also be verified by consideration of the reflections from planes containing these atoms. In Figure 25 the relative intensities of all reflections except the (222) are plotted for six specimens which vary in chemistry. Inspection of the unit cell indicates that the (400) and (220) planes contain important contributions to F (p.83) from the As-Sb positions. Since Sb, with higher atomic number, has a larger scattering factor, these reflections ought to increase in intensity with Sb. In the top diagram of Figure 25, the (220) reflection shows such an increase, but the (400) does not. The (400) plane includes contributions to F from many Cu positions, which can be interpreted as obscuring the effect of Sb. Figure 26, in which all specimens are plotted, shows the increase in intensity with Sb for the (220) reflection. This technique demonstrates the disordering of As and Sb in sites in these planes.

It is possible that Fe, Zn and Ag, as well as other substituting atoms disorder preferentially on Cu-I or Cu-II sites. Possibilities for Ag merit consideration for several reasons: (1) Silver is an important constituent of the tetrahedrite series; (2) because of its large size, silver might be expected to disorder on

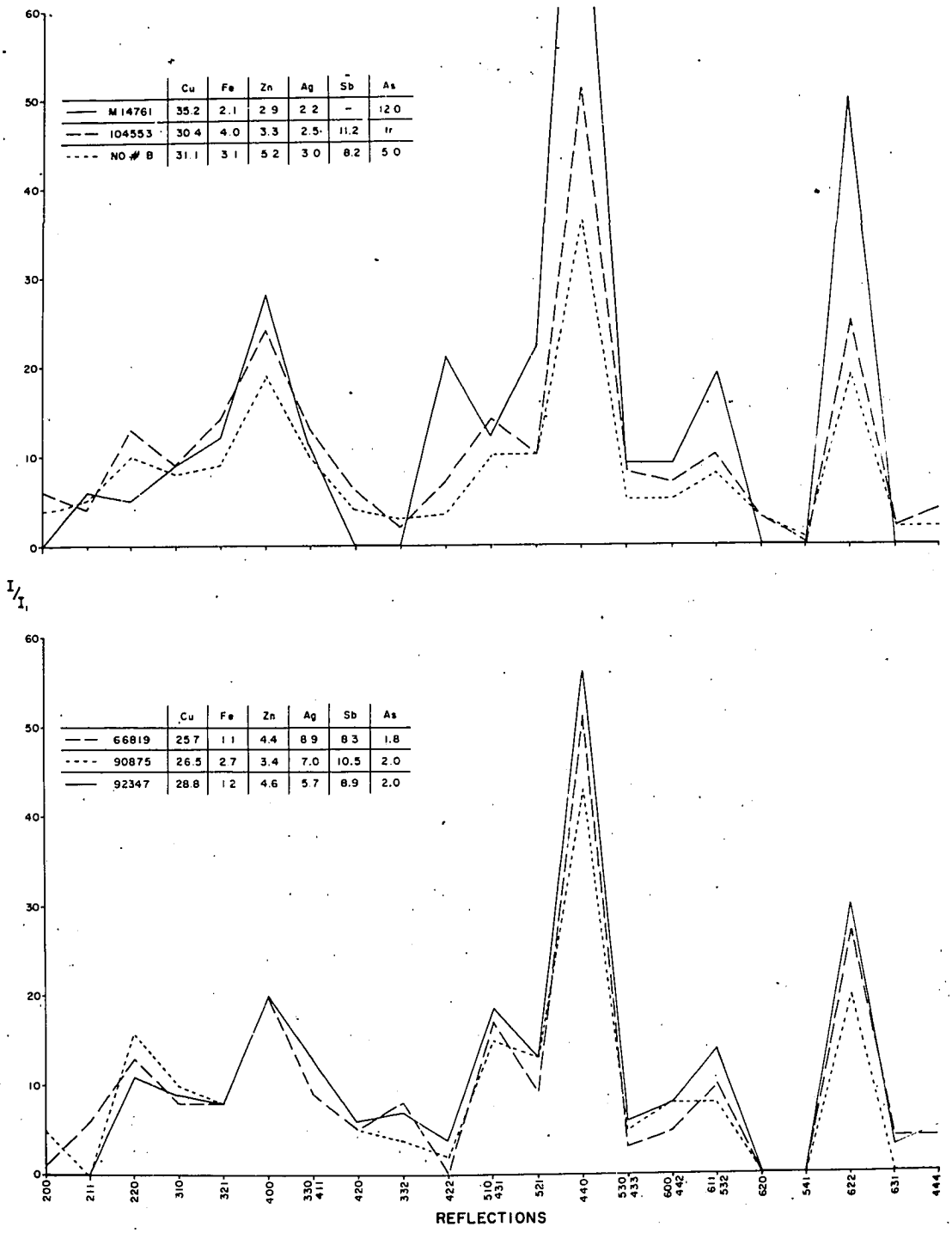

Figure 25. Variation of intensity of reflections in tetrahedrite series.

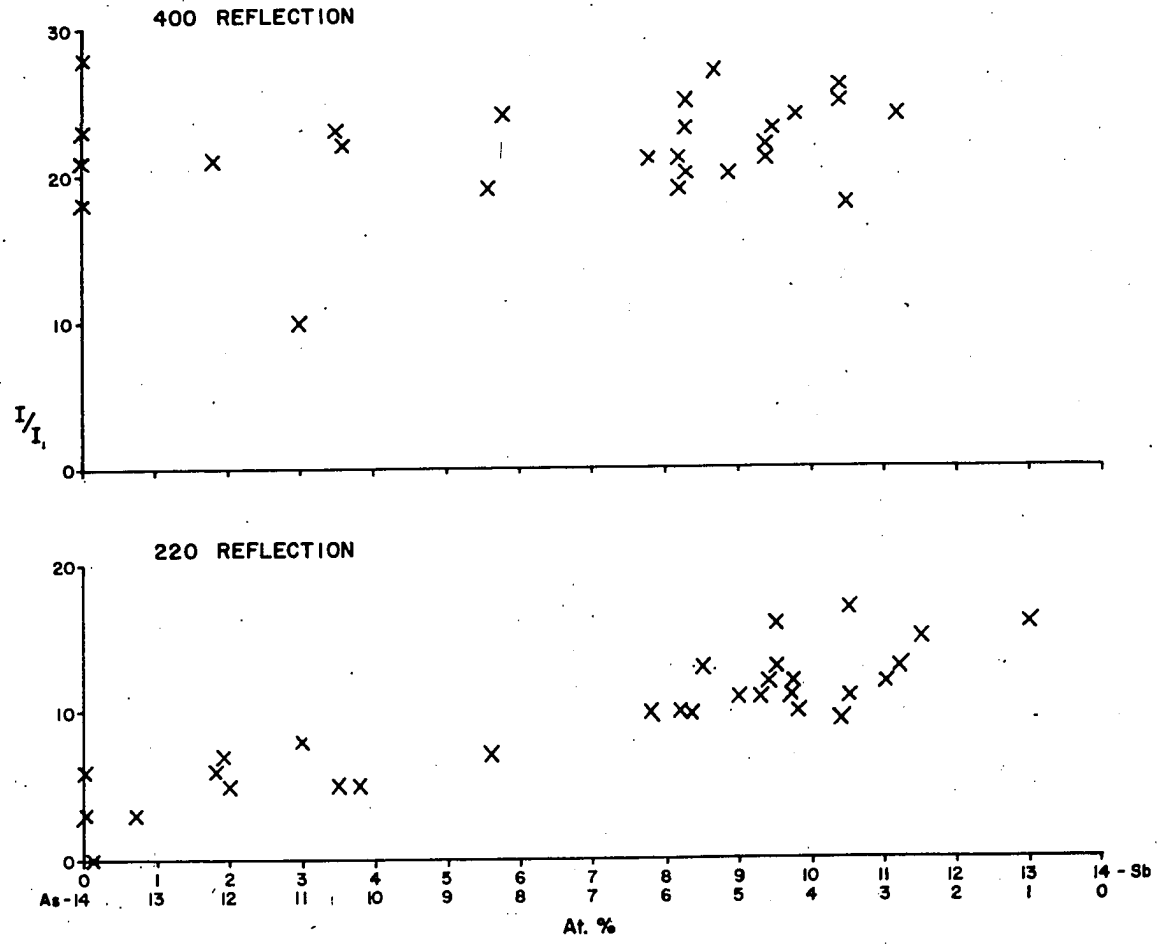

Figure 26. Variation of intensity of (400) and (220) with Sb-As.

selective sites; (3) the high scattering factor ought to make the effect of the silver atoms on certain planes detectable. The bottom diagram of Figure 25 shows the intensity of reflections plotted for three specimens which vary in silver content, and Figure 27 shows several reflections plotted for all silver-bearing specimens. The strongest upward trend with silver occurs with the (510, 431) reflection. The (510) plane is strongly affected by Cu-II sites, but the (431) has not been assessed. Silver may disorder on Cu-II sites, but this conclusion is not yet justified.

"EXTRA" REFLECTIONS BELONGING TO TETRAHEDRITE STRUCTURE

Nonius-Guinier powder camera photographs of several specimens of the tetrahedrite series reveal two additional lines belonging to the mineral structure but never previously reported. The lines are brought out by long exposure (15 hours) on a Nonius-Guinier camera using a curved quartz monochrometer. These reflections are anomalous lines for x-ray powder diffraction patterns of a cubic body-centered lattice and do not both have rational indices.

The lines occur between the (310) and (222) reflections very close to the (222). Table 9 shows the positioning and d-values for these lines as well as a persistent blurry region. The reflections are present

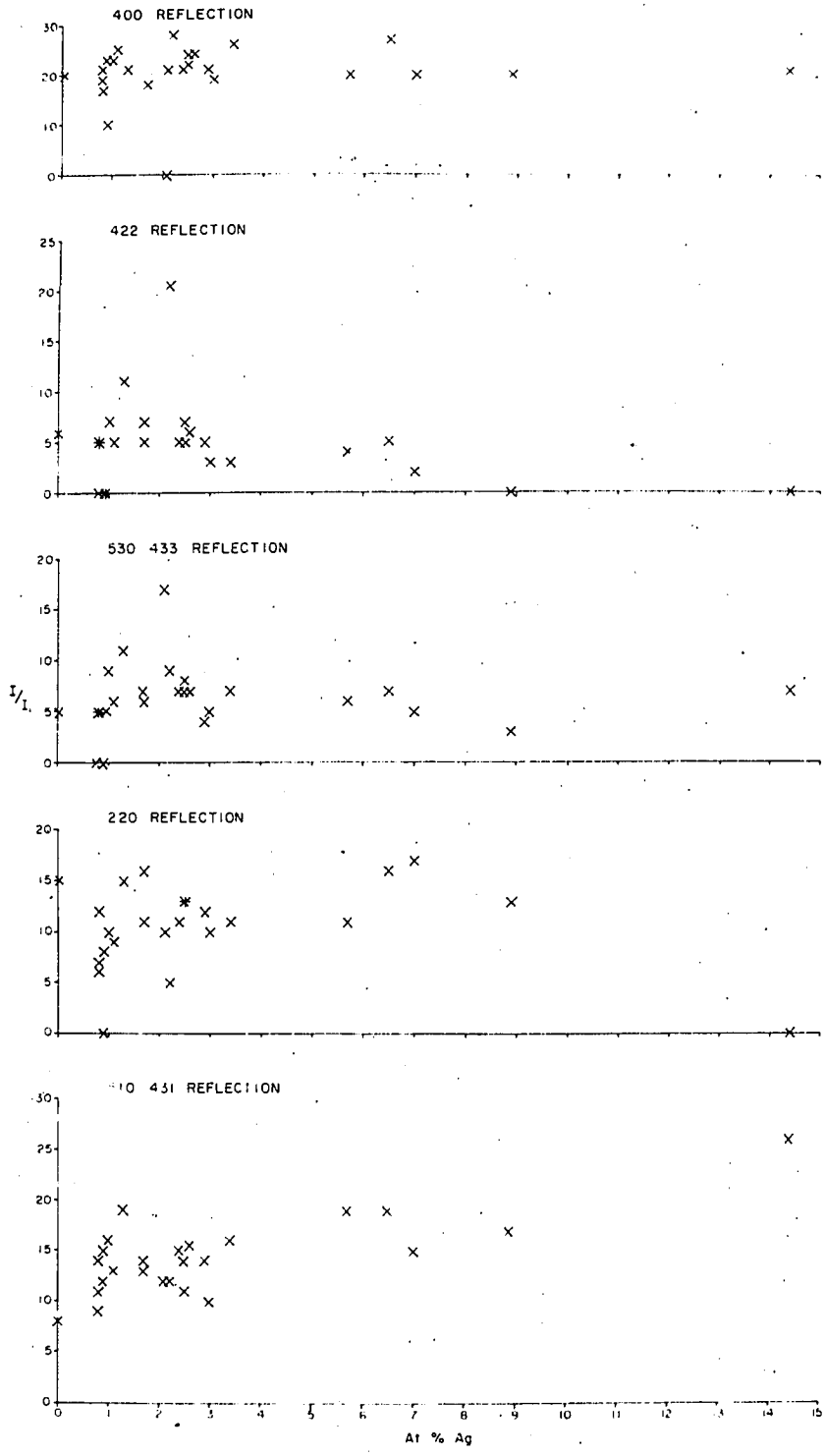

Figure 27. Variation of intensity of reflections with Ag.

in specimens widely different in co chemistry and cell dimensions. Further, the three spqpecimens illustrate that both lines and the blurry regpegion increase in d-spacing along with other reflectioo.ons with increasing cell dimensions. The possibility v of some persistent contaminant is consequently ruled I out. The lines must belong to the mineral structure oftof the tetrahedrite series.

These lines may indicate an co ordering of atoms not shown in the published structure, , since other possibilities do not account for the lines. Tabdable 10 shows that the lines cannot be accounted for as (1) Co K_B peaks of (222), or as (2) simple harmonics s of the next most intense lines (440) and (622). A A search of 0, 1, and 2-level x-ray photographs taken omon the Buerger precession camera shows no symmetrically arrärranged extra spots, though any very weak reflections could beoe missed.

TETRAHEDRITE AS A DERIVATIVE STRUCTURE

Emphasis has been place on tetetrahedrite-tennantite as a derivative structure of the s simple basic sphalerite structure. The basis for this thinking is the similar cubic-closest packed arrangement o of sulfur atoms with metals completely filling the tetrahedral interstitial sites. The structure is regarded as defective in that

TABLE 9

■ NONIUS GUINIER X-RAY DATA SHOWING "EXTRA" LINES

	C819 $a_o = 10.26$		88118 $a_o = 10.35$		66819 $a_o = 10.55$	
hkl	θ	d	θ	d	θ	d
110	7.06	7.277	7.05	7.287	6.90	7.445
- blurry	8.76	5.873	8.63	5.960	8.55	6.016
200	10.02	5.140	9.95	5.176	9.80	5.255
211	12.33	4.188	12.23	4.222	12.05	4.284
220	14.30	3.621	12.92	4.000	12.67	4.078
310	16.06	3.233	15.91	3.262	15.66	3.313
---	16.87	3.082	16.73	3.107	16.42	3.164
---	17.17	3.029	17.17	3.029	16.70	3.112
222	17.61	2.956	17.43	2.986	17.13	3.036
321	19.10	2.733	18.90	2.761	18.57	2.808
400	20.46	2.558	20.25	2.584	19.91	2.626
330 411	21.76	2.412	21.55	2.435	21.16	2.477
420	23.02	2.287	22.76	2.312	22.40	2.347
332	23.93	2.205	23.92	2.206	23.52	2.241
422	25.36	2.088	25.07	2.110	24.66	2.143
510 431	26.47	2.006	26.17	2.028	25.70	2.062
521	28.58	1.869	28.28	1.887	27.78	1.919
440	29.63	1.809	29.31	1.827	28.77	1.858
530 433	30.65	1.754	30.28	1.773	29.77	1.801
600 442	31.51	1.711	31.15	1.729	30.57	1.758
611 532	32.46	1.666	32.12	1.682	31.53	1.710
620	33.45	1.622	33.07	1.639	32.50	1.664
541	34.42	1.582	34.05	1.597	33.37	1.626
622	35.30	1.547	34.91	1.562	34.26	1.588
631	36.25	1.512	35.83	1.528	35.17	1.552
444	37.16	1.480	36.75	1.494	36.02	1.521
710 550 543	38.06	1.450	37.62	1.465	36.88	1.490

■ Co Kα = 1.78890 Å

TABLE 10

CALCULATIONS FOR "EXTRA" LINES ON NONIUS GUINIER PHOTOGRAPHS (Co Kα = 1. 78890)

	d	d corr.	$h^2+k^2+l^2$	Co K_B = 1.6174 θ calc	2d for 440	2d for 622	Co Kα = 1.7889 θ corr
C819	a_o = 10.264 Å						
- -	3.0822	3.0893	11.03		3.6288	3.0958	16.83
---	3.0299	3.0368	11.4				17.13
222	2.9565	2.9629	11.97 (12)	15.83			17.57
88118	a_o = 10.350 Å						
- -	3.1072	3.0911	11.20		3.6592	3.1206	16.82
- -	3.0299	3.0316	11.65				17.16
222	2.9861	2.9877	11.99 (12)	15.70			17.42
66819	a_o = 10.552						
- -	3.1642	3.1755	11.03		3.7306	3.1814	16.36
- -	3.1126	3.1235	11.4				16.64
222	3.1368	3.0461	11.99 (12)	15.40			17.07

sulfur atoms are missing from the sulfur layers. This defect could be corrected by filling in the spaces with the missing sulfur atoms. The structure could then be derived from the sphalerite-type by replacing the one metal atom with the variety of metals found in the tetrahedrite series. This thinking reached its culmination with Ross' (1957) structural classification of the sulfides in which tetrahedrite-tennantite appears as a "complex defect derivative structure" under the basic sphalerite type.

Aside from the convenient simple way of looking at these structures from the point of view of similarities in their geometry, some important dynamic relationships follow. In derivative structures, it is necessary only to change the small interstitial metal atoms without rearranging the stacking of the large sulfurs to revert back to the simple basic type and vice versa. Thus, both chalcopyrite and tetrahedrite (fig. 8, 23, 22) can revert geometrically to the sphalerite structure merely by changing the metal atoms to one atom type and, in the latter case, correcting the defects by filling in the sulfur network. Such a transition is not only geometrically instructive but also may be real in a dynamic sense.

For example, according to order-disorder theory by

Buerger and others, at sufficiently high temperature (550°C) the Fe and Cu atoms in chalcopyrite may actively exchange tetrahedral interstitial sites within the stable sulfur network. In this manner, the atoms become randomly distributed or disordered in sites formerly occupied by ordered Fe and Cu atoms. At this time, for any particular site we have a hybridized atom which is half the time Fe and half Cu and so acts like a single metal atom. When this high-temperature disordered phase is quickly cooled and frozen in, its unit cell is face-centered cubic, similar to the sphalerite cell with slightly different cell dimensions.

Since tetrahedrite-tennantite can be considered a complex defect derivative of the sphalerite-type structure, one of the objectives of this study was to find evidence (or the lack of it) for an order-disorder relationship similar to that for chalcopyrite and other minerals. Such a relationship would have important implications in geothermometry and in the interpretation of the paragenesis of ore minerals from textural relationships.

For geothermometry, both any frozen-in disordered phase or a reordered phase theoretically could be detected. (See section on Frueh's work). The critical temperature for the order-disorder transformation would be of interest.

The tetrahedrite series is commonly associated with the structurally-similar chalcopyrite and sphalerite as well as other sulfides. The interpretation of replacement, exsolution, and simultaneous crystallization textures is a difficult procedure because of confusion of these processes. Were the above three minerals to have a common high temperature phase, they could be expected to exsolve upon cooling.

Most of the structural work in this paper has been done on natural and some synthetic material on recorded diffraction patterns obtained by the powder method. All of this data for 41 natural members of the tetrahedrite series and about 5 synthetic specimens appears in Appendix C. For this material, representing worldwide occurrences, all of the reflections that were detected have been accounted for as belonging to the tetrahedrite structural pattern.

Synthetic members of the tetrahedrite series, quenched just below melting point for stoichiometric mixtures (table 3) do not show a different high temerature phase. All are typical tetrahedrites. Natural materials show only those reflections accounted for by the determined tetrahedrite structure. Those that are missing are weak and lost in the background. For some specimens, these reflections have been verified by means

of Nonius-Guinier photographs. Thus no obvious high temperature phase has been frozen-in to natural members of the tetrahedrite series.

In view of this evidence, the tentative conclusion is held that there is not an order-disorder relationship for all the metal atoms in the tetrahedrite series, resulting in a high temperature phase in common with either sphalerite or chalcopyrite. Such a view leads naturally to an emphasis of the differences, rather than the similarities, in chemistry and structure between sphalerite and tetrahedrite.

Differences in Chemistry.

The tetrahedrite series is chemically complex, with a number of substituting atoms which differ considerably in size. Chemical analyses have shown that the substituting elements As, Sb, Bi, Ag, Hg are in part mutually exclusive. These atoms might show great resistance to exchanging sites because of size and valence differences. From Buerger (1949) the interchange of atoms to produce disorder depends on the energy required to break bonds and to stuff an atom into an unfavorable interstitial position. Thus, it might require too great energy to stuff the large Ag atom into any site or to change As or Sb from a kind of trigonal coordination to tetrahedral coordination. Such difficulties

are not encountered in the chalcopyrite case, where Fe and Cu have similar size and valence states and similarly coordinated sites.

Differences in Stacking.

Strock (1936) classified "defect" structures as those departing from the "structure theory", with defects characterized by:

1. Equivalent points not completely filled.
2. Equivalent points occupied by different atoms.
3. Combination of 1 and 2.

Now consider the tetrahedrite structure (fig. 7). Sulfur atoms are missing; that is, the sulfur lattice has points not filled, as in number 1 above. However, this is not a defect in the sense that Fe is missing from pyrrhotite ($Fe_{1-x}S$).. The S-II atoms are out of position by one-half layer, and the entire arrangement caused, apparently, by the failure of As or Sb to coordinate tetrahedrally with S. Thus the "defect" is not simply a case of a sulfur lattice with equivalent points not completely filled or occupied by different atoms.

It follows that the "abnormalities" (in the sulfur lattice) in the perfect interpenetration of metal and sulfur lattices are not deficiency defects that can be corrected by filling in the empty spaces. From the point of view of stacking, the tetrahedrite series is not a

good derivative of sphalerite. Disorder cannot be expected since differences in the Cu-I and Cu-II sites are caused by the S geometry and not the metal type.

Differences in Structure.

Past workers on the structure of the tetrahedrite series (Machatschki, 1928; Pauling and Neumann, 1934) have called attention to the similarity of the structure to that of sphalerite. Machatschki's structure, which is missing the uniquely positioned S-II atoms, probably has exerted a considerable influence on thought. Such a structure required only the filling of empty spaces in the sulfur lattice and conversion of metal atoms to a single type in order to revert to the simpler face-centered sphalerite structure. This kind of thinking has placed tetrahedrite as a defect derivative structure of sphalerite.

Recently Wuensch (1963) has called attention to the variety of coordination polyhedra comprising the tetrahedrite structure. The planar Cu-II - S_3 groups form a six-bladed spinner as central axis of the unit cell. In contrast to the $metal_4$ - S tetrahedra in the structures of sphalerite and chalcopyrite, the tetrahedrite structure has several polyhedra. They are the $metal_4$-S-I tetrahedron, the flat Sb -S_3 (or As - S_3) polyhedron and the Cu-II_6-S

octahedron coordinated between two sulfur layers. According to Wuensch, "it is misleading to conceive of the tetrahedrite structure in terms of ordered Sb or As substitutions in tetrahedral Cu sites."

Both theoretical considerations and structural investigations of natural and synthetic materials agree that the tetrahedrite series ought not to show dynamic disorder leading to a more simple sphalerite-type cell. Further structural studies would best be directed toward elucidating the limited isomorphous series and the disordering sites of various substituting elements within the tetrahedrite structure.

CONCLUSIONS

From the results of work presented in this paper, the following conclusions are drawn.

1. In the tetrahedrite series, complete solid solution exists between Sb and As only for certain varieties. For varieties with greater than 2.5 atomic percent silver or other large atoms, a gap exists in the series from about 6 to 11 atomic percent arsenic. This gap is transgressed by small atom varieties in the series.

2. Evidence from chemical analysis and x-ray diffraction patterns suggests that the composition gap

between Sb and As marks an unmixing field for varieties having greater than 2.5 atomic percent silver.

3. From chemical analyses, the extent of solid solution of bismuth in the tetrahedrite series is suggested. Solid solution between As and Bi is quite restricted, but is extensive between Sb and Bi. A solid solution field has been delimited on the As-Sb-Bi composition triangle.

4. High amounts of the large elements Ag, Bi, and Hg associate preferentially in the tetrahedrite field. In tennantites, Ag is limited to less than 2.5 atomic percent. The very large atoms Bi and Hg tend to occur together in tetrahedrites. Exceptionally high Ag analyses are from nearly pure tetrahedrites or bismuthian varieties.

5. Zinc and iron are randomly distributed in the tetrahedrite series. The sum Fe + Zn in atomic percent tends to have a fixed value, especially in the tennantite field, near 6.5. For tennantites, the formula $Cu_{10}(Fe,Zn)_2(As,Sb)_4S_{13}$ may be indicated.

6. Though classed as a derivative structure of the basic sphalerite type, x-ray diffraction results on natural specimens and synthetics quenched at high temperature indicate no evidence of a high-temperature disordered phase. These results are in keeping with chemical,

coordination, and structural differences in tetrahedrite from sphalerite. Tetrahedrite is not a good derivative of sphalerite either from a dynamic point of view or from the point of view of stacking geometry.

7. New lines, definitely related to the mineral structure, appear in long-exposure Nonius-Guinier photographs. These are probably related to a slight ordering of atoms.

8. Cell dimensions in the tetrahedrite series cover a range from about 10.18 Å to 10.55 Å. Since Fe and/or Zn is almost invariably present in substantial amount, few specimens have cell dimensions lower than 10.25 Å. The graph of cell size variation for the tetrahedrite series may be used to make a rough estimate of the chemistry of a specimen from its cell size.

9. The brown streak color is related to the relatively non-metallic character of As and Zn in the tetrahedrite series. The brown color is related to the Zn content and in a permissive way to the As content. Light brown streak is limited to Zn-bearing tennantites.

10. Further work with natural specimens ought to be done on the disordering sites of various substituting elements. Both natural and synthetic specimens can be investigated for exsolved phases in the tetrahedrite series.

APPENDIX A

DETAILED PROCEDURES

Separatory Procedure. Tetrahedrite-tennantite was separated from specimens by means of Clerici solution and the Frantz Isodynamic Separator. First a crude hand-picking was done where practicable. Generally about 5 to 25 grams of sample were necessary to obtain 3 to 10 grams of pure separate. This amount was suitable for x-ray work, furnace trials and chemical analysis. The sample was crushed and ground in a mortar and pestle, and screened to the size range 115-170 mesh. This size provides for good separation of attached mineral grains and is convenient for techniques with Clerici solution and the magnetic separator. Further, this size is convenient for investigation of grains with the binocular microscope.

Dust was thoroughly washed from the grains with water and acetone. Acetone dries fast and, because of its small surface tension, was particularly effective in wetting the grains and removing the dust. Removal of dust was essential, since dust would contaminate the Clerici solution and interfere with separation in the magnetic separator.

The Clerici solution was adjusted with water until chalcopyrite just floated. The dry sample grains were added to Clerici in a separatory funnel. This gravi-

metrically separated such minerals as chalcopyrite, sphalerite and the light gangue minerals as the light fraction. Tetrahedrite-tennantite, along, with such minerals as bornite, pyrite, galena, and others were collected as the heavy fraction. A grade of coarse, perforated filter paper was found which allowed very rapid filtration (about 100 ml. per half hour) of the Clerici solution despite its high viscosity. Since the filtrate consisted of coarse grains, the filtered solution was perfectly clean. The heavy fraction of the filtrate was again washed and dried before proceeding to the magnetic separator.

The general procedure was to separate first a highly magnetic fraction from the fraction containing tetrahedrite-tennantite and then to separate tetrahedrite-tennantite from a non-magnetic fraction. Individual samples required different numbers of passes as well as slightly different settings of the magnetic separator depending on the minerals present and the susceptibility of the species of tetrahedrite-tennantite. Several samples required re-processing in Clerici solution to remove several percent of quartz, sphalerite or other minerals. Separations were made with side tilt between 1 and 5 degrees and forward tilt about 30 degrees. A highly magnetic fraction (usually bornite when present) separated cleanly with only minor loss of tetrahedrite at about 0.60 amperes. Tetrahedrite

then separated cleanly from the more non-magnetic material by making passes with settings ranging from 0.65 to 1.50 amperes.

Mineral Synthesis Procedure. Synthetics were prepared by heating stoichiometric amounts of material in evacuated silica glass tubing. A pelletizer was fashioned from a headless drill bushing with 3/16" hole fitted with a dowell pin 3/16" plus 0.0002". A plug was formed by cutting a small section from one end of the dowell pin. Drill rod was used for a pusher. All these pieces were hardened steel. This tight-fitting assembly prevented loss of sample in the pelletizing procedure.

With the plug in place, sample was introduced into the cylinder and the dowell pin inserted. The sample was compressed under 1380 pounds pressure (50,000 psi). To achieve a uniformly dense pellet, it was pressed from both sides. The pressed-out pellets weighed about one-half gram each. Pellets were stored in dessicator until sealed in glass tubes.

The pellets were sealed in Vycor Brand silica glass tubing for synthesis in the furnace. The outside diameter was 9 mm. and wall thickness 1 mm. This tubing has about 99 percent silica, softens over a range so that it can be sealed easily, melts around 1500°C., and has small coefficient of expansion so that it can be quenched in

ice water right from the furnace.

The Vycor was melted by torch using a mixture of lab gas and oxygen. First one end of the tube was sealed and the pellets inserted. The tube was then heated 2-3 inches above the pellets (to prevent volatilization and loss of any material) and drawn out to leave a small opening. A Duo-Seal Vaccuum Pump (Patent No. 2337849, W. M. Welch Manufacturing Co., Chicago) was attached to the tube and contents evacuated for 15 minutes. With pump still running, the small section of tube with the pellets was sealed off, ready for the furnace.

For heating the tubes, a Hoskins Electric Furnace (Type FD202c) equipped with Variac and Micromax (Leeds and Northrup) was used. The thermocouple was chromel vs alumel, and temperature was read with Leeds and Northrup Portable Precision Potentiometer No. 8662. Temperature was controlled to about plus or minus 10°C. Samples remained in furnace about 24 hours and were quenched immediately in cold water.

APPENDIX B

POLISHED SECTION DATA

The following 13 plates contain photomicrographs of textures and mineral associations of 26 specimens in polished sections. The scale shown in Plate 1 is the same for all specimens.

Plate 1.

Figure 1. 108759
Qtz, gn, py, tn. Section has blocky chunks of gn and tn with euhedral and subhedral py scattered through. Some qtz is euhedral with inclusions of tn. Tn one phase only.

Figure 2. 74553
Qtz, ccp, gn, td, bn, sp. Coarse-grained intergrowth. Some wormy-looking ccp and bn in td. Some qtz euhedral. Td one phase. Sp more associated with gn, bn with ccp and td.

Plate 2.

Figure 1. 96332
Qtz, td. Td veined with qtz and one other highly reflective mineral. May be a silver sulfide or silver. High silver analysis for this specimen is in question.

Figure 2. 51746
Intergrowth of td-tn and ccp. Qtz.

Plate 3.

Figure 1. Sunshine 3
Sid, qtz, py, td. Td veins sid. Qtz may be xenolithic. Py as remnants (sometimes subhedral) in td. Td probably replaces py.

Figure 2. M609
Ccp, qtz, py, tn. Subhedral py distributed through field of ccp. Tn appears to replace both. Tn one phase.

Plate 4:

Figure 1. No # B
Rock fragments, gn, ccp, td. Td is one phase; ccp apparently veins td.

Figure 2. C5262
Qtz, py, ccp, td. Section is cross-section of vein. Ccp fills minute fractures in qtz with replacement boundaries. Most ccp distributed in masses of partly euhedral py. Td veins and replaces ccp preferentially as well as py.

Plate 5.

Figure 1. 103164
Py, ccp, td, qtz. Possibly ccp and td interstitial to granular masses of euhedral py. Td essentially without ccp inclusions; the two form an intergrowth. Some qtz euhedral.

Figure 2. M728
Td, py, gn, qtz, bn. Coarse open-structured specimen. Py subhedral. Td one phase.

Plate 6.

Figure 1. 61823
Tn, ccp, qtz. Tn one phase.

Figure 2. M631
One phase td-tn.

Plate 7.

Figure 1. Wedge 2
Ccp, py, td.

Figure 2. 64941
Py, qtz, and two other phases.

Plate 8.

Figure 1. 90942
Field of td-tn, py((one large zoned py), euhedral qtz.

Figure 2. R1096
Py, gn, sp, tn. Tn one phase with blebs of py along boundary between tn and sp. Py blebs also in tn near contact, none in sp. Occasional angular bits of sp in tn.

Plate 9.

Figure 1. M14761
Py, ccp, bn, tn. Part of euhedral crystal of ccp. Tn apparently replaces ccp and bn.

Figure 2. 142652
Td-tn, ccp, bn, qtz.

Plate 10.

Figure 1. 61901
Gn, ccp, qtz, td-tn. Intergrowth.

Figure 2. M11654
Py, td, qtz, ?

Plate 11.

Figure 1. R1110
Fractured py crystals, tn, gn, ccp.

Figure 2. 115256
Ccp, td. One phase of td veined by ccp.

Plate 12.

Figure 1. 90864
Field of td-tn, euhedral py and qtz.

Figure 2. M18004
Droplet py in td-tn. Py apparently crystallographically oriented.

Plate 13.

Figure 1. 90776
Ccp veins broken py. Tn in ccp has droplet inclusions of ccp, crystallographically oriented.

Figure 2. 39599
Py, gn, td-tn, sid. Grid pattern of gn in td-tn.

PLATE 1

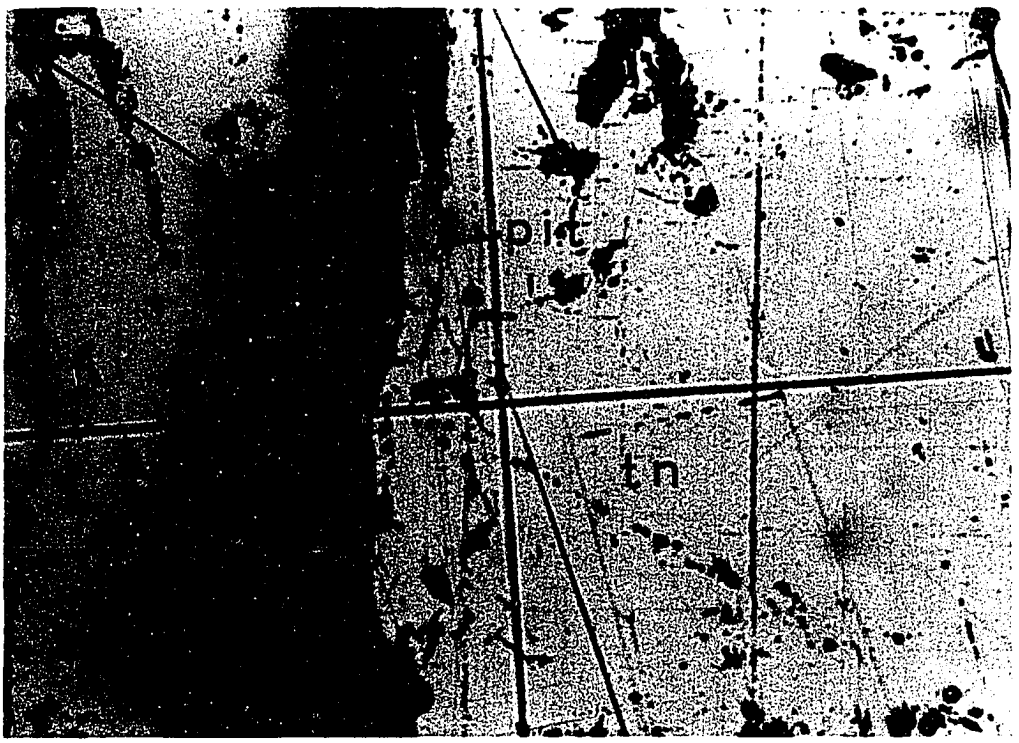

Figure 1. 108759

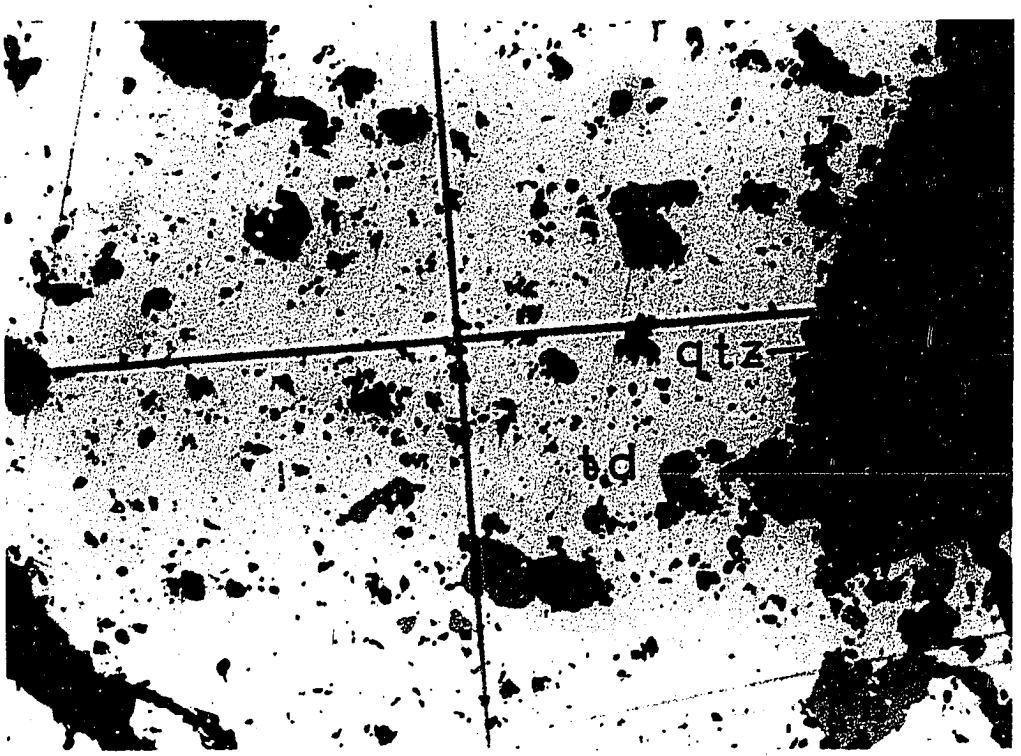

Figure 2. 74553

PLATE 2

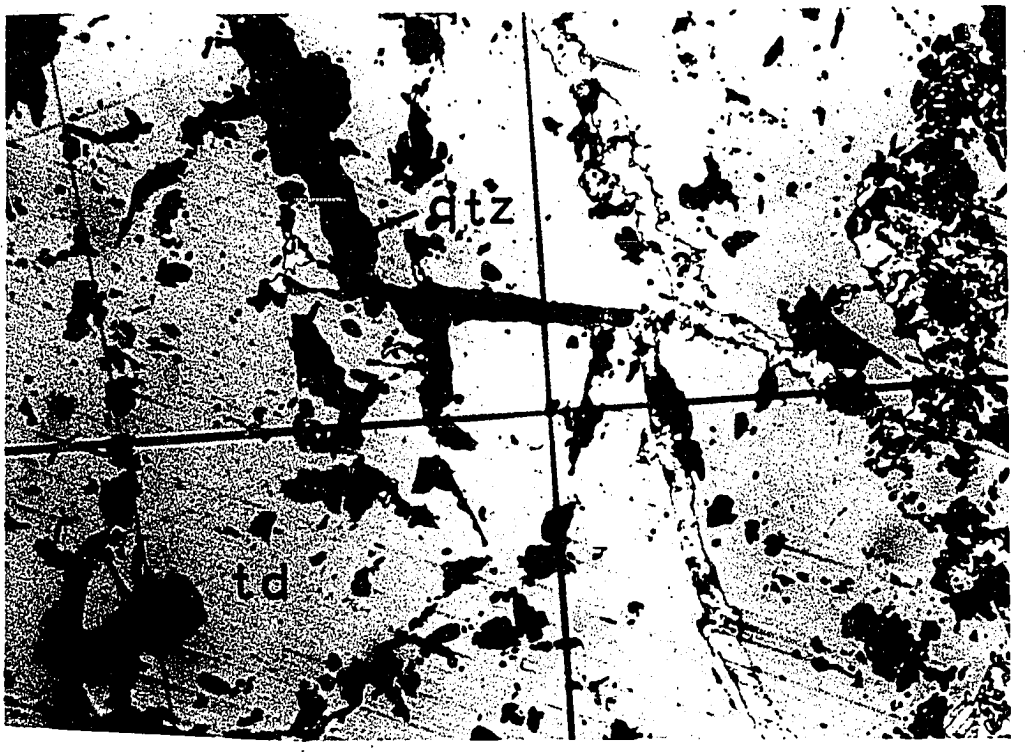

Figure 1. 96332

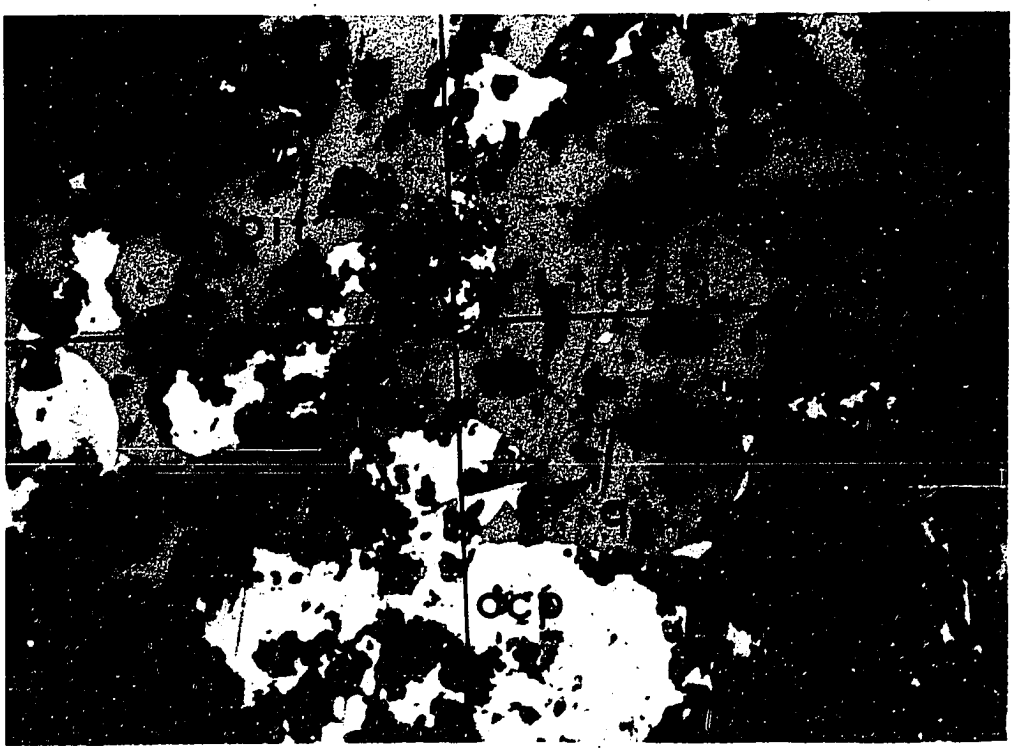

Figure 2. 51746

PLATE 3

Figure 1. Sunshine 3

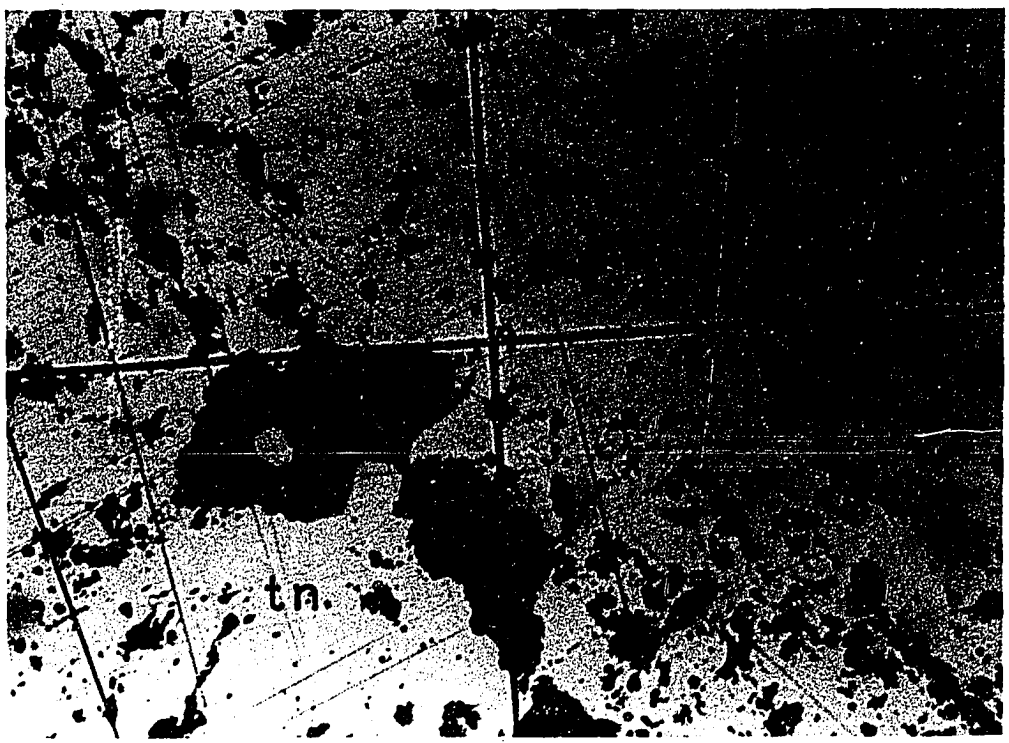

Figure 2. M609

PLATE 4

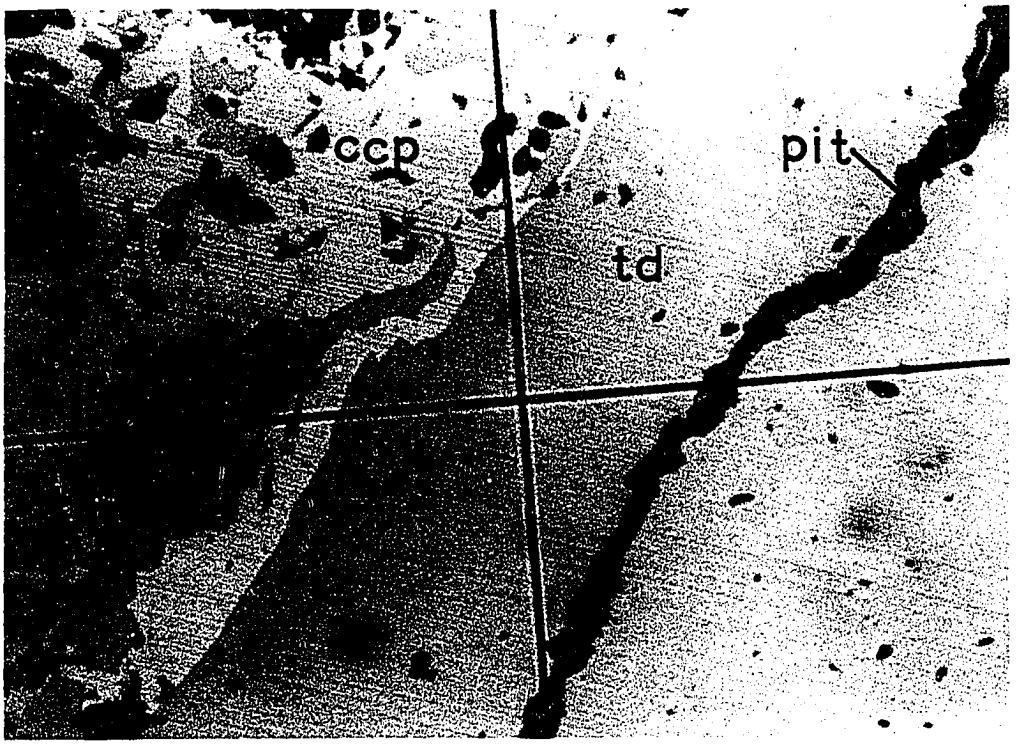

Figure 1. No # B

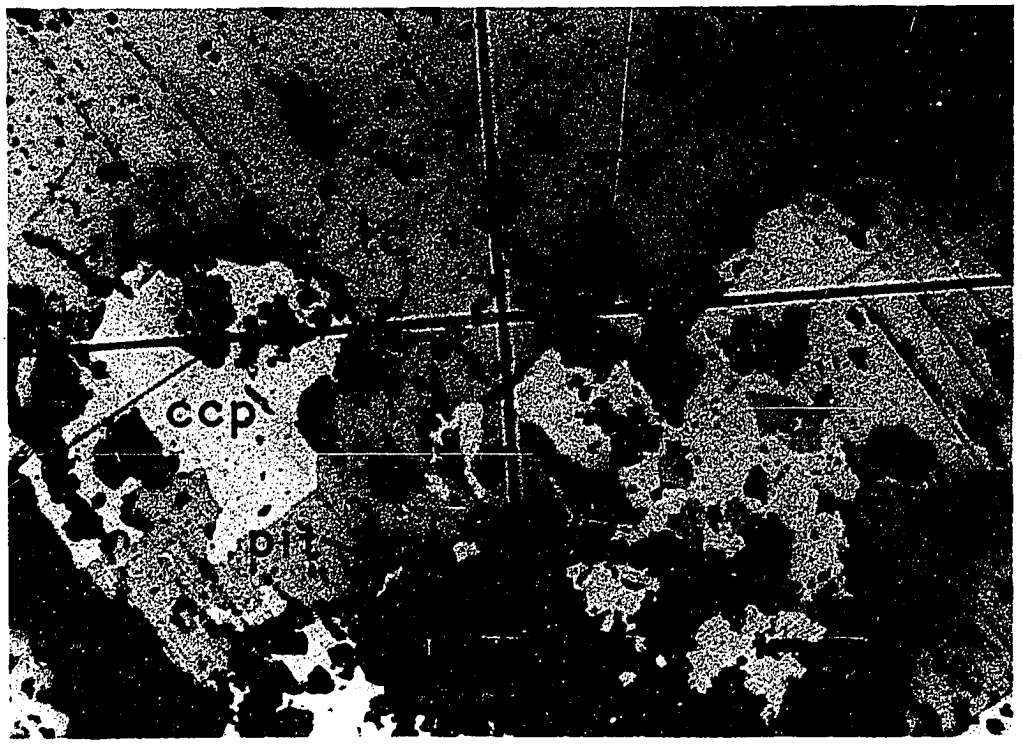

Figure 2. C5262

PLATE 5

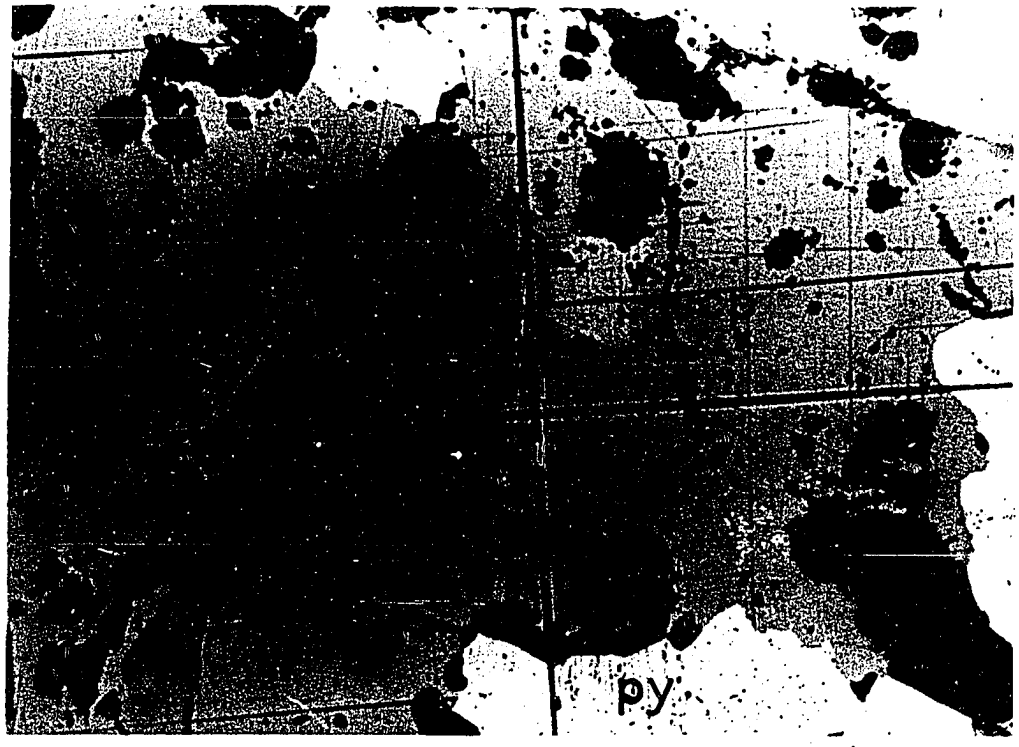

Figure 1. 103164

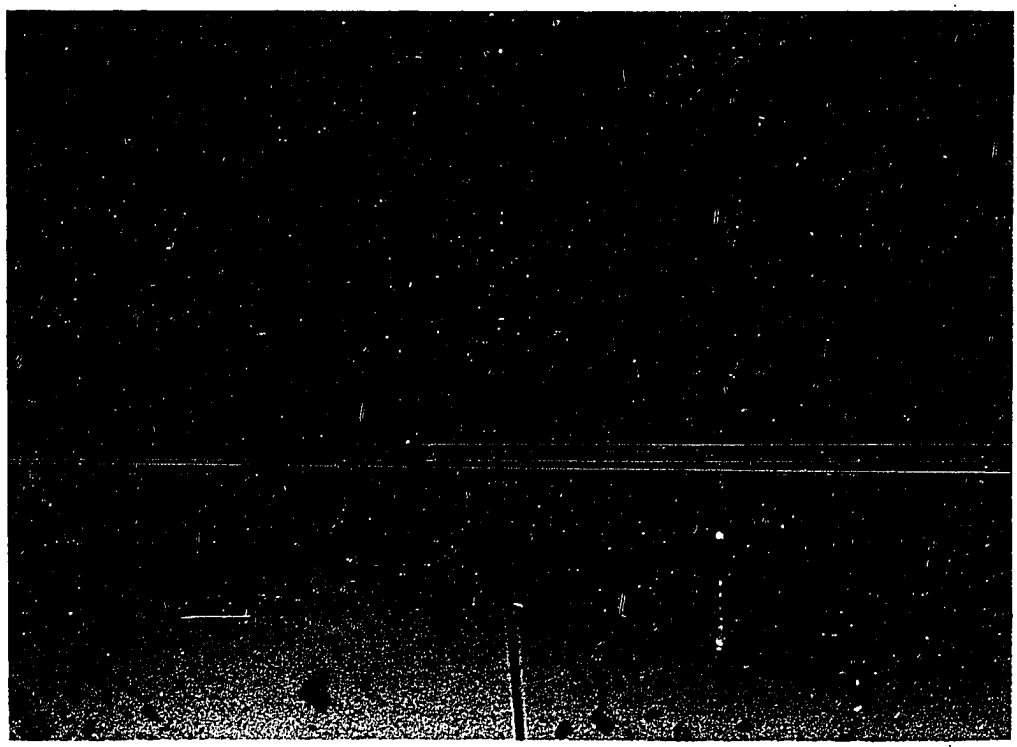

Figure 2. M728

PLATE 6

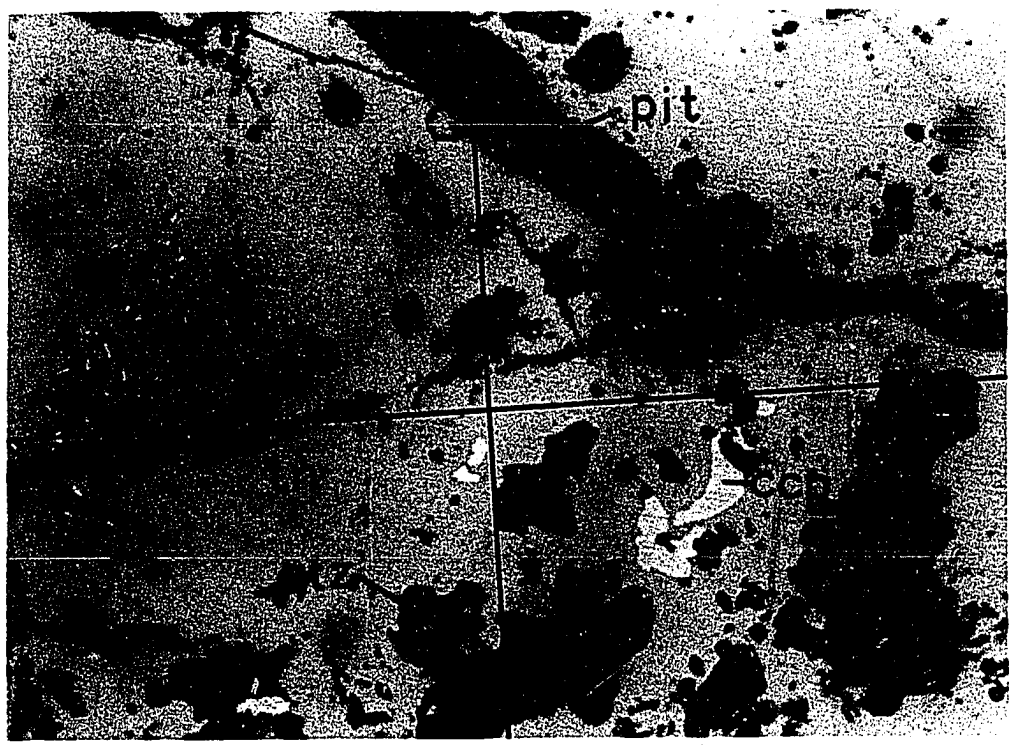

Figure 1. 61823

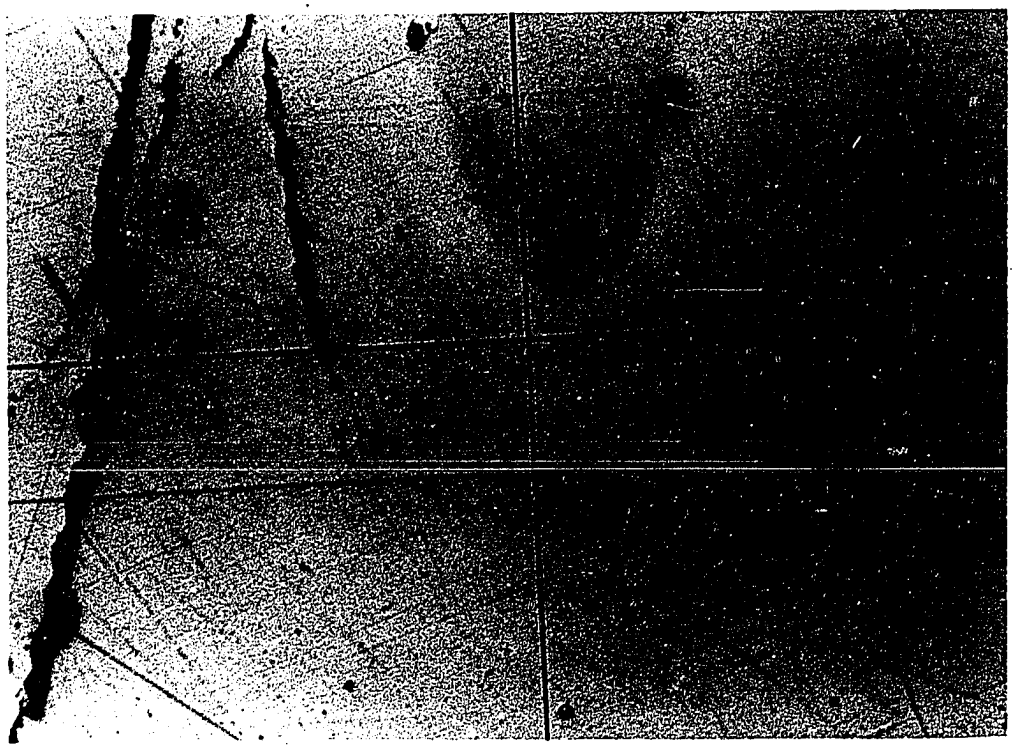

Figure 2. M631

PLATE 7

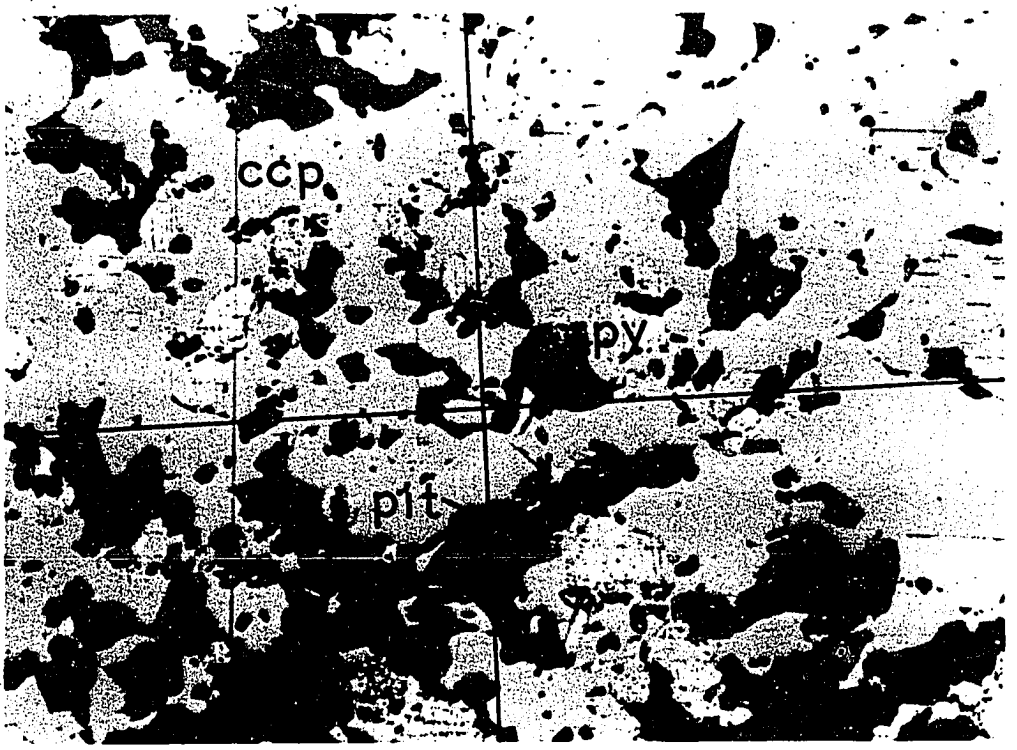

Figure 1. Wedge 2

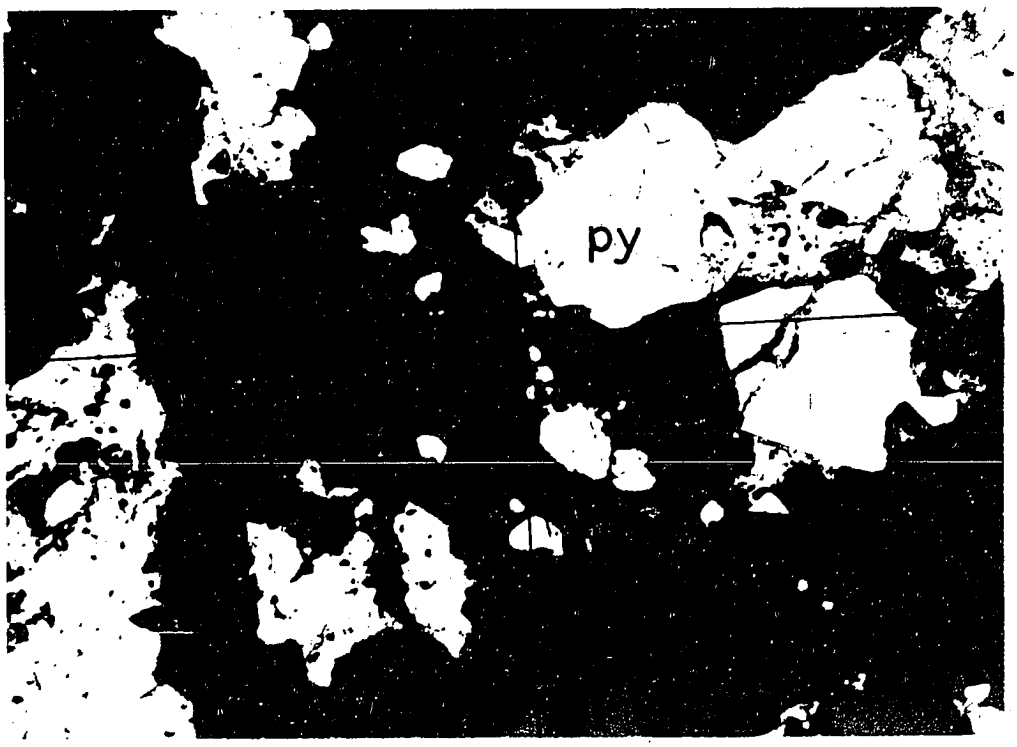

Figure 2. 64941

PLATE 8

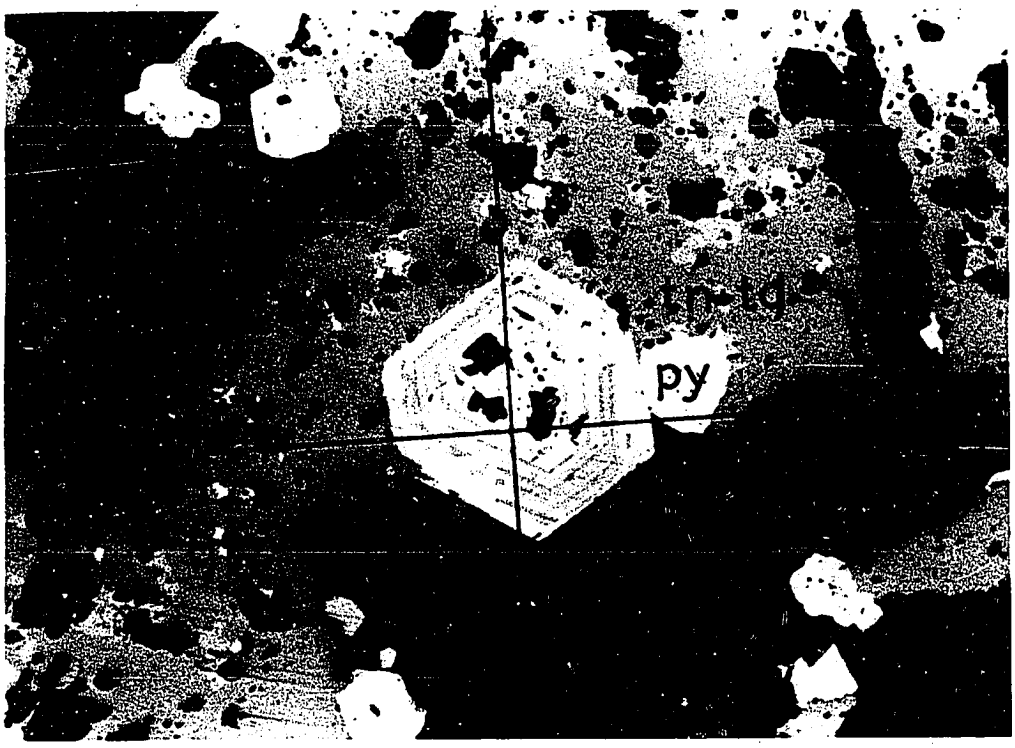

Figure 1. 90942

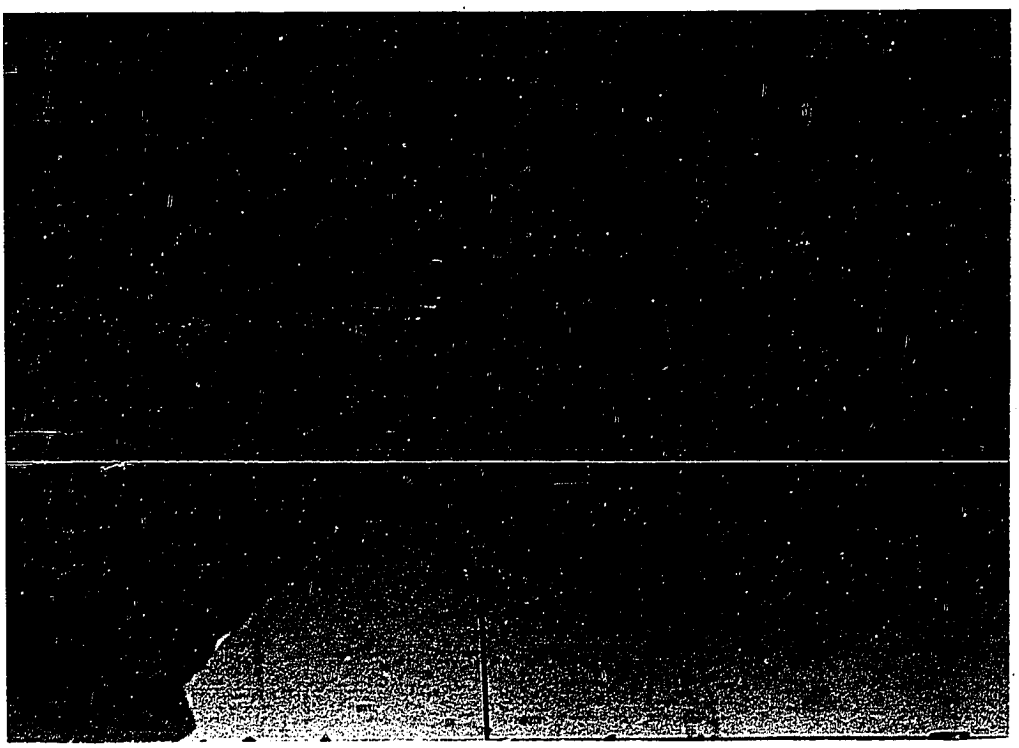

Figure 2. R1096

PLATE 9

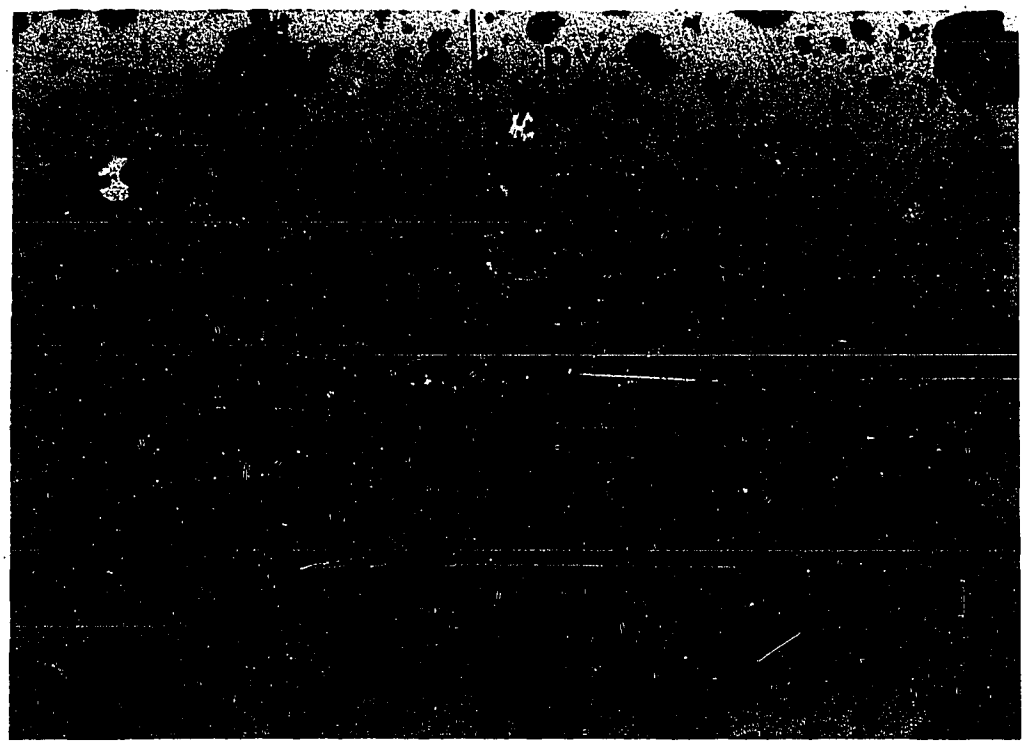

Figure 1. M14761

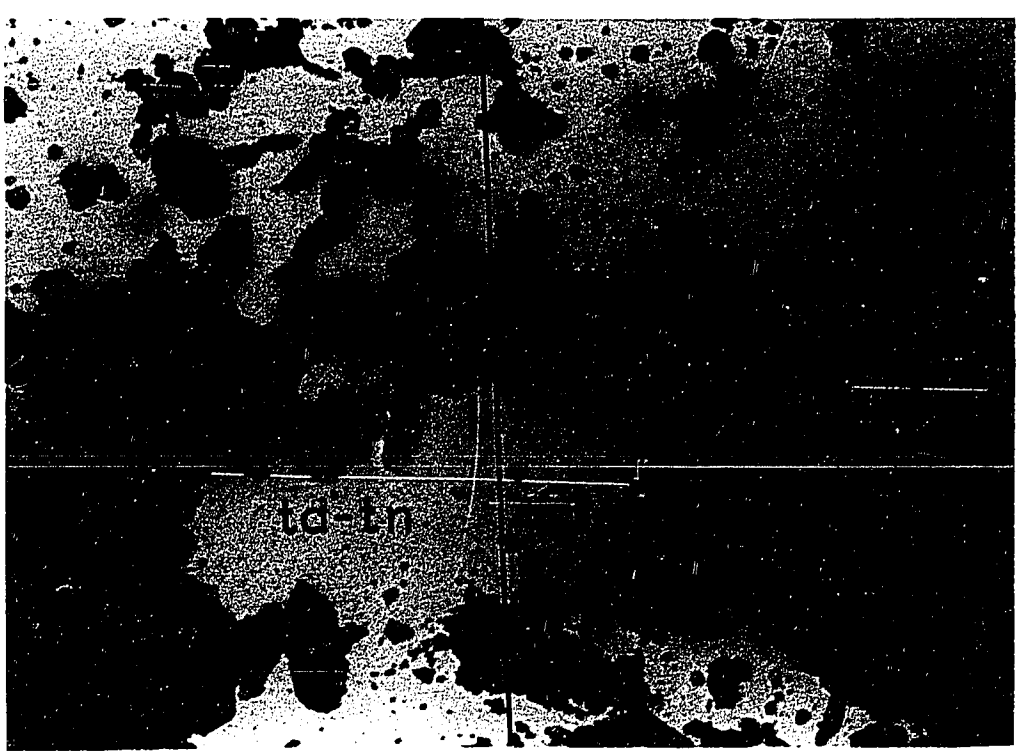

Figure 2. 142652

PLATE 10

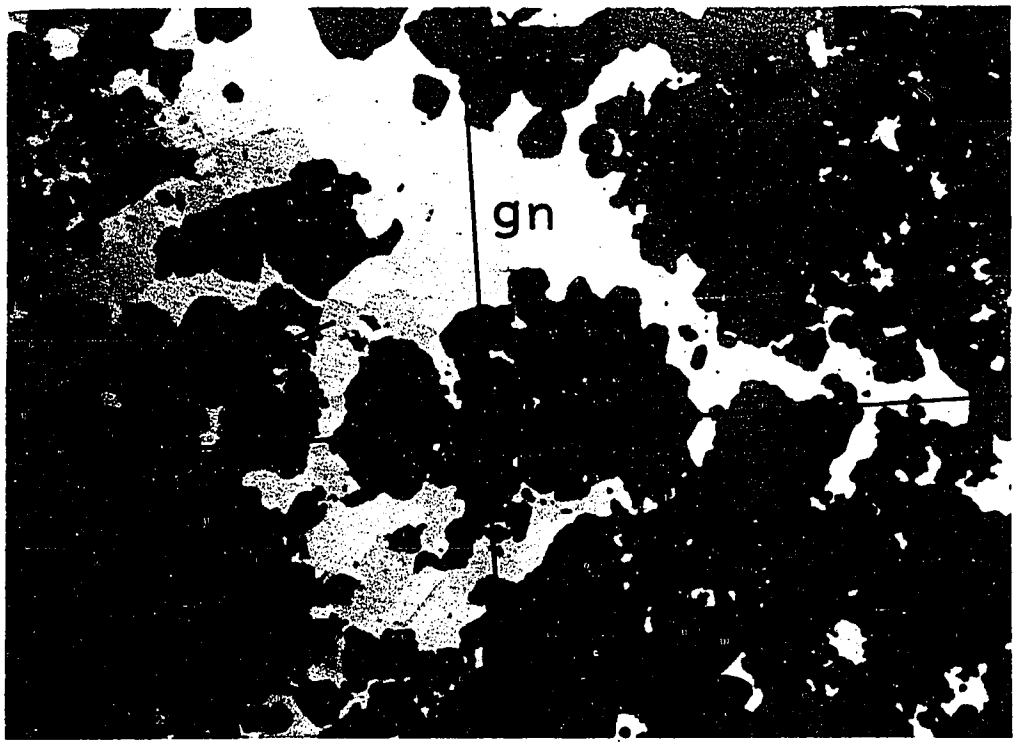

Figure 1. 61901

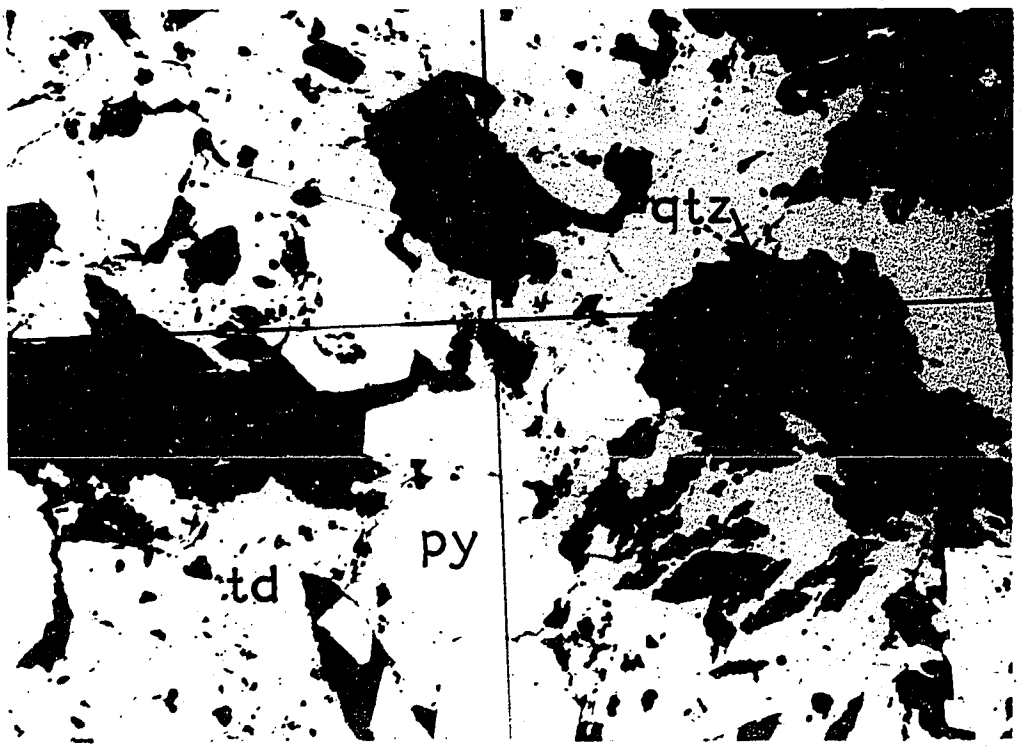

Figure 2. M11654

PLATE 11

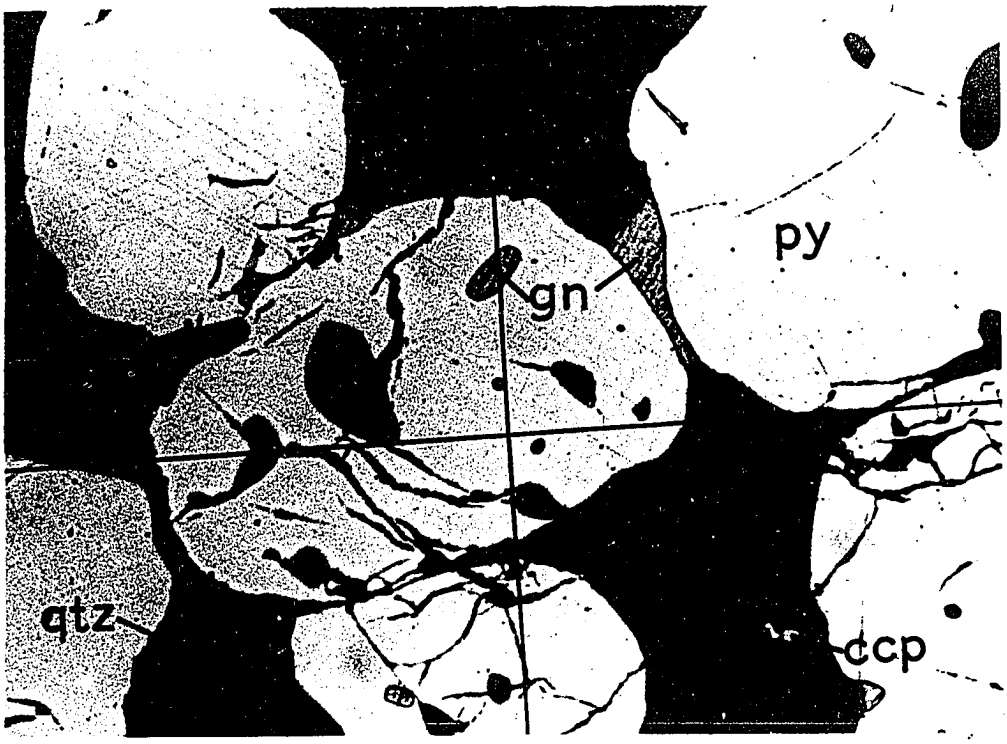

Figure 1. R1110

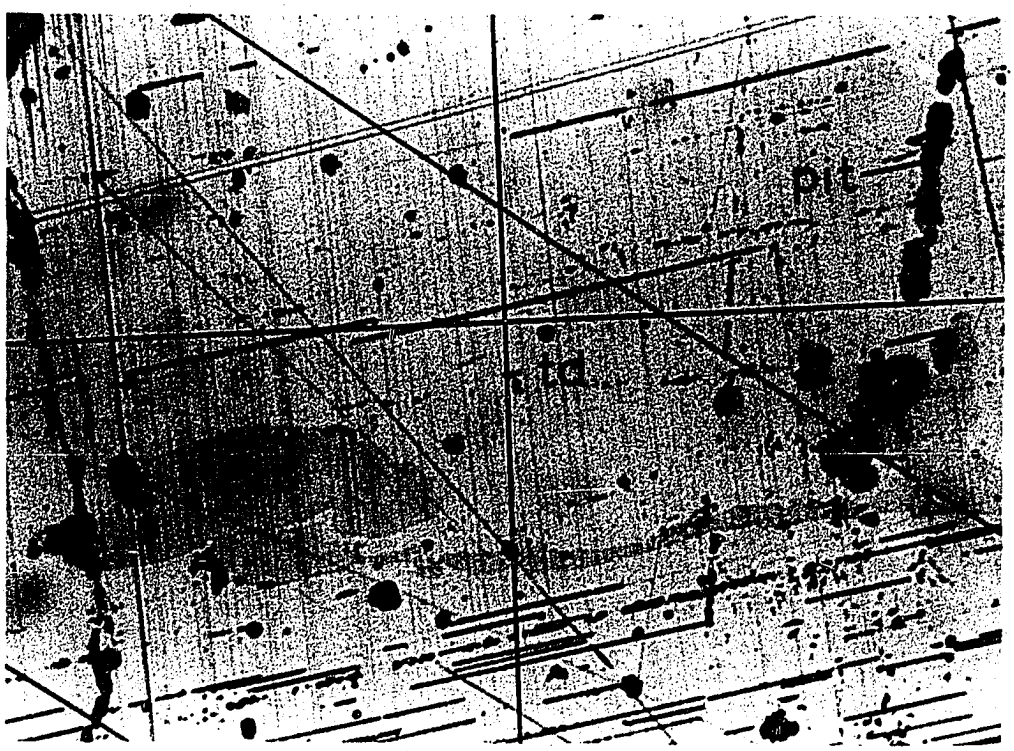

Figure 2. 115256

PLATE 12

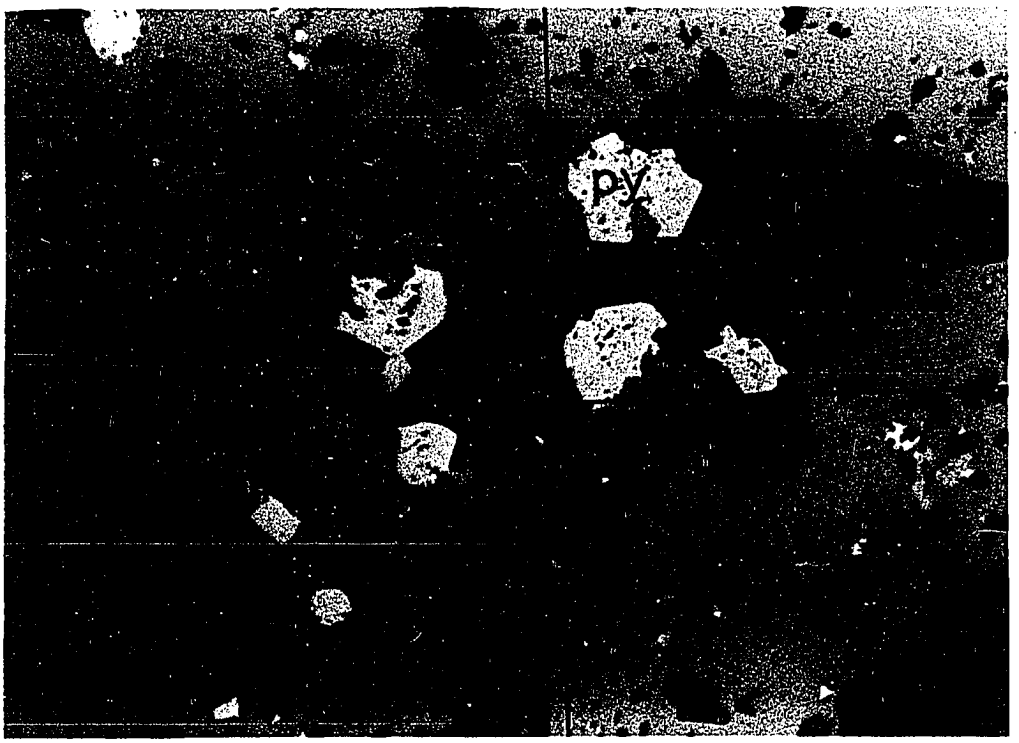

Figure 1. 90864

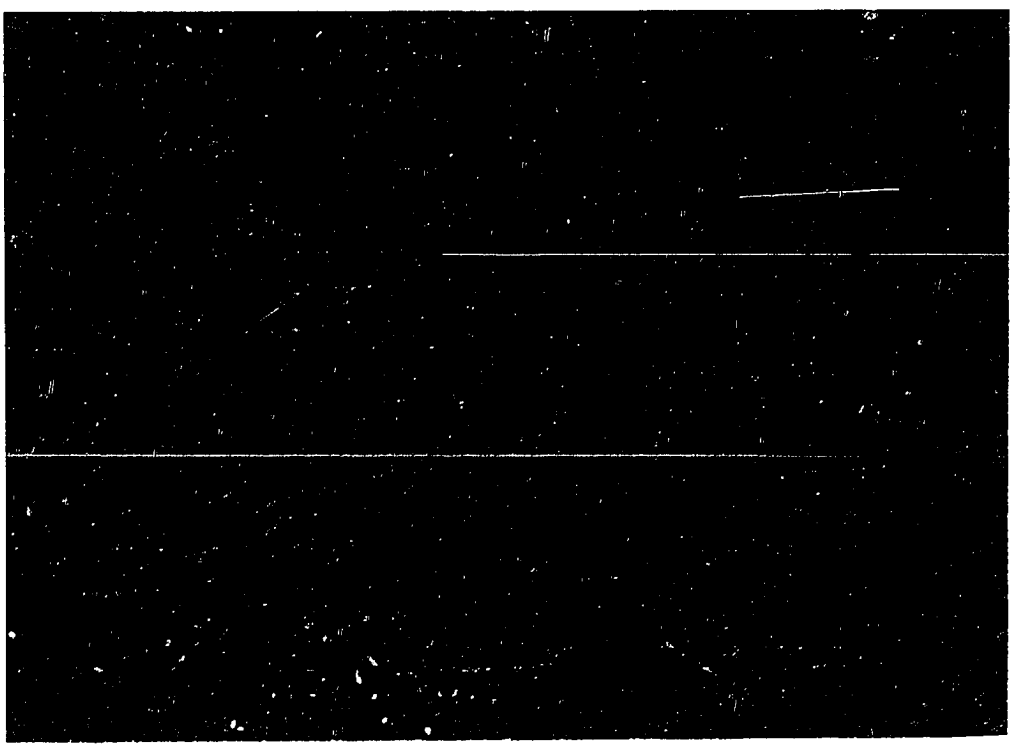

Figure 2. M18004

PLATE 13

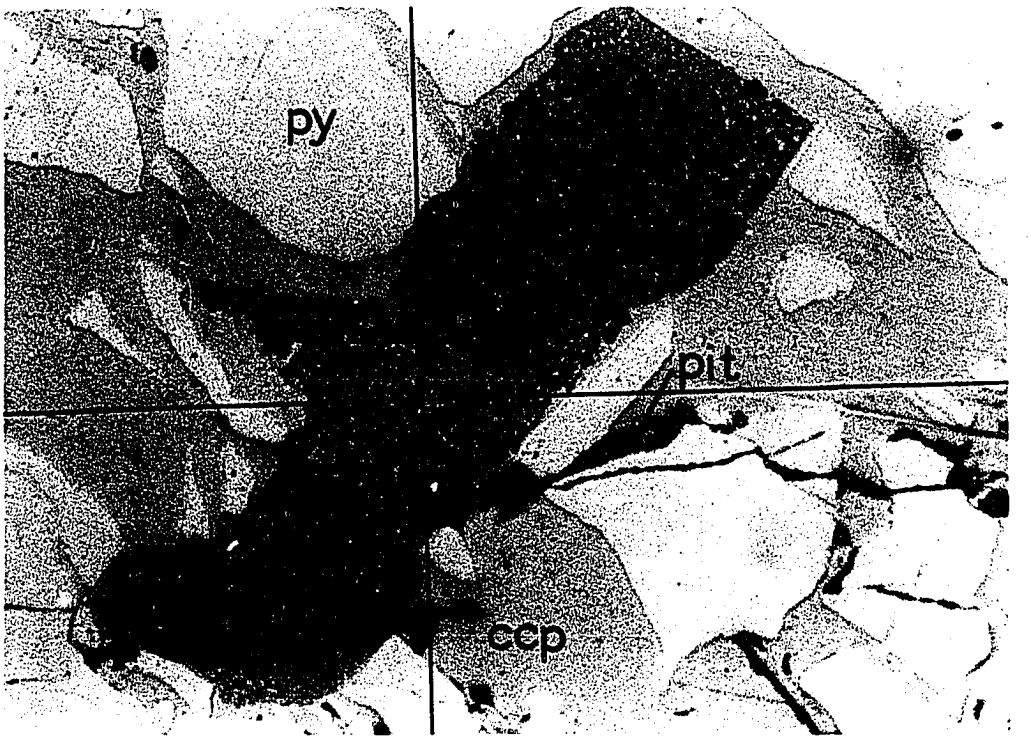

Figure 1. 90776

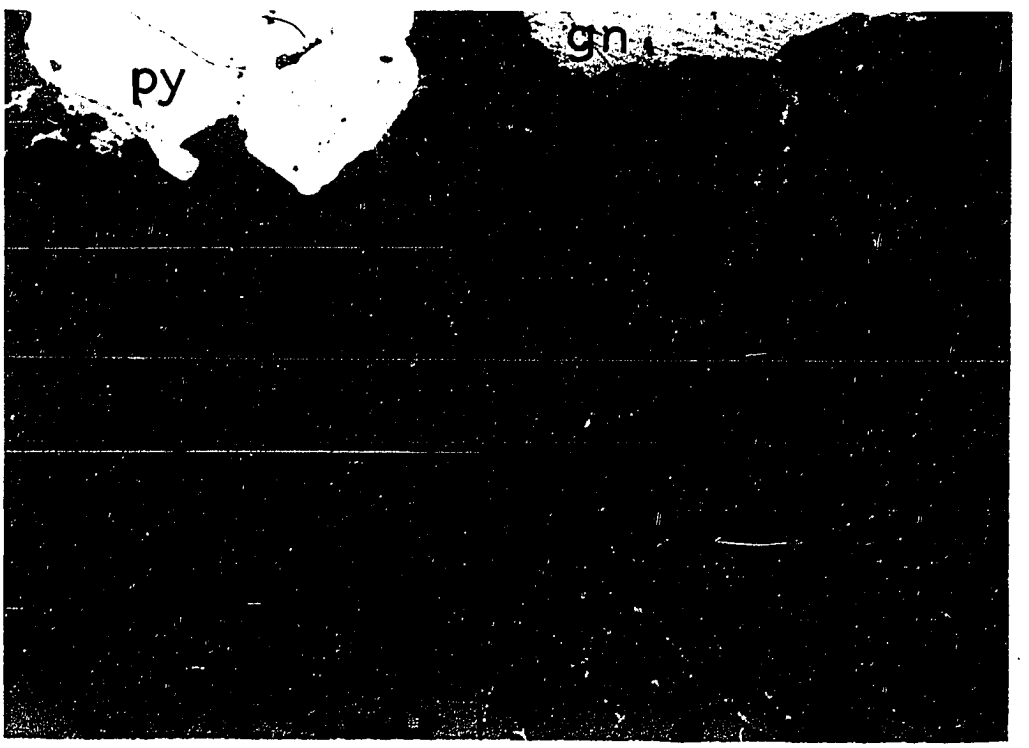

Figure 2. 39599

APPENDIX C

DATA FROM X-RAY DIFFRACTION POWDER PATTERNS

Specimens on the following pages appear in the order of increasing cell dimensions. The information shown below applies to all specimens x-rayed.

GE XRD-5 and diffractometer.
Radiation: Cu Kα (1.54050 Å).
40 kv, 16 ma
Slit system: 1°-3° MR
Ni filter.
Recordings (2θ) at 2°/minute.

Spec: S5-1B a_o = 10.188 ± .005

hkl	I/I_1	2θ	d	N	a_o	d calc	N calc
110	(not scanned)						
200	(undetected)						
211	11	21.33	4.1620	6	10.194	4.1592	5.99
220	(weak)						
310	12	27.39	3.2533	10	10.288	3.2217	9.80
222	100	30.42	2.9358	12	10.170	2.9410	12.04
321	7	32.76	2.7313	14	10.219	2.7228	13.91
400	22	35.25	2.5438	16	10.175	2.5470	16.03
330 411	14	37.46	2.3987	18	10.176	2.4013	18.03
420	(undetected)						
332	(undetected)						
422	(undetected)						
510 431	15	45.40	1.9959	26	10.177	1.9980	26.05
521	19	48.98	1.8581	30	10.177	1.8600	30.06
440	64	50.67	1.8000	32	10.182	1.8010	32.03
530 433	8	52.34	1.7464	34	10.183	1.7472	34.03
600 442	6	53.82	1.7018	36	10.211	1.6980	35.83
611 532	15	55.53	1.6534	38	10.192	1.6527	37.96
620	5	57.13	1.6108	40	10.188	1.6108	39.99
541	(undetected)						
622	27	60.20	1.5358	44	10.187	1.5358	44.00
631	(undetected)						
444	8	63.13	1.4714	48	10.194	1.4705	47.93
710 550 543	10	64.62	1.4410	50	10.189	1.4408	49.98

Spec: S3-1B a_o = 10.200 ± .005

hkl	I/I_1	2θ	d	N	a_o	d calc	N calc
110	(not scanned)						
200	(undetected)						
211	6	21.35	4.1581	6	10.185	4.1641	6.01
220	5	24.68	3.6041	8	10.194	3.6062	8.00
310	7	27.28	3.2662	10	10.328	3.2255	9.75
222	100	30.36	2.9415	12	10.189	2.9444	12.02
321	6	32.78	2.7296	14	10.213	2.7260	13.96
400	26	35.12	2.5529	16	10.211	2.5500	15.96
330 411	9	37.31	2.4080	18	10.216	2.4041	17.94
420	(undetected)						
332	(undetected)						
422	(undetected)						
510 431	8	45.24	2.0026	26	10.211	2.0003	25.94
521	14	48.82	1.8638	30	10.208	1.8622	29.94
440	40	50.58	1.8030	32	10.199	1.8031	32.00
530 433	(weak)						
600 442	(undetected)						
611 532	8	55.49	1.6545	38	10.199	1.6546	38.00
620	(weak)						
541	(undetected)						
622	26	60.07	1.5388	44	10.207	1.5377	43.93
631	(undetected)						
444	(weak)						
710 550 543	4	64.59	1.4416	50	10.194	1.4424	50.05

Spec: M14761 a_o = 10.200 ± .005

hkl	I/I_1	2θ	d	N	a_o	d calc	N calc
110	(not scanned)						
200	6	18.70	4.7410	4	9.482	5.1000	4.62
211	6	21.24	4.1794	6	10.237	4.1641	5.95
220	5	24.55	3.6229	8	10.247	3.6062	7.92
310	9	27.24	3.2709	10	10.343	3.2255	9.72
222	100	30.24	2.9529	12	10.229	2.9444	11.93
321	12	32.74	2.7329	14	10.225	2.7260	13.92
400	28	35.05	2.5579	16	10.231	2.5500	15.90
330 411	11	37.28	2.4098	18	10.224	2.4041	17.91
420	(weak)						
332	(weak)						
422	21	43.20	2.0923	24	10.250	2.0820	23.76
510 431	12	45.30	2.0001	26	10.198	2.0003	26.00
521	22	48.83	1.8634	30	10.206	1.8622	29.96
440	95	50.54	1.8043	32	10.206	1.8031	31.95
530 433	9	52.20	1.7508	34	10.208	1.7492	33.94
600 442	9	53.90	1.6995	36	10.197	1.7000	36.01
611 532	19	55.51	1.6539	38	10.195	1.6546	38.03
620	(weak)						
541	(weak)						
622	50	60.10	1.5381	44	10.203	1.5377	43.97

Spec: 103201 a_o = 10.252 ± .005

hkl	I/I_1	2θ	d	N	a_o	d calc	N calc
110	(not scanned)						
200	(undetected)						
211	5	21.10	4.2068	6	10.304	4.1853	5.93
220	3	24.40	3.6448	8	10.309	3.6246	7.91
310	9	27.09	3.2887	10	10.399	3.2419	9.71
222	100	30.07	2.9692	12	10.285	2.9594	11.92
321	7	32.55	2.7484	14	10.283	2.7399	13.91
400	21	34.89	2.5692	16	10.277	2.5630	15.92
330 411	10	37.10	2.4211	18	10.272	2.4164	17.92
420	(undetected)						
332	(undetected)						
422	3	43.30	2.0877	24	10.227	2.0926	24.11
510 431	11	45.05	2.0106	26	10.252	2.0105	25.99
521	14	48.58	1.8724	30	10.255	1.8717	29.97
440	64	50.28	1.8130	32	10.256	1.8123	31.97
530 433	3	51.85	1.7618	34	10.272	1.7582	33.86
600 442	3	53.45	1.7127	36	10.276	1.7086	35.82
611 532	10	55.13	1.6644	38	10.260	1.6630	37.93
620	4	56.68	1.6225	40	10.262	1.6209	39.92
541	(undetected)						
622	35	59.80	1.5451	44	10.249	1.5455	44.02
631	(undetected)						
444	5	62.70	1.4804	48	10.257	1.4797	47.95
710 550 543	5	64.15	1.4504	50	10.256	1.4498	49.95

Spec: M8380 a_o = 10.252 ± .005

hkl	I/I_1	2θ	d	N	a_o	d calc	N calc
110	(not scanned)						
200	(undetected)						
211	(undetected)						
220	6	24.53	3.6258	8	10.255	3.6246	7.99
310	5	27.20	3.2756	10	10.358	3.2419	9.79
222	100	30.21	2.9558	12	10.239	2.9594	12.02
321	7	32.67	2.7386	14	10.247	2.7399	14.01
400	18	35.00	2.5614	16	10.245	2.5630	16.01
330 411	16	37.17	2.4167	18	10.253	2.4164	17.99
420	(undetected)						
332	5	41.20	2.1891	22	10.268	2.1857	21.93
422	(undetected)						
510 431	16	45.15	2.0064	26	10.230	2.0105	26.10
521	18	48.65	1.8699	30	10.242	1.8717	30.05
440	64	50.40	1.8090	32	10.233	1.8123	32.11
530 433	5	52.04	1.7558	34	10.238	1.7582	34.09
600 442	6	53.60	1.7083	36	10.250	1.7086	36.01
611 532	8	55.28	1.6603	38	10.234	1.6630	38.12
620	14	56.27	1.6334	40	10.200	1.6416	39.39
541	4	57.88	1.5917	42	10.192	1.6010	41.48
622	33	59.88	1.5433	44	10.237	1.5455	44.12

Spec: BINGHAM a_o = 10.255 ± .005

hkl	I/I	2θ	d	N	a_o	d calc	N calc
110	(not scanned)						
200	(undetected)						
211	(undetected)						
220	(undetected)						
310	9	27.07	3.2911	10	10.407	3.2429	9.70
222	100	30.02	2.9740	12	10.302	2.9603	11.88
321	15	32.82	2.7264	14	10.201	2.7407	14.14
400	23	34.82	2.5743	16	10.297	2.5637	15.86
330 411	15	36.98	2.4287	18	10.304	2.4171	17.82
420	(undetected)						
332	9	40.63	2.2185	22	10.166	2.2378	21.36
422	(poor peak)						
510 431	15	45.06	2.0102	26	10.250	2.0111	26.02
521	18	48.62	1.8710	30	10.248	1.8722	30.04
440	73	50.37	1.8100	32	10.239	1.8128	32.09
530 433	(weak)						
600 442	7	53.47	1.7121	36	10.273	1.7091	35.87
611 532	9	55.14	1.6642	38	10.258	1.6635	37.97
620	(weak)						
541	(undetected)						
622	33	59.78	1.5456	44	10.252	1.5459	44.02
631	5	61.52	1.5060	46	10.214	1.5120	46.36
444	6	62.80	1.4783	48	10.242	1.4801	48.11
710 550 543	8	64.10	1.4514	50	10.263	1.4502	49.91

Spec: 61823 a_o = 10.255 ± .005

hkl	I/I_1	2θ	d	N	a_o	d calc	N calc
110	(not scanned)						
200	(undetected)						
211	7	21.05	4.2167	6	10.328	4.1865	5.91
220	7	24.42	3.6419	8	10.300	3.6256	7.92
310	8	27.03	3.2958	10	10.422	3.2429	9.68
222	100	30.10	2.9663	12	10.275	2.9603	11.95
321	8	32.54	2.7492	14	10.286	2.7407	13.91
400	22	34.87	2.5707	16	10.282	2.5637	15.91
330 411	9	37.08	2.4224	18	10.277	2.4171	17.92
420	(undetected)						
332	(undetected)						
422	2	43.18	2.0932	24	10.254	2.0932	24.00
510 431	12	45.00	2.0127	26	10.263	2.0111	25.95
521	13	48.58	1.8724	30	10.255	1.8722	29.99
440	56	50.32	1.8117	32	10.248	1.8128	32.03
530 433	4	51.93	1.7592	34	10.258	1.7587	33.97
600 422	3	53.55	1.7098	36	10.258	1.7091	35.97
611 532	8	55.17	1.6633	38	10.253	1.6635	38.00
620	2	56.80	1.6194	40	10.242	1.6214	40.09
541	(undetected)						
622	26	59.83	1.5444	44	10.244	1.5459	44.08
631	(undetected)						
444	(weak)						
710 550 543	3	64.30	1.4474	50	10.235	1.4502	50.19

Spec: R1110 a_o = 10.257 ± .005

hkl	I/I_1	2θ	d	N	ao	d calc	N calc
110	(not scanned)						
200	(undetected)						
211	6	21.03	4.2207	6	10.338	4.1874	5.90
220	3	24.35	3.6522	8	10.330	3.6263	7.88
310	6	27.14	3.2827	10	10.381	3.2435	9.76
222	100	30.05	2.9711	12	10.292	2.9609	11.91
321	16	32.84	2.7248	14	10.195	2.7412	14.16
400	18	34.90	2.5685	16	10.274	2.5642	15.94
330 411	19	37.00	2.4274	18	10.298	2.4175	17.85
420	(undetected)						
332	10	40.60	2.2201	22	10.413	2.1868	21.34
422	12	42.95	2.1039	24	10.307	2.0937	23.76
510 431	11	45.00	2.0127	26	10.263	2.0115	25.96
521	13	48.60	1.8717	30	10.251	1.8726	30.02
440	54	50.32	1.8117	32	10.248	1.8131	32.05
530 433	3	51.98	1.7577	34	10.249	1.7590	34.05
600 442	3	53.55	1.7098	36	10.258	1.7095	35.98
611 532	7	55.20	1.6625	38	10.248	1.6639	38.06
620	18	56.14	1.6369	40	10.352	1.6217	39.26
541	(undetected)						
622	33	59.81	1.5449	44	10.247	1.5463	44.07
631	5	61.54	1.5055	46	10.211	1.5123	46.41
444	5	62.75	1.4794	48	10.249	1.4804	48.06
710 550 543	9	64.20	1.4494	50	10.249	1.4505	50.07

Spec: 90776 a_o = 10.260 ± .005

hkl	I/I_1	2θ	d	N	a_o	d calc	N calc
110	(not scanned)						
200	(weak)						
211	4	21.03	4.2207	6	10.338	4.1886	5.90
220	6	24.35	3.6522	8	10.330	3.6274	7.89
310	9	27.05	3.2935	10	10.414	3.2444	9.70
222	100	30.05	2.9711	12	10.292	2.9618	11.92
321	9	32.50	2.7525	14	10.299	2.7421	13.89
400	21	34.92	2.5671	16	10.268	2.5650	15.97
330 411	11	37.10	2.4211	18	10.272	2.4183	17.95
420	(weak)						
332	(weak)						
422	5	43.20	2.0923	24	10.250	2.0943	24.04
510 431	14	45.02	2.0119	26	10.258	2.0121	26.00
521	15	48.52	1.8746	30	10.267	1.8732	29.95
440	57	50.28	1.8130	32	10.256	1.8137	32.02
530 433	5	51.90	1.7602	34	10.263	1.7595	33.97
600 442	4	53.47	1.7121	36	10.273	1.7100	35.90
611 532	7	55.13	1.6644	38	10.260	1.6643	37.99
620	3	56.70	1.6220	40	10.258	1.6222	40.00
541	(undetected)						
622	30	59.78	1.5456	44	10.252	1.5467	44.06
631	(undetected)						
444	5	62.75	1.4794	48	10.249	1.4809	48.09
710 550 543	5	64.22	1.4490	50	10.246	1.4509	50.13

Spec: C819 a_o = 10.264 ± .005

hkl	I/I_1	2θ	d	N	a_o	d calc	N calc
110	(not scanned)						
200	2	17.16	5.1628	4	10.325	5.1320	3.95
211	7	20.96	4.2346	6	10.372	4.1902	5.87
220	8	24.35	3.6522	8	10.330	3.6288	7.89
310	6	27.04	3.2946	10	10.418	3.2457	9.70
222	100	30.01	2.9750	12	10.305	2.9629	11.90
321	22	32.47	2.7550	14	10.308	2.7431	13.87
400	10	34.84	2.5728	16	10.291	2.5660	15.91
330 411	10	37.02	2.4262	18	10.293	2.4192	17.89
420	(undetected)						
332	(undetected)						
422	(undetected)						
510 431	12	44.95	2.0148	26	10.273	2.0129	25.94
521	13	48.44	1.8775	30	10.283	1.8739	29.88
440	48	50.17	1.8167	32	10.277	1.8144	31.91
530 433	5	51.83	1.7624	34	10.276	1.7602	33.91
600 442	3	53.43	1.7133	36	10.280	1.7106	35.88
611 532	8	55.08	1.6658	38	10.269	1.6650	37.96
620	3	56.62	1.6241	40	10.272	1.6228	39.93
541	(undetected)						
622	27	59.68	1.5479	44	10.268	1.5473	43.96
631	(undetected)						
444	5	62.63	1.4819	48	10.267	1.4814	47.96
710 550 543	6	64.10	1.4514	50	10.263	1.4515	50.00

Spec: 108759 a_o = 10.274 ± .005

hkl	I/I_1	2θ	d	N	a_o	d calc	N calc
110	(not scanned)						
200	(undetected)						
211	6	21.07	4.2127	6	10.319	4.1943	5.94
220	5	24.38	3.6478	8	10.317	3.6324	7.93
310	7	27.04	3.2946	10	10.418	3.2489	9.72
222	100	30.05	2.9711	12	10.292	2.9658	11.95
321	7	32.52	2.7509	14	10.293	2.7458	13.94
400	24	34.85	2.5721	16	10.288	2.5685	15.95
330 411	10	37.02	2.4262	18	10.293	2.4216	17.93
420	1	39.06	2.3040	20	10.304	2.2973	19.88
322	2	41.10	2.1942	22	10.292	2.1904	21.92
422	1	43.04	2.0997	24	10.286	2.0971	23.94
510 431	13	44.97	2.0140	26	10.269	2.0148	26.02
512	14	48.10	1.8900	30	10.352	1.8757	29.54
440	51	50.20	1.8157	32	10.271	1.8162	32.01
530 433	4	51.80	1.7633	34	10.282	1.7619	33.94
600 442	3	53.40	1.7142	36	10.285	1.7123	35.91
611 532	8	55.05	1.6667	38	10.274	1.6666	37.99
620	3	56.64	1.6236	40	10.268	1.6244	40.04
541	(undetected)						
622	27	59.68	1.5479	44	10.268	1.5488	44.04
631	(undetected)						
444	4	62.50	1.4847	48	10.286	1.4829	47.88
710 550 543	5	64.02	1.4531	50	10.275	1.4529	49.98

Spec: 90382 a_o = 10.274 ± .005

hkl	I/I_1	2θ	d	N	a_o	d calc	N calc
110	(not scanned)						
200	2	17.17	5.1598	4	10.319	5.1370	3.96
211	5	21.05	4.2167	6	10.328	4.1943	5.93
220	5	24.41	3.6433	8	10.305	3.6324	7.95
310	7	27.04	3.2946	10	10.418	3.2489	9.72
222	100	30.03	2.9731	12	10.299	2.9658	11.94
321	7	32.48	2.7542	14	10.305	2.7458	13.91
400	23	34.80	2.5757	16	10.302	2.5685	15.91
330 411	12	37.04	2.4249	18	10.288	2.4216	17.95
420	(undetected)						
332	2	41.10	2.1942	22	10.292	2.1904	21.92
422	5	42.95	2.1039	24	10.307	2.0971	23.84
510 431	13	44.95	2.0148	26	10.273	2.0148	26.00
521	14	48.50	1.8753	30	10.271	1.8757	30.01
440	57	50.20	1.8157	32	10.271	1.8162	32.01
530 433	5	51.83	1.7624	34	10.276	1.7619	33.98
600 442	1	53.40	1.7142	36	10.285	1.7123	35.91
611 532	8	55.10	1.6653	38	10.265	1.6666	38.06
620	(weak)						
541	(weak)						
622	27	59.72	1.5470	44	10.261	1.5488	44.10
631	(undetected)						
444	5	62.68	1.4809	48	10.260	1.4829	48.12
710 550 543	4	64.18	1.4498	50	10.252	1.4529	50.21

Spec: R1089 a_o = 10.300 ± .005

hkl	I/I_1	2θ	d	N	a_o	d calc	N calc
110	(not scanned)						
200	(undetected)						
211	5	20.76	4.2749	6	10.471	4.2049	5.80
220	5	24.08	3.6925	8	10.444	3.6415	7.78
310	7	26.85	3.3175	10	10.491	3.2571	9.63
222	100	29.83	2.9925	12	10.366	2.9733	11.84
321	5	32.25	2.7733	14	10.376	2.7527	13.79
400	23	34.64	2.5872	16	10.349	2.5750	15.84
330 411	14	36.96	2.4300	18	10.309	2.4277	17.96
420	(undetected)						
332	(undetected)						
422	(undetected)						
510 431	12	44.85	2.0234	26	10.317	2.0199	25.91
521	13	48.27	1.8837	30	10.317	1.8805	29.89
440	52	50.00	1.8225	32	10.309	1.8207	31.93
530 533	(weak)						
600 442	(weak)						
611 532	8	54.91	1.6706	38	10.298	1.6708	38.01
620	(weak)						
541	(weak)						
622	27	59.54	1.5512	44	10.290	1.5527	44.08
631	(undetected)						
444	5	62.60	1.4826	48	10.271	1.4866	48.26
710 550 543	7	64.07	1.4521	50	10.267	1.4566	50.31

Spec: S1-1 a_o = 10.308 ± .005

hkl	I/I_1	2θ	d	N	a_o	d calc	N calc
110	(not scanned)						
200	6	17.20	5.1509	4	10.301	5.1540	4.00
211	4	21.15	4.1970	6	10.280	4.2082	6.03
220	13	24.40	3.6448	8	10.309	3.6444	7.99
310	7	27.00	3.2994	10	10.433	3.2596	9.76
222	100	30.00	2.9760	12	10.309	2.9756	11.99
321	12	32.50	2.7525	14	10.299	2.7549	14.02
400	23	34.75	2.5793	16	10.317	2.5770	15.97
330 411	13	37.00	2.4274	18	10.298	2.4296	18.03
420	7	39.00	2.3074	19	10.319	2.3049	19.95
332	5	40.95	2.2019	22	10.328	2.1976	21.91
422	6	42.95	2.1039	24	10.307	2.1041	24.00
510 431	15	44.75	2.0234	26	10.317	2.0215	25.95
521	15	48.25	1.8845	30	10.321	1.8819	29.91
440	62	50.00	1.8225	32	10.309	1.8222	31.98
530 433	6	51.50	1.7729	34	10.337	1.7678	33.80
600 442	1	53.40	1.7142	36	10.285	1.7180	36.15
611 532	12	54.81	1.6734	38	10.315	1.6721	37.94
620	(weak)						
541	(weak)						
622	30	59.40	1.5546	44	10.312	1.5539	43.96
631	1	60.85	1.5210	46	10.315	1.5198	45.92
444	1	62.35	1.4879	48	10.308	1.4878	47.99
710 550 543	8	63.70	1.4596	50	10.321	1.4577	49.87

Spec: D148, A1772 $a_o = 10.315 \pm .005$

hkl	I/I_1	2θ	d	N	a_o	d calc	N calc
110	(not scanned)						
200	2	17.20	5.1509	4	10.301	5.1575	4.01
211	3	21.15	4.1970	6	10.280	4.2110	6.04
220	10	24.35	3.6522	8	10.330	3.6469	7.97
310	5	27.00	3.2994	10	10.433	3.2618	9.77
222	100	30.00	3.9760	12	10.309	2.9776	12.01
321	8	32.40	2.7608	14	10.330	2.7567	13.95
400	17	34.75	2.5793	16	10.317	2.5787	15.99
300 411	8	36.90	2.4338	18	10.325	2.4312	17.96
420	4	39.00	2.3074	20	10.319	2.3065	19.98
322	2	41.00	2.1994	22	10.316	2.1991	21.99
422	4	42.85	2.1086	24	10.330	2.1055	23.92
510 431	9	44.70	2.0255	26	10.328	2.0229	25.93
521	6	48.30	1.8826	30	10.311	1.8832	30.01
440	40	50.00	1.8225	32	10.309	1.8234	32.03
530 433	3	51.60	1.7697	34	10.319	1.7690	33.97
600 442	2	53.20	1.7202	36	10.321	1.7191	35.95
611 532	6	54.80	1.6737	38	10.317	1.6733	37.98
620	1	56.34	1.6315	40	10.318	1.6309	39.96
541	1	58.08	1.5867	42	10.283	1.5916	42.25
622	14	59.40	1.5546	44	10.312	1.5550	44.02
631	1	60.80	1.5221	46	10.323	1.5208	45.92
444	1	62.26	1.4898	48	10.322	1.4888	47.93
710 550 543	2	63.70	1.4596	50	10.321	1.4587	49.93

Spec: M609 a_o = 10.340 ± .005

hkl	I/I1	2θ	d	N	ao	d calc	N calc
110	(not scanned)						
200	(undetected)						
211	(undetected)						
220	6	24.25	3.6670	8	10.372	3.6557	7.95
310	8	26.95	3.3054	10	10.452	3.2697	9.78
222	100	29.88	2.9876	12	10.349	2.9849	11.97
321	10	31.33	2.8526	14	10.673	2.7634	13.13
400	33	34.67	2.5850	16	10.340	2.5850	15.99
330 411	14	36.89	2.4344	18	10.328	2.4371	18.03
420	3	38.90	2.3131	20	10.344	2.3120	19.98
332	3	41.25	2.1866	22	10.256	2.2044	22.36
422	6	42.80	2.1109	24	10.341	2.1106	23.99
510 431	20	44.62	2.0290	26	10.345	2.0278	25.96
521	19	48.14	1.8885	30	10.344	1.8878	29.97
440	77	49.83	1.8283	32	10.342	1.8278	31.98
530 433	12	51.48	1.7735	34	10.341	1.7732	33.98
600 442	12	52.98	1.7268	36	10.361	1.7233	35.85
611 532	20	54.65	1.6779	38	10.343	1.6773	37.97
620	(undetected)						
541	(undetected)						
622	40	59.20	1.5593	44	10.343	1.5588	43.96
631	8	60.70	1.5243	46	10.338	1.5245	46.00
444	14	62.20	1.4911	48	10.331	1.4924	48.08
710 550 543	15	63.53	1.4631	50	10.345	1.4622	49.94

Spec: 88118 a_o = 10.350 ± .005

hkl	I/I_1	2θ	d	N	a_o	d calc	N calc
110	(not scanned)						
200	4	17.04	5.1989	4	10.397	5.1750	3.96
211	5	20.98	4.2306	6	10.362	4.2253	5.98
220	10	25.25	3.6670	8	10.372	3.6592	7.96
310	10	26.82	3.3212	10	10.502	3.2729	9.71
222	100	29.80	2.9955	12	10.376	2.9877	11.93
321	10	32.25	2.7733	14	10.376	2.7661	13.92
400	23	34.60	2.5901	16	10.360	2.5875	15.96
330 411	14	36.73	2.4447	18	10.371	2.4395	17.92
420	4	38.81	2.3183	20	10.367	2.3143	19.93
332	5	39.74	2.2661	22	10.628	2.2066	20.85
422	7	42.70	2.1156	24	10.364	2.1126	23.93
510 431	16	44.58	2.0307	26	10.354	2.0298	25.97
521	11	48.10	1.8900	30	10.352	1.8896	29.98
440	55	49.78	1.8301	32	10.352	1.8296	31.98
530 433	9	51.40	1.7761	34	10.356	1.7750	33.95
600 442	5	53.00	1.7262	36	10.357	1.7250	35.94
611 532	14	54.62	1.6788	38	10.348	1.6789	38.00
620	4	56.13	1.6371	40	10.354	1.6364	39.96
541	2	57.50	1.6013	42	10.378	1.5970	41.77
622	33	59.18	1.5598	44	10.347	1.5603	44.02
631	2	60.65	1.5255	46	10.346	1.5260	46.02
444	5	62.08	1.4937	48	10.349	1.4938	48.00
710 550 543	8	63.64	1.4608	50	10.329	1.4637	50.19

Spec: D148, A877, d3241 a_o = 10.360 ± .005

hkl	I/I1	2θ	d	N	a_o	d calc	N calc
110	(not scanned)						
200	2	17.05	5.1959	4	10.391	5.1800	3.97
211	2	20.93	4.2406	6	10.387	4.2294	5.96
220	9	24.20	3.6745	8	10.393	3.6628	7.94
310	5	26.85	3.3175	10	10.491	3.2761	9.75
222	100	29.79	2.9965	12	10.380	2.9906	11.95
321	8	32.25	2.7733	14	10.376	2.7688	13.95
400	25	34.54	2.5945	16	10.378	2.5900	15.94
330 411	12	36.68	2.4479	18	10.385	2.4418	17.91
420	5	38.78	2.3200	20	10.375	2.3165	19.93
332	3	40.75	2.2123	22	10.376	2.2087	21.92
422	5	42.72	2.1147	24	10.360	2.1147	23.99
510 431	13	44.50	2.0342	26	10.372	2.0317	25.93
521	9	48.40	1.8790	30	10.291	1.8914	30.39
440	61	49.70	1.8328	32	10.368	1.8314	31.94
530 433	6	51.39	1.7764	34	10.358	1.7767	34.00
600 442	3	52.94	1.7280	36	10.368	1.7266	35.94
611 532	11	54.55	1.6808	38	10.361	1.6806	37.99
620	2	56.06	1.6390	40	10.366	1.6380	39.95
541	(undetected)						
622	26	59.05	1.5629	44	10.367	1.5618	43.93
631	2	60.50	1.5289	46	10.369	1.5274	45.91
444	2	61.95	1.4966	48	10.368	1.4953	47.91
710 550 543	5	63.42	1.4654	50	10.362	1.4651	49.98

Spec: R1096 a_o = 10.360 ± .005

hkl	I/I_1	2θ	d	N	a_o	d calc	N calc
110	(not scanned)						
200	(undetected)						
211	5	20.90	4.2466	6	10.402	4.2294	5.95
220	7	24.00	3.7046	8	10.478	3.6628	7.82
310	7	26.70	3.3358	10	10.548	3.2761	9.64
222	100	29.65	3.0103	12	10.428	2.9906	11.84
321	7	32.13	2.7834	14	10.414	2.7688	13.85
400	19	34.47	2.5996	16	10.398	2.5900	15.88
330 411	16	36.73	2.4447	18	10.371	2.4418	17.95
420	(weak)						
332	8	40.53	2.2238	22	10.430	2.2087	21.70
422	(weak)						
510 431	11	44.43	2.0372	26	10.387	2.0317	25.86
521	11	47.98	1.8944	30	10.376	1.8914	29.90
440	49	49.65	1.8345	32	10.378	1.8314	31.88
530 433	(weak)						
600 442	(weak)						
611 532	11	54.55	1.6808	38	10.361	1.6806	37.99
620	11	55.95	1.6420	40	10.385	1.6380	39.80
541	(undetected)						
622	26	59.10	1.5617	44	10.359	1.5618	44.00
631	(weak)						
444	(weak)						
710 550 543	(weak)						

Spec: 115256 a_o = 10.361 ± .005

hkl	I/I_1	2θ	d	N	a_o	d calc	N calc
110	(not scanned)						
200	10	16.92	5.2355	4	10.471	5.1805	3.91
211	(undetected)						
220	12	24.19	3.6760	8	10.397	3.6631	7.94
310	6	26.87	3.3151	10	10.483	3.2764	9.76
222	100	29.78	2.9975	12	10.3836	2.9909	11.94
321	10	32.21	2.7766	14	10.389	2.7690	13.92
400	17	34.58	2.5916	16	10.366	2.5902	15.98
330 411	12	36.72	2.4453	18	10.374	2.4421	17.95
420	5	38.74	2.3223	20	10.385	2.3167	19.90
332	3	40.80	2.2097	22	10.364	2.2089	21.98
422	5	42.80	2.1109	24	10.341	2.1149	24.08
510 431	9	44.58	2.0307	26	10.354	2.0319	26.03
521	9	48.05	1.8918	30	10.362	1.8916	29.99
440	44	49.79	1.8297	32	10.350	1.8315	32.06
530 433	5	51.46	1.7742	34	10.345	1.7768	34.10
600 442	5	52.94	1.7280	36	10.368	1.7268	35.94
611 532	9	54.61	1.6791	38	10.350	1.6807	38.07
620	3	56.10	1.6379	40	10.359	1.6382	40.01
541	2	57.74	1.5953	42	10.338	1.5987	42.18
622	17	59.16	1.5603	44	10.350	1.5619	44.09
631	(undetected)						
444	2	62.07	1.4940	48	10.350	1.4954	48.09
710 550 543	3	63.56	1.4625	50	10.341	1.4652	50.18

Spec: S4-1B a_o = 10.365 ± .005

hkl	I/I1	2θ	d	N	a_o	d calc	N calc
110	(not scanned)						
200	6	17.02	5.2050	4	10.410	5.1825	3.96
211	3	20.93	4.2406	6	10.387	4.2314	5.97
220	11	24.21	3.6730	8	10.388	3.6645	7.96
310	6	26.88	3.3139	10	10.479	3.2777	9.78
222	100	29.85	2.9906	12	10.359	2.9921	12.01
321	9	32.31	2.7683	14	10.358	2.7701	14.01
400	21	34.57	2.5923	16	10.369	2.5912	15.98
330 411	12	36.77	2.4421	18	10.361	2.4430	18.01
420	6	38.80	2.3189	20	10.370	2.3176	19.97
332	4	40.80	2.2097	22	10.364	2.2098	22.00
422	5	42.68	2.1166	24	10.369	2.1157	23.97
510 431	11	44.52	2.0333	26	10.368	2.0327	25.98
521	11	47.98	1.8944	30	10.376	1.8923	29.93
440	42	49.68	1.8335	32	10.372	1.8322	31.95
530 433	8	51.29	1.7797	34	10.377	1.7775	33.91
600 442	6	52.90	1.7292	36	10.375	1.7275	35.92
611 532	12	54.48	1.6828	38	10.373	1.6814	37.93
620	7	56.13	1.6371	40	10.354	1.6388	40.08
541	(weak)						
622	29	59.06	1.5627	44	10.366	1.5625	43.99
631	5	60.43	1.5305	46	10.380	1.5282	45.86
444	4	62.04	1.4946	48	10.355	1.4960	48.09
710 550	5	63.36	1.4666	50	10.370	1.4658	49.94

Spec: 148,A320,d3241 $a_o = 10.365 \pm .005$

hkl	I/I_1	2θ	d	N	a_o	d calc	N calc
110	(not scanned)						
200	5	17.15	5.1658	4	10.331	5.1825	4.02
211	8	20.85	4.2567	6	10.426	4.2314	5.92
220	12	24.18	3.6775	8	10.401	3.6645	7.94
310	44	26.59	3.3494	10	10.591	3.2777	9.57
222	100	29.78	2.9975	12	10.383	2.9921	11.95
321	6	32.20	2.7775	14	10.392	2.7701	13.92
400	18	34.52	2.5959	16	10.383	2.5912	15.94
330 411	12	36.65	2.4498	18	10.393	2.4430	17.90
420	(undetected)						
332	(undetected)						
422	8	42.58	2.1213	24	10.392	2.1157	23.87
510 431	10	44.49	2.0346	26	10.374	2.0327	25.95
521	9	48.01	1.8933	30	10.370	1.8923	29.96
440	51	49.70	1.8328	32	10.368	1.8322	31.97
530 433	5	51.30	1.7793	34	10.375	1.7775	33.93
600 442	3	52.82	1.7317	36	10.390	1.7275	35.82
611 532	10	54.52	1.6816	38	10.366	1.6814	37.98
620	(undetected)						
541	(undetected)						
622	17	59.08	1.5622	44	10.362	1.5625	44.01
631	(undetected)						
444	2	62.00	1.4955	48	10.361	1.4960	48.03
710 550	2	63.50	1.4637	50	10.350	1.4658	50.14

543

Spec: M354 $a_o = 10.366 \pm .005$

hkl	I/I_1	2θ	d	N	a_o	d calc	N calc
110	(not scanned)						
200	(undetected)						
211	(undetected)						
220	15	24.27	3.6640	8	10.363	3.6649	8.00
310	6	26.90	3.3115	10	10.471	3.2780	9.79
222	100	29.85	2.9906	12	10.359	2.9924	12.01
321	9	32.25	2.7733	14	10.376	2.7704	13.97
400	21	34.57	2.5923	16	10.369	2.5915	15.98
330 411	12	36.74	2.4440	18	10.369	2.4432	17.98
420	6	38.85	2.3160	20	10.357	2.3179	20.03
332	6	40.73	2.2133	22	10.381	2.2100	21.93
422	11	42.68	2.1166	24	10.369	2.1159	23.98
510 431	19	44.53	2.0329	26	10.365	2.0329	26.00
521	9	48.05	1.8918	30	10.362	1.8925	30.02
440	71	49.70	1.8328	32	10.368	1.8324	31.98
530 433	11	51.32	1.7787	34	10.371	1.7777	33.96
600 422	5	52.77	1.7332	36	10.399	1.7276	35.76
611 532	12	54.50	1.6822	38	10.369	1.6815	37.97
620	(weak)						
541	(undetected)						
622	34	59.07	1.5625	44	10.364	1.5627	44.01
631	4	60.56	1.5275	46	10.360	1.5283	46.04
444	7	61.98	1.4959	48	10.364	1.4962	48.01
710 550 543	6	63.38	1.4662	50	10.367	1.4659	49.98

Spec: M631 #148 a_o = 10.370 ± .005

hkl	I/I$_1$	2θ	d	N	a_o	d calc	N calc
110	(not scanned)						
200	7	16.93	5.2324	4	10.464	5.1850	3.92
211	4	20.76	4.2749	6	10.471	4.2335	5.88
220	13	24.09	3.6910	8	10.439	3.6663	7.89
310	7	26.67	3.3395	10	10.560	3.2792	9.64
222	100	29.70	3.0053	12	10.410	2.9935	11.90
321	13	32.15	2.7817	14	10.408	2.7714	13.89
400	22	34.44	2.6018	16	10.407	2.5925	15.88
330 411	14	36.64	2.4504	18	10.396	2.4442	17.90
420	5	38.73	2.3229	20	10.388	2.3188	19.92
332	6	40.65	2.2175	22	10.401	2.2108	21.86
422	6	42.62	2.1194	24	10.383	2.1167	23.93
510 431	21	44.45	2.0363	26	10.383	2.0337	25.93
521	15	48.00	1.8937	30	10.372	1.8932	29.98
440	75	49.64	1.8349	32	10.379	1.8331	31.93
530 433	9	51.12	1.7852	34	10.409	1.7784	33.74
600 442	5	52.85	1.7307	36	10.384	1.7283	35.89
611 532	18	54.50	1.6822	38	10.369	1.6822	38.00
620	6	56.05	1.6393	40	10.368	1.6396	40.01
541	(weak)						
622	33	59.05	1.5629	44	10.367	1.5633	44.01

Spec: WEDGE MINE #1 a_o = 10.377 ± .005

hkl	I/I_1	2θ	d	N	a_o	d calc	N calc
110	(not scanned)						
200	(undetected)						
211	(undetected)						
220	13	24.15	3.6820	8	10.414	3.6688	7.94
310	11	26.75	3.3297	10	10.529	3.2814	9.71
222	100	29.64	3.0113	12	10.431	2.9955	11.87
321	13	32.10	2.7859	14	10.424	2.7733	13.87
400	27	34.40	2.6047	16	10.419	2.5942	15.87
330 411	17	36.60	2.4530	18	10.407	2.4458	17.89
420	10	40.70	2.2149	22	10.388	2.2123	21.95
332	8	40.65	2.2175	22	10.401	2.2123	21.89
422	7	42.59	2.1209	24	10.390	2.1181	23.93
510 431	22	44.44	2.0368	26	10.385	2.0350	25.95
521	17	47.96	1.8952	30	10.380	1.8945	29.97
440	70	49.64	1.8349	32	10.379	1.8344	31.98
530 433	6	51.27	1.7803	34	10.381	1.7796	33.97
600 442	8	52.80	1.7323	36	10.393	1.7295	35.88
611 532	15	54.45	1.6836	38	10.378	1.6833	37.98
620	5	56.09	1.6382	40	10.361	1.6407	40.12
541	3	57.70	1.5963	42	10.345	1.6012	42.25
622	36	59.05	1.5629	44	10.367	1.5643	44.07
631	7	60.50	1.5289	46	10.369	1.5300	46.06
444	8	61.95	1.4966	48	10.368	1.4977	48.07
710 550 543	8	63.40	1.4658	50	10.364	1.4675	50.11

Spec: S2-1A $a_o = 10.380 \pm .005$

hkl	I/I_1	2θ	d	N	a_o	d calc	N calc
110	(not scanned)						
200	12	16.98	5.2171	4	10.434	5.1900	3.95
211	9	20.87	4.2527	6	10.416	4.2376	5.95
220	25	24.17	3.6790	8	10.405	3.6698	7.96
310	6	26.75	3.3297	10	10.529	3.2824	9.71
222	100	29.77	2.9984	12	10.387	2.9964	11.98
321	12	32.25	2.7733	14	10.376	2.7741	14.00
400	18	34.51	2.5967	16	10.386	2.5950	15.97
330 411	15	36.69	2.4472	18	10.382	2.4465	17.98
420	6	38.72	2.3235	20	10.391	2.3210	19.95
332	7	40.69	2.2154	22	10.391	2.2130	21.95
422	1	42.53	2.1237	24	10.404	2.1188	23.88
510 431	18	44.40	2.0385	26	10.394	2.0356	25.92
521	12	47.96	1.8952	30	10.380	1.8951	29.99
440	58	49.56	1.8377	32	10.395	1.8349	31.90
530 433	6	51.25	1.7810	34	10.384	1.7801	33.96
600 442	3	52.73	1.7344	36	10.406	1.7300	35.81
611 532	10	54.42	1.6845	38	10.384	1.6838	37.97
620	(undetected)						
541	(undetected)						
622	26	58.98	1.5646	44	10.378	1.5648	44.00
631	1	60.40	1.5312	46	10.385	1.5304	45.95

Spec: 103658 a_o = 10.392 ± .005

hkl	I/I_1	2θ	d	N	a_o	d calc	N calc
110	(not scanned)						
200	(undetected)						
211	(undetected)						
220	10	24.08	3.6925	8	10.444	3.6741	7.92
310	7	26.80	3.3236	10	10.510	3.2862	9.77
222	100	29.68	3.0073	12	10.417	2.9999	11.94
321	10	32.07	2.7884	14	10.433	2.7773	13.88
400	21	34.40	2.6047	16	10.419	2.5980	15.91
330 411	11	36.56	2.4556	18	10.418	2.4494	17.90
420	3	38.65	2.3275	20	10.409	2.3237	19.93
332	2	40.65	2.2175	22	10.401	2.2155	21.96
422	25	42.85	2.1086	24	10.330	2.1212	24.28
510 431	12	44.37	2.0398	26	10.401	2.0380	25.95
521	9	47.94	1.8959	30	10.384	1.8973	30.04
440	47	49.57	1.8373	32	10.393	1.8370	31.98
530 433	17	51.00	1.7891	34	10.432	1.7822	33.73
600 422	8	53.20	1.7202	36	10.321	1.7320	36.49
611 532	12	54.36	1.6862	38	10.394	1.6858	37.98
620	2	55.90	1.6433	40	10.393	1.6431	39.98
541	(weak)						
622	25	58.93	1.5658	44	10.386	1.5666	44.04
631	3	60.32	1.5330	46	10.397	1.5322	45.94
444	(weak)						
710 550 543	6	63.33	1.4672	50	10.375	1.4696	50.16

Spec: 14252 a_o = 10.398 ± .005

hkl	I/I_1	2θ	d	N	a_o	d calc	N calc
110	(not scanned)						
200	8	16.88	5.2479	4	10.495	5.1990	3.92
211	13	20.73	4.2811	6	10.486	4.2449	5.89
220	10	24.02	3.7016	8	10.469	3.6762	7.89
310	22	26.53	3.3568	10	10.615	3.2881	9.59
222	100	29.65	3.0103	12	10.428	3.0016	11.93
321	12	32.12	2.7842	14	10.417	2.7789	13.94
400	24	34.39	2.6054	16	10.421	2.5995	15.92
330 411	13	36.52	2.4582	18	10.429	2.4508	17.89
420	4	38.65	2.3275	20	10.409	2.3250	19.95
332	4	40.62	2.2191	22	10.408	2.2168	21.95
422	6	42.48	2.1261	24	10.415	2.1224	23.91
510 431	16	44.35	2.0407	26	10.405	2.0392	25.96
521	11	47.85	1.8993	30	10.402	1.8984	29.97
440	53	49.53	1.8387	32	10.401	1.8381	31.97
530 433	7	51.10	1.7858	34	10.413	1.7832	33.89
600 442	4	52.68	1.7359	36	10.415	1.7330	35.87
611 532	12	54.34	1.6868	38	10.398	1.6867	37.99
620	(undetected)						
541	(undetected)						
622	27	58.88	1.5671	44	10.394	1.5675	44.02
631	4	60.00	1.5405	46	10.448	1.5331	45.55
444	4	61.83	1.4992	48	10.386	1.5008	48.10
710 550 543	2	63.20	1.4699	50	10.394	1.4704	50.03

Spec: 46455 a_o = 10.405 ± .005

hkl	I/I_1	2θ	d	N	a_o	d calc	N calc
110	(not scanned)						
200	4	16.76	5.2851	4	10.570	5.2025	3.87
211	5	20.74	4.2790	6	10.481	4.2478	5.91
220	12	24.00	3.7046	8	10.478	3.6787	7.88
310	6	26.62	3.3457	10	10.580	3.2903	9.67
222	100	29.60	3.0153	12	10.445	3.0036	11.90
321	9	32.00	2.7944	14	10.455	2.7808	13.86
400	24	34.38	2.6062	16	10.424	2.6012	15.93
330 411	11	36.58	2.4543	18	10.413	2.4524	17.97
420	4	38.60	2.3304	20	10.422	2.3266	19.93
332	3	40.70	2.2149	22	10.388	2.2183	22.06
422	4	42.44	2.1280	24	10.425	2.1239	23.90
510 431	11	44.38	2.0394	26	10.399	2.0405	26.02
521	9	47.82	1.9004	30	10.409	1.8996	29.97
440	46	49.56	1.8377	32	10.395	1.8393	32.05
530 433	5	51.18	1.7832	34	10.398	1.7844	34.04
600 442	4	52.66	1.7365	36	10.419	1.7341	35.89
611 532	10	54.38	1.6856	38	10.391	1.6879	38.10
620	5	55.98	1.6412	40	10.379	1.6451	40.19
541	1	57.39	1.6041	42	10.396	1.6055	42.06
622	22	58.94	1.5656	44	10.385	1.5686	44.16
631	4	60.44	1.5303	46	10.379	1.5341	46.22
444	2	61.90	1.4976	48	10.376	1.5018	48.26
710 550 543	5	63.30	1.4679	50	10.379	1.4714	50.24

Spec: C5262 a_o = 10.412 ± .005

hkl	I/I_1	2θ	d	N	a_o	d calc	N calc
110	(not scanned)						
200	3	16.92	5.2356	4	10.471	5.2060	3.95
211	(undetected)						
220	15	24.07	3.6940	8	10.448	3.6811	7.94
310	4	26.66	3.3407	10	10.564	3.2925	9.71
222	100	29.62	3.0133	12	10.438	3.0056	11.93
321	12	31.98	2.7961	14	10.462	2.7827	13.86
400	20	34.33	2.6099	16	10.439	2.6030	15.91
330 411	12	36.50	2.4595	18	10.435	2.4541	17.92
420	5	38.55	2.3333	20	10.435	2.3281	19.91
332	7	40.49	2.2259	22	10.440	2.2198	21.87
422	6	42.43	2.1285	24	10.427	2.1253	23.92
510 431	8	44.22	2.0464	26	10.434	2.0419	25.88
521	7	47.80	1.9011	30	10.413	1.9009	29.99
440	37	49.42	1.8425	32	10.423	1.8405	31.93
530 433	5	51.05	1.7875	34	10.422	1.7856	33.92
600 442	3	52.60	1.7384	36	10.430	1.7353	35.87
611 532	9	54.20	1.6908	38	10.422	1.6890	37.91
620	5	55.90	1.6433	40	10.393	1.6462	40.14
541	3	57.30	1.6065	42	10.411	1.6066	42.00
622	20	58.74	1.5705	44	10.417	1.5696	43.95
631	3	60.20	1.5358	46	10.416	1.5351	45.95
444	(weak)						
710 550 543	5	63.05	1.4731	50	10.416	1.4724	49.95

Spec: 115110 a_o = 10.415 ± .005

hkl	I/I$_1$	2θ	d	N	a_o	d calc	N calc
110	(not scanned)						
200	(undetected)						
211	5	20.68	4.2913	6	10.511	4.2519	5.89
220	11	24.00	3.7046	8	10.478	3.6822	7.90
310	14	26.43	3.3693	10	10.654	3.2935	9.55
222	100	29.55	3.0203	12	10.462	3.0065	11.89
321	14	31.82	2.8098	14	10.513	2.7835	13.73
400	25	34.26	2.6150	16	10.460	2.6037	15.86
330 411	11	36.42	2.4647	18	10.457	2.4548	17.85
420	4	38.40	2.3421	20	10.474	2.3288	19.77
332	2	40.48	2.2264	22	10.443	2.2204	21.88
422	3	42.36	2.1318	24	10.444	2.1259	23.86
510 431	12	44.30	2.0429	26	10.416	2.0425	25.99
521	8	47.75	1.9030	30	10.423	1.9015	29.95
440	47	49.43	1.8422	32	10.421	1.8411	31.96
530 433	5	51.03	1.7881	34	10.426	1.7861	33.92
600 442	4	52.60	1.7384	36	10.430	1.7358	35.89
611 532	9	54.27	1.6888	38	10.410	1.6895	38.03
620	1	55.85	1.6447	40	10.402	1.6467	40.09
541	(undetected)						
622	23	58.78	1.5695	44	10.411	1.5701	44.03
631	(undetected)						
444	5	61.70	1.5020	48	10.406	1.5032	48.07
710 550 543	5	63.28	1.4683	50	10.382	1.4729	50.31

Spec: 103164 a_o = 10.416 ± .005

hkl	I/I_1	2θ	d	N	a_o	d calc	N calc
110	(not scanned)						
200	6	16.84	5.2602	4	10.520	5.2080	3.92
211	3	20.60	4.3078	6	10.551	4.2523	5.84
220	11	24.00	3.7046	8	10.478	3.6826	7.90
310	10	26.60	3.3481	10	10.587	3.2938	9.67
222	100	29.60	3.0153	12	10.445	3.0068	11.93
321	12	32.02	2.7927	14	10.449	2.7837	13.91
400	18	34.36	2.6077	16	10.430	2.6040	15.95
330 411	11	36.57	2.4550	18	10.415	2.4550	18.00
420	7	38.60	2.3304	20	10.422	2.3290	19.97
332	4	40.49	2.2259	22	10.440	2.2206	21.89
422	5	42.50	2.1251	24	10.411	2.1261	24.02
510 431	13	44.33	2.0416	26	10.410	2.0427	26.02
521	10	47.82	1.9004	30	10.409	1.9016	30.03
440	49	49.50	1.8397	32	10.407	1.8413	32.05
530 433	6	51.18	1.7832	34	10.398	1.7863	34.11
600 422	(weak)						
611 532	11	54.25	1.6894	38	10.414	1.6896	38.01
620	3	55.90	1.6433	40	10.393	1.6469	40.17
541	(weak)						
622	23	58.82	1.5685	44	10.404	1.5702	44.09
631	4	60.23	1.5351	46	10.412	1.5357	46.03
444	3	61.70	1.5020	48	10.406	1.5034	48.08
710 550 543	5	63.18	1.4703	50	10.397	1.4730	50.18

Spec: 98503 a_o = 10.424 ± .005

hkl	I/I_1	2θ	d	N	a_o	d calc	N calc
110	(not scanned)						
200	5	16.80	5.2726	4	10.543	5.2120	3.90
211	3	20.64	4.2995	6	10.531	4.2555	5.87
220	12	23,90	3.7199	8	10.521	3.6854	7.85
310	8	26.52	3.3581	10	10.619	3.2963	9.63
222	100	29.50	3.0253	12	10.479	3.0091	11.87
321	8	31.95	2.7986	14	10.471	2.7859	13.87
400	21	34.22	2.6180	16	10.472	2.6060	15.85
330 411	12	36.42	2.4647	18	10.457	2.4569	17.88
420	5	38.50	2.3362	20	10.448	2.3308	19.90
332	3	40.44	2.2285	22	10.452	2.2224	21.87
422	5	42.36	2.1318	24	10.444	2.1277	23.90
510 431	14	44.20	2.0473	26	10.439	2.0443	25.92
521	12	47.70	1.9049	30	10.433	1.9031	29.94
440	52	49.40	1.8432	32	10.427	1.8427	31.98
530 433	4	51.05	1.7875	34	10.422	1.7877	34.00
600 442	5	52.60	1.7384	36	10.430	1.7373	35.95
611 532	11	54.20	1.6908	38	10.422	1.6909	38.00
620	3	55.78	1.6466	40	10.414	1.6481	40.07
541	(weak)						
622	26	58.78	1.5695	44	10.411	1.5714	44.10
631	2	60.22	1.5353	46	10.413	1.5369	46.09
444	5	61.64	1.5033	48	10.415	1.5045	48.07
710 550 543	5	63.11	1.4718	50	10.407	1.4741	50.15

Spec: D148,A315 a_o = 10.424 ± .005

hkl	I/I_1	2θ	d	N	a_o	d calc	N calc
110	(not scanned)						
200	(undetected)						
211	(undetected)						
220	11	24.05	3.6971	8	10.457	3.6854	7.94
310	9	26.60	3.3481	10	10.587	3.2963	9.69
222	100	29.58	3.0173	12	10.452	3.0091	11.93
321	14	32.05	2.7901	14	10.439	2.7859	13.95
400	21	34.35	2.6084	16	10.433	2.6060	15.97
330 411	11	36.55	2.4563	18	10.421	2.4569	18.00
420	5	38.50	2.3362	20	10.448	2.3308	19.90
332	4	40.50	2.2254	22	10.438	2.2224	21.94
422	5	42.38	2.1309	24	10.439	2.1277	23.92
510 431	15	44.20	2.0473	26	10.439	2.0443	25.92
521	9	47.65	1.9068	30	10.444	1.9031	29.88
440	52	49.35	1.8450	32	10.437	1.8427	31.91
530 433	7	50.95	1.7907	34	10.442	1.7877	33.88
600 442	5	52.60	1.7384	36	10.430	1.7373	35.95
611 532	10	54.10	1.6937	38	10.440	1.6909	37.87
620	3	55.72	1.6482	40	10.424	1.6481	39.99
541	(undetected)						
622	25	58.70	1.5714	44	10.424	1.5714	43.99
631	5	60.13	1.5374	46	10.427	1.5369	45.96
444	7	61.64	1.5033	48	10.415	1.5045	48.07
710 550 543	7	62.98	1.4745	50	10.426	1.4741	49.97

Spec: 18267 a_o = 10.430 ± .005

hkl	I/I_1	2θ	d	N	a_o	d calc	N calc
110	(not scanned)						
200	3	16.65	5.3198	4	10.639	5.2150	3.84
211	5	20.61	4.3057	6	10.546	4.2580	5.86
220	13	23.84	3.7291	8	10.547	3.6875	7.82
310	11	26.38	3.3756	10	10.674	3.2982	9.54
222	100	29.45	3.0303	12	10.497	3.0108	11.84
321	8	31.86	2.8063	14	10.500	2.7875	13.81
400	22	34.20	2.6195	16	10.478	2.6075	15.85
330 411	12	36.35	2.4693	18	10.476	2.4583	17.83
420	4	38.45	2.3392	20	10.461	2.3322	19.88
332	3	40.41	2.2301	22	10.460	2.2236	21.87
422	5	42.40	2.1299	24	10.434	2.1290	23.97
510 431	11	44.14	2.0499	26	10.452	2.0454	25.88
521	8	47.64	1.9071	30	10.446	1.9042	29.90
440	52	49.35	1.8450	32	10.437	1.8437	31.95
530 433	7	50.95	1.7907	34	10.442	1.7887	33.92
600 442	3	52.48	1.7421	36	10.452	1.7383	35.84
611 532	9	54.15	1.6922	38	10.431	1.6919	37.98
620	2	55.65	1.6501	40	10.436	1.6491	39.94
541	2	57.35	1.6052	42	10.403	1.6093	42.21
622	25	58.68	1.5719	44	10.427	1.5723	44.02
631	(poor)						
444	3	61.60	1.5043	48	10.468	1.5054	48.07

Spec: No#B a_o = 10.433 ± .005

hkl	I/I_1	2θ	d	N	a_o	d calc	N calc
110	(not scanned)						
200	4	16.65	5.3198	4	10.639	5.2165	3.84
211	5	20.40	4.3496	6	10.654	4.2592	5.75
220	10	23.70	3.7509	8	10.609	3.6886	7.73
310	8	26.30	3.3856	10	10.157	3.4776	9.49
222	100	29.30	3.0455	12	10.549	3.0117	11.73
321	9	31.70	2.8201	14	10.552	2.7883	13.68
400	19	34.03	2.6322	16	10.528	2.6082	15.70
330 411	10	36.20	2.4792	18	10.518	2.4590	17.70
420	4	38.32	2.3468	20	10.495	2.3328	19.76
332	3	40.25	2.2386	22	10.500	2.2243	21.71
422	3	42.22	2.1386	24	10.477	2.1296	23.79
510 431	10	44.17	2.0486	26	10.446	2.0460	25.93
521	10	47.67	1.9060	30	10.439	1.9047	29.95
440	36	49.30	1.8467	32	10.447	1.8443	31.91
530 433	5	50.90	1.7924	34	10.451	1.7892	33.87
600 442	5	52.44	1.7433	36	10.460	1.7388	35.81
611 532	8	54.08	1.6943	38	10.444	1.6924	37.91
620	3	55.59	1.6518	40	10.446	1.6496	39.89
541	1	56.94	1.6158	42	10.471	1.6098	41.69
622	19	58.62	1.5734	44	10.436	1.5728	43.96
631	2	60.10	1.5381	46	10.432	1.5382	46.00
444	2	61.67	1.5027	48	10.411	1.5058	48.20
710 550 543	3	63.00	1.4741	50	10.423	1.4754	50.08

Spec: M11654 a_o = 10.433 ± .005

hkl	I/I_1	2θ	d	N	a_o	d calc	N calc
110	(not scanned)						
200	(undetected)						
211	(undetected)						
220	(undetected)						
310	36	26.43	3.3693	10	10.654	3.2992	9.58
222	100	29.53	3.0223	12	10.469	3.0117	11.91
321	27	31.85	2.8072	14	10.503	2.7883	13.81
400	24	34.22	2.6180	16	10.472	2.6082	15.88
330 411	16	36.44	2.4634	18	10.451	2.4590	17.93
420	(undetected)						
332	27	40.56	2.2222	22	10.423	2.2243	22.04
422	16	42.26	2.1367	24	10.467	2.1296	23.84
510 431	11	44.19	2.0477	26	10.441	2.0460	25.95
521	27	47.25	1.9220	30	10.350	1.9373	29.46
440	55	49.32	1.8460	32	10.443	1.8443	31.93
530 433	(undetected)						
600 442	(undetected)						
611 532	(undetected)						
620	44	56.07	1.6387	40	10.493	1.6293	40.52
541	(weak)						
622	50	58.55	1.5751	44	10.448	1.5728	43.87
631	(undetected)						
444	13	61.52	1.5060	48	10.434	1.5058	47.98
710 550 543	(undetected)						

Spec: 104553 a_o = 10.445 ± .005

hkl	I/I_1	2θ	d	N	a_o	d calc	N calc
110	(not scanned)						
200	6	16.80	5.2726	4	10.545	5.2225	3.92
211	4	20.65	4.2975	6	10.526	4.2641	5.90
220	13	23.95	3.7123	8	10.500	3.6928	7.91
310	9	26.48	3.3630	10	10.635	3.3029	9.64
222	100	29.46	3.0293	12	10.493	3.0152	11.88
321	14	31.90	2.8029	14	10.487	2.7915	13.88
400	24	34.18	2.6210	16	10.484	2.6112	15.88
330 411	13	36.37	2.4680	18	10.471	2.4619	17.91
420	6	38.40	2.3421	20	10.474	2.3355	19.88
332	2	40.38	2.2317	22	10.467	2.2268	21.90
422	7	42.25	2.1371	24	10.470	2.1320	23.88
510 431	14	44.16	2.0490	26	10.448	2.0484	25.98
521	10	47.62	1.9079	30	10.450	1.9069	29.96
440	51	49.28	1.8474	32	10.451	1.8484	31.96
530 433	8	50.90	1.7924	34	10.451	1.7913	33.95
600 442	7	52.50	1.7415	36	10.449	1.7408	35.97
611 532	10	54.09	1.6940	38	10.442	1.6944	38.01
620	3	55.60	1.6515	40	10.445	1.6514	39.99
541	(very weak)						
622	25	58.56	1.5749	44	10.446	1.5746	43.98
631	2	59.93	1.5421	46	10.459	1.5400	45.87
444	4	61.48	1.5069	48	10.440	1.5076	48.04
710 550 543	6	62.84	1.4775	50	10.447	1.4771	49.97

Spec: 74553 a_o = 10.448 ± .005

hkl	I/I1	2θ	d	N	a_o	d calc	N calc
110	(not scanned)						
200	5	16.68	5.3103	4	10.620	5.2240	3.87
211	12	20.49	4.3307	6	10.608	4.2653	5.82
220	16	23.82	3.7322	8	10.556	3.6939	7.83
310	28	26.30	3.3856	10	10.706	3.3039	9.52
222	100	29.42	3.0333	12	10.507	3.0160	11.86
321	11	31.82	2.8098	14	10.513	2.7923	13.82
400	23	34.16	2.6225	16	10.490	2.6120	15.87
330 411	15	36.28	2.4739	18	10.496	2.4626	17.83
420	5	38.37	2.3438	20	10.482	2.3362	19.86
332	3	40.37	2.2322	22	10.470	2.2275	21.90
422	7	42.22	2.1386	24	10.477	2.1326	23.86
510 431	14	44.16	2.0490	26	10.448	2.0490	25.99
521	13	47.63	1.9075	30	10.448	1.9075	29.99
440	53	49.33	1.8457	32	10.441	1.8469	32.04
530 433	7	50.90	1.7924	34	10.451	1.7918	33.97
600 442	4	52.45	1.7430	36	10.458	1.7413	35.92
611 532	9	54.13	1.6928	38	10.435	1.6948	38.09
620	8	56.03	1.6398	40	10.500	1.6317	40.59
541	(weak)						
622	27	58.65	1.5726	44	10.432	1.5750	44.13
631	(weak)						
444	5	61.52	1.5060	48	10.434	1.5080	48.12
710 550 543	5	63.02	1.4737	50	10.420	1.4775	50.25

Spec: SUNSHINE MINE #3 $a_o = 10.453 \pm .005$

hkl	I/I_1	2θ	d	N	a_o	d calc	N calc
110	(not scanned)						
200	5	16.81	5.2695	4	10.539	5.2265	3.93
211	4	20.70	4.2872	6	10.501	4.2674	5.94
220	11	23.95	3.7123	8	10.500	3.6956	7.92
310	8	26.51	3.3593	10	10.623	3.3055	9.68
222	100	29.44	3.0313	12	10.500	3.0175	11.89
321	12	31.90	2.8029	14	10.487	2.7936	13.90
400	26	34.15	2.6232	16	10.493	2.6132	15.87
330 411	10	36.32	2.4713	18	10.485	2.4637	17.89
420	4	38,35	2.3450	20	10.487	2.3373	19.86
332	6	40.42	2.2296	22	10.457	2.2285	21.97
422	3	42.30	2.1347	24	10.458	2.1337	23.97
510 431	16	44.08	2.0526	26	10.466	2.0500	25.93
521	10	47.58	1.9094	30	10.458	1.9084	29.96
440	51	49.25	1.8485	32	10.456	1.8478	31.97
530 433	7	50.90	1.7924	34	10.451	1.7926	34.00
600 442	5	52.54	1.7402	36	10.441	1.7421	36.07
611 532	11	54.04	1.6954	38	10.451	1.6957	38.01
620	4	55.60	1.6515	40	10.445	1.6527	40.05
541	(weak)						
622	26	58.54	1.5753	44	10.449	1.5758	44.02
631	(very weak)						
444	5	61.40	1.5086	48	10.452	1.5087	48.00
710 550 543	5	62.82	1.4779	50	10.450	1.4782	50.02

Spec: 92347 a_o = 10.487 ± .005

hkl	I/I_1	2θ	d	N	a_o	d calc	N calc
110	(not scanned)						
200	(undetected)						
211	(undetected)						
220	11	23.88	3.7230	8	10.530	3.7077	7.93
310	9	26.47	3.3643	10	10.638	3.3162	9.71
222	100	29.39	3.0363	12	10.518	3.0273	11.92
321	8	31.84	2.8081	14	10.506	2.8027	13.94
400	20	34.12	2.6254	16	10.501	2.6217	15.95
330 411	13	36.24	2.4766	18	10.507	2.4718	17.93
420	6	38.30	2.3480	20	10.500	2.3449	19.94
332	7	40.25	2.2386	22	10.500	2.2358	21.94
422	4	42.17	2.1410	24	10.488	2.1406	23.99
510 431	19	43.98	2.0570	26	10.488	2.0566	25.99
521	13	47.39	1.9166	30	10.498	1.9146	29.93
440	56	49.03	1.8563	32	10.500	1.8538	31.91
530 433	6	50.66	1.8003	34	10.497	1.7985	33.93
600 442	8	52.25	1.7492	36	10.495	1.7478	35.94
611 532	14	53.80	1.7024	38	10.494	1.7012	37.94
620	(weak)						
541	(weak)						
622	30	58.33	1.5805	44	10.484	1.5809	44.02
631	3	59.80	1.5451	46	10.479	1.5462	46.06
444	5	61.17	1.5138	48	10.487	1.5136	47.99
710 550 543	5	62.52	1.4843	50	10.495	1.4830	49.91

Spec: C4995 a_o = 10.502 ± .005

hkl	I/I_1	2θ	d	N	a_o	d calc	N calc
110	(not scanned)						
200	6	16.67	5.3135	4	10.627	5.2510	3.90
211	5	20.55	4.3182	6	10.577	4.2874	5.91
220	16	23.78	3.7384	8	10.573	3.7130	7.89
310	10	26.31	3.3844	10	10.702	3.3210	9.62
222	100	29.28	3.0475	12	10.556	3.0316	11.87
321	11	31.70	2.8201	14	10.552	2.8067	13.86
400	27	34.00	2.6344	16	10.537	2.6255	15.89
330 411	17	36.15	2.4825	18	10.532	2.4753	17.89
420	8	38.23	2.3521	20	10.519	2.3483	19.93
332	5	40.20	2.2413	22	10.512	2.2390	21.95
422	5	42.07	2.1459	24	10.512	2.1437	23.95
510 431	19	43.90	2.0606	26	10.507	2.0596	25.97
521	13	47.30	1.9201	30	10.516	1.9173	29.91
440	57	48.98	1.8581	32	10.511	1.8565	31.94
530 433	7	50.58	1.8030	34	10.513	1.8010	33.92
600 442	3	52.17	1.7517	36	10.510	1.7503	35.94
611 532	11	53.75	1.7039	38	10.503	1.7036	37.98
620	(weak)						
541	(weak)						
622	30	58.23	1.5830	44	10.500	1.5832	44.01
631	4	59.74	1.5465	46	10.489	1.5484	46.11
444	4	61.08	1.5158	48	10.501	1.5158	48.00
710 550 543	4	62.47	1.4853	50	10.503	1.4852	49.98

Spec: 90875 a_o = 10.512 ± .005

hkl	I/I1	2θ	d	N	a_o	d calc	N calc
110	(not scanned)						
200	5	16.77	5.2820	4	10.564	5.2560	3.96
211	(undetected)						
220	17	23.80	3.7353	8	10.565	3.7165	7.91
310	10	26.45	3.3668	10	10.646	3.3241	9.74
222	100	29.34	3.0414	12	10.535	3.0345	11.94
321	8	31.80	2.8115	14	10.519	2.8094	13.97
400	20	34.06	2.6299	16	10.519	2.6280	15.97
330 411	9	36.15	2.4825	18	10.532	2.4777	17.92
420	5	38.28	2.3492	20	10.505	2.3505	20.02
332	4	40.20	2.2413	22	10.512	2.2411	21.99
422	2	42.45	2.1275	24	10.422	2.1457	24.41
510 431	15	43.85	2.0628	26	10.518	2.0615	25.96
521	13	47.33	1.9189	30	10.510	1.9192	30.00
440	43	49.01	1.8570	32	10.505	1.8582	32.04
530 433	5	50.65	1.8006	34	10.499	1.8027	34.07
600 442	8	51.98	1.7577	36	10.546	1.7520	35.76
611 532	8	53.70	1.7053	38	10.512	1.7052	37.99
620	(weak)						
541	(undetected)						
622	20	58.21	1.5835	44	10.503	1.5847	44.06

Spec: 96332 a_o = 10.530 ± .005

hkl	I/I_1	2θ	d	N	a_o	d calc	N calc
222	100	29.26	3.0495	12	10.564	3.0397	11.92
321	16	31.62	2.8271	14	10.578	2.8142	13.87
400	21	33.97	2.6367	16	10.546	2.6325	15.94
330 411	14	36.11	2.4852	18	10.543	2.4819	17.95
420	6	38.10	2.3598	20	10.553	2.3545	19.91
332	20	40.13	2.2450	22	10.530	2.2450	21.99
422	(undetected)						
510 431	26	43.80	2.0650	26	10.529	2.0651	26.00
521	10	47.28	1.9208	30	10.521	1.9225	30.05
440	40	48.90	1.8609	32	10.527	1.8614	32.01
530 433	7	50.45	1.8073	34	10.538	1.8058	33.94
600 442	7	52.07	1.7548	36	10.529	1.7550	36.00
611 532	13	53.63	1.7074	38	10.525	1.7081	38.03
620	5	55.15	1.6639	40	10.523	1.6649	40.04
541	(weak)						
622	21	58.14	1.5852	44	10.515	1.5874	44.12
631	7	59.53	1.5515	46	10.523	1.5525	46.06
444	3	60.97	1.5182	48	10.519	1.5198	48.09
710 550 543	7	62.34	1.4881	50	10.523	1.4891	50.06

Spec: 66819 a_o = 10.552 ± .005

hkl	I/I_1	2θ	d	N	a_o	d calc	N calc
110	(not scanned)						
200	1	16.62	5.3293	4	10.658	5.2760	3.92
211	6	20.46	4.3369	6	10.623	4.3078	5.91
220	13	23.66	3.7571	8	10.626	3.7306	7.88
310	8	26.24	3.3933	10	10.730	3.3368	9.66
222	100	29.17	3.0587	12	10.595	3.0461	11.90
321	8	31.56	2.8323	14	10.597	2.8201	13.87
400	20	33.85	2.6458	16	10.583	2.6380	15.90
330 411	9	35.98	2.4939	18	10.580	2.4871	17.90
420	5	38.02	2.3646	20	10.575	2.3594	19.91
332	8	39.98	2.2531	22	10.568	2.2496	21.93
422	(undetected)						
510 431	17	43.66	2.0713	26	10.561	2.0694	25.95
521	9	47.08	1.9285	30	10.563	1.9265	29.93
440	51	48.73	1.8670	32	10.561	1.8653	31.94
530 433	3	50.28	1.8130	34	10.571	1.8096	33.87
600 442	5	51.90	1.7602	36	10.561	1.7586	35.93
611 532	10	53.50	1.7112	38	10.549	1.7117	38.02
620	(undetected)						
541	(undetected)						
622	27	57.97	1.5895	44	10.543	1.5907	44.06
631	4	59.40	1.5546	46	10.543	1.5558	46.07
444	4	60.88	1.5203	48	10.533	1.5230	48.17
710 550 543	4	62.33	1.4883	50	10.524	1.4922	50.26

REFERENCES

Azaroff, L.V., 1960, Introduction to solids: New York, McGraw-Hill Book Company, Inc., 460 p.

Berry, L.G., 1943, Studies of mineral sulpho-salts: VII - a systematic arrangement on the basis of cell dimensions: Univ. of Toronto Studies Geol. Series, No. 48, p. 9-30.

_____ and Thompson, R.M., 1962, X-ray powder data for ore minerals: Geol. Soc. American Mem. 85, 281 p.

Buerger, M.J., 1949, Disorder in crystals of non-metals: Anais da Academia Brasileira de Ciencias, v. 21, p. 155-266.

Chace, F.M., 1956, Abbreviations in field and mine geological mapping: Econ. Geology, v. 51, p. 712-723.

Commission on New Minerals and Mineral Names, IMA, 1960, 1962, Annual review of new names and suggested changes in nomenclature: Am. Mineralogist, v. 49, p. 223-224, (1964).

Frueh, A.J., Jr., 1950, Disorder in sulfides (abs.): Am. Mineralogist, v. 35, p. 282.

_____1958, Some applications of x-ray crystallography to geologic thermometry: Jour. Geology, v. 66, p. 218-223.

Gaudin, A.M., and Dicke, Gunther, 1939, The pyrosynthesis, microscopic study and iridescent filming of sulfide compounds of copper with arsenic, antimony and bismuth: Econ. Geology, v. 34, p. 49-81, 214-232.

Harcourt, G.A., 1942, Tables for the identification of ore minerals by x-ray powder patterns: Am. Mineralogist, v. 27, p. 63-113.

Hiller, J.E., 1953, Eine kristallchemische Systematik der Sulfide, Selenid- und Telluridminerale: Neues Jahrb. Mineralogie, Monatsh., p. 145-153.

Hurlbut, C.S., Jr., 1959, Dana's manuel of mineralogy, (17th ed.): New York, John Wiley and Sons, Inc., 609 p.

Machatschki, Felix, 1928, Prazisionsmessungen der Gitterkonstanten verschiedener Fahlerze. Formel und Struktur derselben: Zeitschr. Kristallographie, v. 68, p. 204-222.

Palache, Charles, Berman, Harry, and Frondel, Clifford, 1944, Dana's system of mineralogy, v. 1, (7th ed.): New York, John Wiley and Sons, Inc., 834 p.

Pauling, Linus, 1948, The nature of the chemical bond, (2d ed.): Ithaca, N.Y., Cornell University Press.

——— and Neuman, E.W., 1934, The crystal structure of binnite, $(Cu,Fe)_{12}As_4S_{13}$, and the chemical composition and structure of minerals of the tetrahedrite group: Zeitschr. Kristallographie, v. 88, p. 54-62.

Prior, G.T., 1908, Analyses of seligmannite, zinciferous tennantite (binnite), and fuchsite from the Lengenbach quarry, Binnenthal: Mineralog. Mag., v. 15, p. 385-387.

Rosenblum, S., 1958, Magnetic susceptibilities of minerals in the Frantz Isodynamic Separator: Am. Mineralogist, v. 43, p. 170.

Ross, Virginia, 1957, Geochemistry, crystal structure and mineralogy of the sulfides: Econ. Geology, v. 52, p. 755-774.

Sampson, E.A., 1949, A method for polishing sections of ores: Econ. Geology, v. 44, p. 119-127.

———1956, A procedure for polishing ore sections with diamond abrasive: Econ. Geology, v. 51, p. 482-484.

Skinner, B.J., 1961, Unit-cell edges of natural and synthetic sphalerites: Am. Mineralogist, v. 46, p. 1399-1411.

——— and Bethke, P.M., 1961, The relationship between unit-cell edges and composition of synthetic wurtzites: Am. Mineralogist, v. 46, p. 1382-1398.

Strock, L.W., 1936, A classification of crystal structures with defect lattices: Zeitschr. Kristallographie, v. 93, p. 285-311.

Waldo, A.W., 1935, Identification of the copper ore minerals by means of x-ray powder diffraction patterns: Am. Mineralogist, v. 20, p. 575-594.

Wherry, E.T., and Foshag, W.F., 1921, A new classification of the sulfo-salt minerals: Jour. Washington Acad. Sci., v. 11, p. 1-8.

Winchell, A.N., 1926, The chemical constitution of the tetrahedrite-tennantite system: Am. Mineralogist, v. 11, p. 181-185.

Wuensch, B.J., 1963, Confirmation of the crystal structure of tetrahedrite, $Cu_{12}Sb_4S_{13}$: Science, v. 141, p. 804-805.